Notes for Solid State Theory
FYST25/EXTP90/NAFY017

Andreas Wacker
Matematisk Fysik
Lunds Universitet

Vårtermin 2019

LUNDS UNIVERSITET

These notes give a summary of the lecture and present additional material, which may be less accessible by standard text books. They should be studied together with standard text books of solid state physics, such as Snoke (2008), Hofmann (2008), Ibach and Lüth (2003) or Kittel (1996), to which is frequently referred.

Solid state theory is a large field and thus a 7.5 point course must restrict the material. E.g., important issues such as calculation schemes for the electronic structure or a detailed account of crystal symmetries is not contained in this course.

Sections marked with a * present additional material on an advanced level, which may be treated very briefly or even skipped. They will not be relevant for the exam. The same holds for footnotes which shall point towards more sophisticated problems.

Note that there are two different usages for the symbol e: In these note $e > 0$ denotes the *elementary charge*, which consistent with most textbooks (including Snoke (2008),Ibach and Lüth (2003), and Kittel (1996)). In contrast sometimes $e < 0$ denotes the *charge of the electron*, which I also used in previous versions of these notes. Thus, there may still be some places, where I forgot to change. Please report these together with other misprints and any other suggestion for improvement.

I want the thank all former students for helping in improving the text. Any further suggestions as well as reports of misprints are welcome! Special thanks to Rikard Nelander for critical reading and preparing several figures.

Bibliography

D. W. Snoke, *Solid State Physics: Essential Concepts* (Addison-Wesley, 2008).

P. Hofmann, *Solid State Physics* (Viley-VCH, Weinheim, 2008).

H. Ibach and H. Lüth, *Solid-state physics* (Springer, Berlin, 2003).

C. Kittel, *Introduction to Solid State Physics* (John Wiley & Sons, New York, 1996).

N. W. Ashcroft and N. D. Mermin, *Solid State Physics* (Thomson Learning, 1979).

G. Czycholl, *Festkörperphysik* (Springer, Berlin, 2004).

D. Ferry, *Semiconductors* (Macmillan Publishing Company, New York, 1991).

E. Kaxiras, *Atomic and Electronic Structure of Solids* (Cambridge University Press, Cambridge, 2003).

C. Kittel, *Quantum Theory of Solids* (John Wiley & Sons, New York, 1987).

M. P. Marder, *Condensed Matter Physics* (John Wiley & Sons, New York, 2000).

J. R. Schrieffer, *Theory of Superconductivity* (Perseus, 1983).

K. Seeger, *Semiconductor Physics* (Springer, Berlin, 1989).

P. Y. Yu and M. Cardona, *Fundamentals of Semiconductors* (Springer, Berlin, 1999).

C. Kittel and H. Krömer, *Thermal Physics* (Freeman and Company, San Francisco, 1980).

J. D. Jackson, *Classical Electrodynamics* (John Wiley & Sons, New York, 1998), 3rd ed.

W. W. Chow and S. W. Koch, *Semiconductor-Laser Fundamentals* (Springer, Berlin, 1999).

List of symbols

symbol	meaning	page
$A(\mathbf{r},t)$	magnetic vector potential	11
$\mathbf{a}_i$	primitive lattice vector	1
$\mathbf{B}(\mathbf{r},t)$	magnetic field	11
$D(E)$	density of states	7
E_F	Fermi energy	7
$E_n(\mathbf{k})$	Energy of Bloch state with band index n and Bloch vector $\mathbf{k}$	2
e	elementary charge (positive!)	
$\mathbf{F}(\mathbf{r},t)$	electric field	11
$f(\mathbf{k})$	occupation probability	16
g_e	Landé factor of the electron	30
$\mathbf{g}_i$	primitive vector of reciprocal lattice	1
$\mathbf{G}$	reciprocal lattice vector	1
$\mathbf{H}$	magnetizing field	29
I	radiation intensity	Eq. (4.10)
$\mathbf{M}$	Magnetization	29
m_e	electron mass	
m_n	effective mass m_{eff} of band n	10
N	Number of unit cells in normalization volume	3
n	electron density (or spin density) with unit 1/Volume	7
n	refractive index	41
$\mathbf{P}_{m,n}(\mathbf{k})$	momentum matrix element	10
$\mathbf{R}$	lattice vector	1
$u_{n\mathbf{k}}(\mathbf{r})$	lattice periodic function of Bloch state $(n,\mathbf{k})$	1
V	Normalization volume	3
V_c	volume of unit cell	1
$v_n(\mathbf{k})$	velocity of Bloch state with band index n and Bloch vector $\mathbf{k}$	10
α	absorption coefficient	41
$\phi(\mathbf{r},t)$	electrical potential	11
$\boldsymbol{\mu}$	magnetic dipole moment	29
μ	chemical potential	16
μ_0	vacuum permeability	29
μ_B	Bohr magneton	30
μ_k	electric dipole moment	44
$\tilde{\mu}$	mobility	17
ν	number of nearest neighbor sites in the lattice	36
χ	magnetic/electric susceptibility	29/39

Contents

Chapter 1

Band structure

1.1 Bloch's theorem

Most solid materials (a famous exception is glass) show a crystalline structure [1] which exhibits a translation symmetry. The crystal is invariant under translations by all *lattice vectors*

$$\mathbf{R}_l = l_1\mathbf{a}_1 + l_2\mathbf{a}_2 + l_3\mathbf{a}_3 \tag{1.1}$$

where $l_i \in \mathbb{Z}$. The set of points associated with the end points of these vectors is called the *Bravais lattice*. The *primitive vectors* $\mathbf{a}_i$ span the Bravais lattice and can be determined by X-ray spectroscopy for each material. The volume of the unit cell is $V_c = \mathbf{a}_1 \cdot (\mathbf{a}_2 \times \mathbf{a}_3)$. In order to characterize the energy eigenstates of such a crystal, the following theorem is of utmost importance:

Bloch's Theorem: The eigenstates of a lattice-periodic Hamiltonian satisfying $\hat{H}(\mathbf{r}) = \hat{H}(\mathbf{r} + \mathbf{R_l})$ for all $l_i \in \mathbb{Z}$ can be written as *Bloch functions* in the form

$$\Psi_{n,\mathbf{k}}(\mathbf{r}) = \mathrm{e}^{\mathrm{i}\mathbf{k}\cdot\mathbf{r}} u_{n,\mathbf{k}}(\mathbf{r}) \tag{1.2}$$

where $\mathbf{k}$ is the *Bloch vector* and $u_{n,\mathbf{k}}(\mathbf{r})$ is a lattice-periodic function.

An equivalent defining relation for the Bloch functions is $\Psi_{n,\mathbf{k}}(\mathbf{r} + \mathbf{R}_l) = \mathrm{e}^{\mathrm{i}\mathbf{k}\cdot\mathbf{R}_l}\Psi_{n,\mathbf{k}}(\mathbf{r})$ for all lattice vectors $\mathbf{R}_l$ (sometimes called Bloch condition).

For each Bravais lattice one can construct the corresponding primitive vectors of the *reciprocal lattice* $\mathbf{g}_i$ by the relations

$$\mathbf{g}_i \cdot \mathbf{a}_j = 2\pi\delta_{ij}\,. \tag{1.3}$$

In analogy to the real lattice, they span the reciprocal lattice with vectors $\mathbf{G}_m = m_1\mathbf{g}_1 + m_2\mathbf{g}_2 + m_3\mathbf{g}_3$. More details on the real and reciprocal lattice are found in your textbook.

We define the *first Brillouin zone* by the set of vectors $\mathbf{k}$, satisfying $|\mathbf{k}| \leq |\mathbf{k} - \mathbf{G}_m|$ for all G_n, i.e. they are closer to the origin than to any other vector of the reciprocal lattice. Thus the first Brillouin zone is confined by the planes $\mathbf{k}\cdot\mathbf{G}_m = |\mathbf{G}_m|^2/2$. Then we can write each vector $\mathbf{k}$ as $\mathbf{k} = \tilde{\mathbf{k}} + \mathbf{G}_m$, where $\tilde{\mathbf{k}}$ is within the first Brillouin zone and $\mathbf{G}_m$ is a vector of the reciprocal lattice. (This decomposition is unique unless $\tilde{\mathbf{k}}$ is on the boundary of the first Brillouin zone.) Then we have

$$\Psi_{n,\mathbf{k}}(\mathbf{r}) = \mathrm{e}^{\mathrm{i}\tilde{\mathbf{k}}\cdot\mathbf{r}}\mathrm{e}^{\mathrm{i}\mathbf{G}_n\cdot\mathbf{r}} u_{n,\mathbf{k}}(\mathbf{r}) = \mathrm{e}^{\mathrm{i}\tilde{\mathbf{k}}\cdot\mathbf{r}} u_{\tilde{n},\tilde{\mathbf{k}}}(\mathbf{r}) = \Psi_{\tilde{n},\tilde{\mathbf{k}}}(\mathbf{r})$$

[1] Another rare sort of solid materials with high symmetry are quasi-crystals, which do not have an underlying Bravais lattice. Their discovery in 1984 was awarded with the Nobel price in Chemistry 2011 `http://www.nobelprize.org/nobel_prizes/chemistry/laureates/2011/sciback_2011.pdf`

as $u_{\tilde{n},\tilde{\mathbf{k}}}(\mathbf{r})$ is also a lattice-periodic function. Therefore we can restrict our Bloch vectors to the first Brillouin zone without loss of generality.

Band structure: For each $\mathbf{k}$ belonging to the first Brillouin zone, we have set of eigenstates of the Hamiltonian

$$\hat{H}\Psi_{n,\mathbf{k}}(\mathbf{r}) = E_n(\mathbf{k})\Psi_{n,\mathbf{k}}(\mathbf{r}) \tag{1.4}$$

where $E_n(\mathbf{k})$ is a continuous function in $\mathbf{k}$ for each *band index* n.

Bloch's theorem can be derived by examining the plane wave expansion of arbitrary wave functions and using

$$u_{n,\mathbf{k}}(\mathbf{r}) = \sum_{\{m_i\}} a_m^{(n,\mathbf{k})} \mathrm{e}^{\mathrm{i}\mathbf{G}_m\cdot\mathbf{r}},$$

see, e.g. chapter 7.1 of Ibach and Lüth (2003) or chapter 7 of Kittel (1996). In the subsequent section an alternate proof is given on the basis of the crystal symmetry. The treatment follows essentially chapter 8 of Ashcroft and Mermin (1979) and chapter 1.3 of Snoke (2008).

1.1.1 Derivation of Bloch's theorem by lattice symmetry

We define the *translation operator* $\hat{T}_{\mathbf{R}}$ by its action on arbitrary wave functions $\Psi(\mathbf{r})$ by

$$\hat{T}_{\mathbf{R}}\Psi(\mathbf{r}) = \Psi(\mathbf{r}+\mathbf{R})$$

where $\mathbf{R}$ is an arbitrary lattice vector. We find for arbitrary wave functions:

$$\hat{T}_{\mathbf{R}}\hat{T}_{\mathbf{R}'}\Psi(\mathbf{r}) = \hat{T}_{\mathbf{R}}\Psi(\mathbf{r}+\mathbf{R}') = \Psi(\mathbf{r}+\mathbf{R}+\mathbf{R}') = \hat{T}_{\mathbf{R}+\mathbf{R}'}\Psi(\mathbf{r}) \tag{1.5}$$

As $\hat{T}_{\mathbf{R}+\mathbf{R}'} = \hat{T}_{\mathbf{R}'+\mathbf{R}}$ we find the commutation relation

$$[\hat{T}_{\mathbf{R}}, \hat{T}_{\mathbf{R}'}] = 0 \tag{1.6}$$

for all pairs of lattice vectors $\mathbf{R}, \mathbf{R}'$. Thus, there is a complete set of common eigenfunctions $\Psi_\alpha(\mathbf{r})$ to all translation operators, satisfying

$$\hat{T}_{\mathbf{R}}\Psi_\alpha(\mathbf{r}) = c_\alpha(\mathbf{R})\Psi_\alpha(\mathbf{r})$$

Let us write without loss of generality $c_\alpha(\mathbf{a}_i) = \mathrm{e}^{2\pi\mathrm{i}x_i^\alpha}$ for the primitive lattice vectors $\mathbf{a}_i$ with $x_i^\alpha \in \mathbb{C}$ (it will be shown below that only $x_i^\alpha \in \mathbb{R}$ is of relevance for bulk crystals). From Eqs. (1.1,1.6) we find

$$\hat{T}_{\mathbf{R}_n}\Psi_\alpha(\mathbf{r}) = \hat{T}_{\mathbf{a}_1}^{n_1}\hat{T}_{\mathbf{a}_2}^{n_2}\hat{T}_{\mathbf{a}_3}^{n_3}\Psi_\alpha(\mathbf{r}) = \mathrm{e}^{2\pi\mathrm{i}(n_1x_1^\alpha+n_2x_2^\alpha+n_3x_3^\alpha)}\Psi_\alpha(\mathbf{r}) = \mathrm{e}^{\mathrm{i}\mathbf{k}_\alpha\cdot\mathbf{R}_n}\Psi_\alpha(\mathbf{r})$$

where $\mathbf{k}_\alpha = x_1^\alpha\mathbf{g}_1 + x_2^\alpha\mathbf{g}_2 + x_3^\alpha\mathbf{g}_3$ and Eq. (1.3) is used.

Now we define $u_\alpha(\mathbf{r}) = \mathrm{e}^{-\mathrm{i}\mathbf{k}_\alpha\cdot\mathbf{r}}\Psi_\alpha(\mathbf{r})$ and find

$$u_\alpha(\mathbf{r}-\mathbf{R}_n) = \mathrm{e}^{-\mathrm{i}\mathbf{k}_\alpha\cdot(\mathbf{r}-\mathbf{R}_n)}\Psi_\alpha(\mathbf{r}-\mathbf{R}_n) = \mathrm{e}^{-\mathrm{i}\mathbf{k}_\alpha\cdot\mathbf{r}}\underbrace{\mathrm{e}^{\mathrm{i}\mathbf{k}_\alpha\cdot\mathbf{R}_\mathbf{n}}\Psi_\alpha(\mathbf{r}-\mathbf{R}_n)}_{=\Psi_\alpha(\mathbf{r})} = u_\alpha(\mathbf{r})$$

Thus we find:

If $\Psi_\alpha(\mathbf{r})$ is eigenfunction to all translation-operators $\hat{T}_{\mathbf{R}}$ of the lattice, it has the form

$$\Psi_\alpha(\mathbf{r}) = \mathrm{e}^{\mathrm{i}\mathbf{k}_\alpha\cdot\mathbf{r}}u_\alpha(\mathbf{r}) \tag{1.7}$$

where $u_\alpha(\mathbf{r})$ is a lattice periodic function. The vector $\mathbf{k}_\alpha$ is called *Bloch vector*.

For infinite crystals we have $\mathbf{k}_\alpha \in \mathbb{R}$. This is proven by contradiction. Let, e.g., $\mathrm{Im}\{\mathbf{k}_\alpha \cdot \mathbf{a}_1\} = \lambda > 0$. Then we find

$$|\Psi_\alpha(-n\mathbf{a}_1)|^2 = |T_{-n\mathbf{a}_1}\Psi_\alpha(0)|^2 = |\mathrm{e}^{-2\pi n i \mathbf{k}_\alpha\cdot\mathbf{a}_1}\Psi_\alpha(0)|^2 = \mathrm{e}^{4\pi n\lambda}|\Psi_\alpha(0)|^2$$

and the wave function diverges for $n \to -\infty$, i.e. in the direction opposite to $\mathbf{a}_1$. Thus $\Psi_\alpha(\mathbf{r})$ has its weight at the boundaries of the crystal but does not contribute in the bulk of the crystal.[2]

As the crystal lattice is invariant to translations by lattice vectors $\mathbf{R}$, the *Hamiltonian* $\hat{H}(\mathbf{r})$ for the electrons in the crystal satisfies

$$\hat{H}(\mathbf{r}) = \hat{H}(\mathbf{r}+\mathbf{R})$$

for all lattice vectors $\mathbf{R}$. Thus we find

$$\hat{T}_\mathbf{R}\hat{H}(\mathbf{r})\Psi(\mathbf{r}) = \hat{H}(\mathbf{r}+\mathbf{R})\Psi(\mathbf{r}+\mathbf{R}) = \hat{H}(\mathbf{r})\hat{T}_\mathbf{R}\Psi(\mathbf{r})$$

or

$$\underbrace{\left(\hat{T}_\mathbf{R}\hat{H}(\mathbf{r}) - \hat{H}(\mathbf{r})\hat{T}_\mathbf{R}\right)}_{=[\hat{T}_\mathbf{R},\hat{H}(\mathbf{r})]}\Psi(\mathbf{r}) = 0$$

As this holds for arbitrary wave functions we find the *commutation relation* $[\hat{T}_\mathbf{R}, \hat{H}(\mathbf{r})] = 0$.

Thus $\{\hat{H}, \hat{T}_\mathbf{R}, \hat{T}_{\mathbf{R}'}, \ldots\}$ are a set of pairwise commuting operators and quantum mechanics tells us, that there is a complete set of functions $\Psi_\alpha(\mathbf{r})$, which are eigenfunctions to each of these operators, i.e.

$$\hat{H}\Psi_\alpha(\mathbf{r}) = E_\alpha\Psi_\alpha(\mathbf{r}) \quad \text{and} \quad \hat{T}_\mathbf{R}\Psi_\alpha(\mathbf{r}) = c_\alpha(\mathbf{R})\Psi_\alpha(\mathbf{r})$$

As Eq. (1.7) holds, we may replace the index α by $n, \mathbf{k}$, where $\mathbf{k} = \mathbf{k}_\alpha$ is the Bloch vector and n describes different energy states for a fixed $\mathbf{k}$. This provides us with Bloch's theorem.

1.1.2 Born-von Kármán boundary conditions

In order to count the Bloch states and obtain normalizable wave functions one can use the following trick.

We assume a finite crystal in the shape of a parallelepiped with $N_1N_2N_3$ unit cells. Thus the entire volume is $V = N_1N_2N_3V_c$. For the wave functions we assume periodic boundary conditions $\Psi(\mathbf{r}+N_i\mathbf{a}_i) = \Psi(\mathbf{r})$ for simplicity. For the Bloch functions this requires $\mathbf{k}\cdot N_i\mathbf{a}_i = 2\pi n_i$ with $n_i \in \mathbb{Z}$ or

$$\mathbf{k} = \frac{n_1}{N_1}\mathbf{g}_1 + \frac{n_2}{N_2}\mathbf{g}_2 + \frac{n_3}{N_3}\mathbf{g}_3$$

Restricting to the first Brillouin zone[3] gives $N_1N_2N_3$ different values for $\mathbf{k}$. Thus,

Each band n has within the Brillouin zone as many states as there are unit cells in the crystal (twice as many for spin degeneracy).

If all N_i become large, the values $\mathbf{k}$ become close to each other and we can replace a sum over $\mathbf{k}$ by an integral. As the volume of the Brillouin zone is $Vol(\mathbf{g}_1, \mathbf{g}_2, \mathbf{g}_3) = (2\pi)^3/V_c$ we find that

[2] This does not hold close to a surface perpendicular to $\mathbf{a}_1$. Therefor surface states can be described by a complex Bloch vector $\mathbf{k}_\alpha$.

[3] If the Brillouin zone is a parallelepiped, we can write $-N_i/2 < n_i < N_i/2$. But typically the Brillouin zone is more complicated.

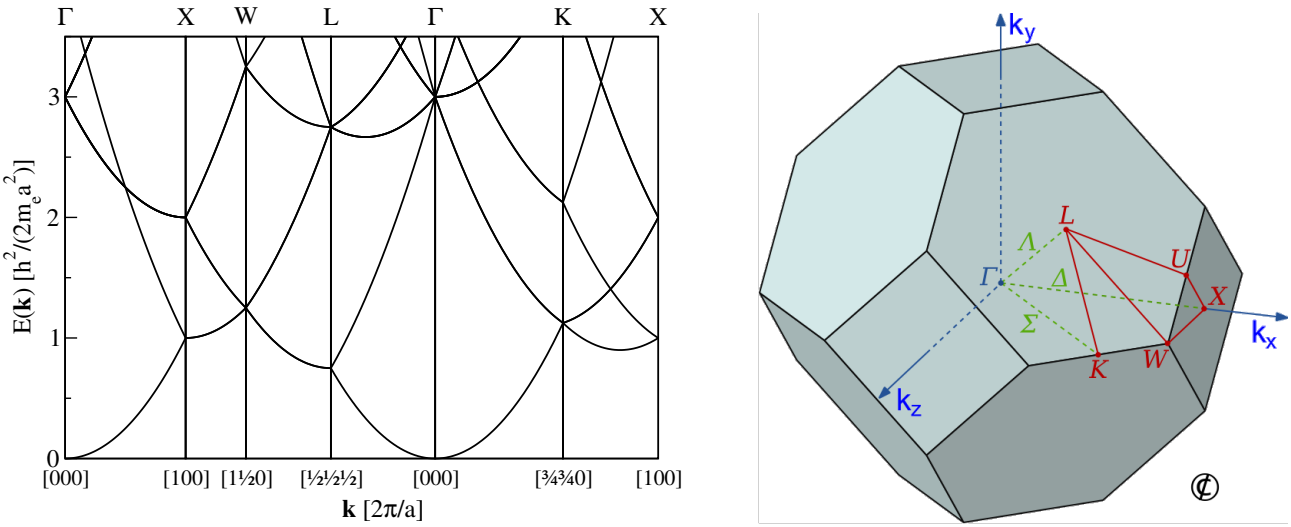

Figure 1.1: Free electron band structure for an fcc crystal together with a sketch of the Brillouin zone (modified file from Wikipedia). The energy scale is $\hbar^2/2m \times (2\pi/a)^2$. For the lattice constant $a = 4.05$Å of Al, we obtain 9.17 eV or 0.67 Rydberg.

the *continuum limit* is given by

$$\sum_{\mathbf{k}} f(\mathbf{k}) = \frac{V_c N_1 N_2 N_3}{(2\pi)^3} \sum_{\mathbf{k}} Vol(\Delta k_1, \Delta k_2, \Delta k_3) f(\mathbf{k}) \to \frac{V}{(2\pi)^3} \int \mathrm{d}^3 k f(\mathbf{k}) \tag{1.8}$$

for arbitrary functions $f(\mathbf{k})$.

1.2 Examples of band structures

The calculation of the band structure for a crystal is an intricate task and many approximation schemes have been developed, see, e.g., chapter 10 of Marder (2000). Here we discuss two simple approximations in order to provide insight into the main features.

1.2.1 Plane wave expansion for a weak potential

In case of a constant potential U_0 the eigenstates of the Hamiltonian are free particle states, i.e. plan waves $\mathrm{e}^{\mathrm{i}\mathbf{k}\cdot\mathbf{r}}$ with energy $\hbar^2 k^2/2m + U_0$. These can be written as Bloch states by decomposing $\mathbf{k} = \tilde{\mathbf{k}} + \mathbf{G}_n$, where $\tilde{\mathbf{k}}$ is within the first Brillouin zone. Then we find

$$\Psi_{n\tilde{\mathbf{k}}}(\mathbf{r}) = \mathrm{e}^{\mathrm{i}\tilde{\mathbf{k}}\cdot\mathbf{r}} u_{n\tilde{\mathbf{k}}}(\mathbf{r}) \quad \text{and} \quad E_n(\tilde{\mathbf{k}}) = \frac{\hbar^2(\tilde{\mathbf{k}} + \mathbf{G}_n)^2}{2m} + U_0$$

The corresponding band structure is shown in Fig. 1.1 for a fcc lattice. A weak periodic potential will split the degeneracies at crossings (in particular at zone boundaries and at $\tilde{\mathbf{k}} = 0$), thus providing gaps (see exercise 2). In this way the band structure of many metals such as aluminum can be well understood, see Fig. 1.2.

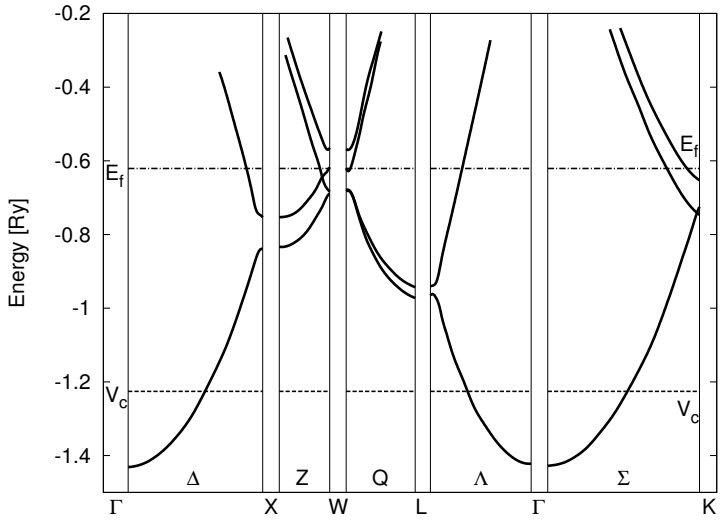

Figure 1.2: Calculated band structure of aluminum. [After E.C. Snow, Phys. Rev. **158**, 683 (1967)]

1.2.2 Superposition of localized orbits for bound electrons

Alternatively, one may start from a set of localized atomic wave functions $\phi_j(\mathbf{r})$ satisfying

$$\left[-\frac{\hbar^2}{2m}\Delta + V_A(\mathbf{r})\right]\phi_j(\mathbf{r}) = E_j\phi_j(\mathbf{r})$$

for the atomic potential $V_A(\mathbf{r})$ of a single unit cell. The total crystal potential is given by $\sum_l V_A(\mathbf{r}-\mathbf{R}_l)$ and we construct Bloch states as

$$\Psi_{n\mathbf{k}}(\mathbf{r}) = \frac{1}{\sqrt{N}}\sum_{l,j} \mathrm{e}^{\mathrm{i}\mathbf{k}\cdot\mathbf{R}_l} c_j^{(n,\mathbf{k})}\phi_j(\mathbf{r}-\mathbf{R}_l)$$

Defining $v(\mathbf{r}) = \sum_{h\neq 0} V_A(\mathbf{r}-\mathbf{R}_h)$ we find

$$\hat{H}\Psi_{n\mathbf{k}}(\mathbf{r}) = \frac{1}{\sqrt{N}}\sum_{lj} \mathrm{e}^{\mathrm{i}\mathbf{k}\cdot\mathbf{R}_l} c_j^{(n,\mathbf{k})}\big[E_j\phi_j(\mathbf{r}-\mathbf{R}_l) + v(\mathbf{r}-\mathbf{R}_l)\phi_j(\mathbf{r}-\mathbf{R}_l)\big] \stackrel{!}{=} E_n(\mathbf{k})\Psi_{n\mathbf{k}}(\mathbf{r})$$

Taking the scalar product by the operation $\sqrt{N}\int \mathrm{d}^3r\phi_i^*(\mathbf{r})$ we find

$$E_i c_i^{(n,\mathbf{k})} + \sum_j \int \mathrm{d}^3r\phi_i^*(\mathbf{r})v(\mathbf{r})\phi_j(\mathbf{r})c_j^{(n,\mathbf{k})} + \sum_{l\neq 0,j} \mathrm{e}^{\mathrm{i}\mathbf{k}\cdot\mathbf{R}_l}\int \mathrm{d}^3r\phi_i^*(\mathbf{r})\big[E_j + v(\mathbf{r}-\mathbf{R}_l)\big]\phi_j(\mathbf{r}-\mathbf{R}_l)c_j^{(n,\mathbf{k})}$$
$$= E_n(\mathbf{k})\left(c_i^{(n,\mathbf{k})} + \sum_{l\neq 0,j}\mathrm{e}^{\mathrm{i}\mathbf{k}\cdot\mathbf{R}_l}\int \mathrm{d}^3r\phi_i^*(\mathbf{r})\phi_j(\mathbf{r}-\mathbf{R}_l)c_j^{(n,\mathbf{k})}\right)$$

which provides a matrix equation for the coefficients $c_i^{(n,\mathbf{k})}$. For a given energy $E_n(\mathbf{k})$, the atomic levels $E_i \approx E_n(\mathbf{k})$ dominate, and thus one can restrict oneself to a finite set of levels in the energy region of interest (e.g., the 3s and 3p levels for the conduction and valence band of Si). Restricting to a single atomic S-level and next-neighbor interactions in a simple cubic crystal with lattice constant a we find

$$E(\mathbf{k}) \approx E_S + \frac{A + 2B(\cos k_x a + \cos k_y a + \cos k_z a)}{1 + 2C(\cos k_x a + \cos k_y a + \cos k_z a)}$$

with

$$A = \int \mathrm{d}^3r\phi_S^*(\mathbf{r})v(\mathbf{r})\phi_S(\mathbf{r})\,, \quad B = \int \mathrm{d}^3r\phi_S^*(\mathbf{r})v(\mathbf{r}-a\mathbf{e}_x)\phi_S(\mathbf{r}-a\mathbf{e}_x)\,, \quad C = \int \mathrm{d}^3r\phi_S^*(\mathbf{r})\phi_S(\mathbf{r}-a\mathbf{e}_x)$$

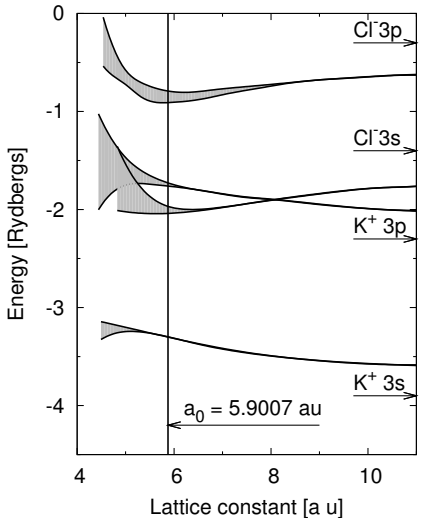

Figure 1.3: Upper filled bands of KCl as a function of the lattice constant in atomic unit (equal to the Bohr radius $a_B = 0.529$Å) [After L.P. Howard, Phys. Rev. **109**, 1927 (1958)]. One can clearly see, how the atomic orbitals of the ions broaden to bands with decreasing distance between the ions.

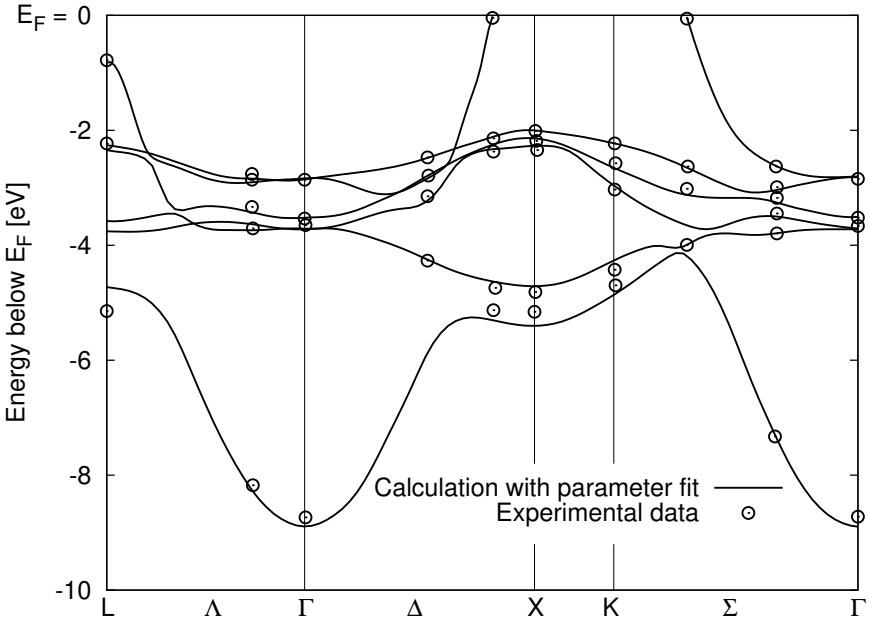

Figure 1.4: Band structure of copper with experimental data. [After R. Courths and S. Hüfner, Physics Reports **112**, 53 (1984)]

Thus the band is essentially of cosine shape, where the band width depends on the overlap B between next-neighbor wave functions.

An example is shown in Fig. 1.3 for Potassium chloride (KCl), where the narrow band can be well described by this approach. The outer shell of transition metals exhibits both s and d electrons. Here the wave function of the 3d-electrons does not reach out as far as the 4s-electrons (with approximately equal total energy), as a part of the total energy is contained in the angular momentum. Thus bands resulting from the d electrons have a much smaller band width compared to bands resulting from the s electrons, which have essentially the character of free electrons. Taking into account avoided crossings, this results in the band structure for copper (Cu) shown in Fig. 1.4.

The band structure of Si and GaAs as well as similar materials is dominated by the outer s and p shells of the constituents. This results in four occupied bands (valence bands) and four empty bands (conduction bands) with a gap of the order of 1 eV between. See Fig. 1.5.

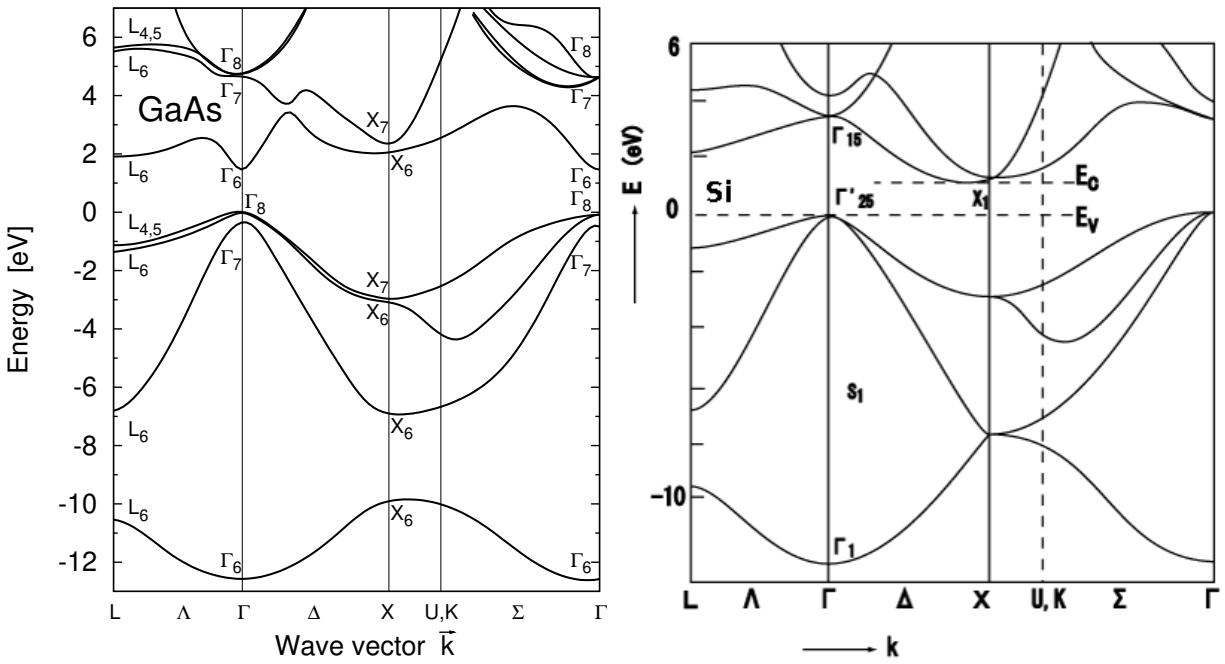

Figure 1.5: Band structure of GaAs [After J.R. Chelikowsky and M.L. Cohen, Phys. Rev B **14**,556 (1976)] and Si [from Wikipedia Commons, after J.R. Chelikowsky and M.L. Cohen, Phys. Rev B **10**,5095 (1974)]

1.3 Density of states and Fermi level

The density of states gives the number of states per volume and energy interval. From Eq. (1.8) we obtain

For a single band n the density of states is defined by

$$D_n(E) = \frac{1}{(2\pi)^3} \int_{1.\mathrm{Bz}} \mathrm{d}^3k \, \delta(E - E_n(\mathbf{k}))$$

The total density of states is then the sum over all bands.

The density of states is obviously zero in a band gap, where there are no states. On the other hand, it is particularly large, if the bands are flat as there are plenty of k-states within a small energy interval. Thus, copper has a large density of states in the energy range of $-4\mathrm{eV} < E < -2\mathrm{eV}$, see Fig. 1.4.

Bulk crystals cannot exhibit macroscopic space charges. Thus, the electron density n must equal the positive charge density of the ions. As double occupancy of levels is forbidden by the Pauli principle, the low lying energy levels with energies up to the *Fermi energy* E_F are occupied at zero temperature. If the Fermi energy E_F is within a band the crystal is a *metal* exhibiting a high electrical conductivity (see the next chapter). In contrast, if the Fermi energy is located in a band gap, we have a *semiconductor* (with moderate conductivity which is strongly increasing with temperature), or an *insulator* (with vanishingly small conductivity). This distinction is not well-defined; semiconductors have typically band gaps of the order of 1 eV, while the band gap is much larger for insulators.

1.3.1 Parabolic and isotropic bands

For a parabolic isotropic band (e.g. close to the Γ point, or in good approximation for metals) we have $E_n(\mathbf{k}) = E_n + \frac{\hbar^2\mathbf{k}^2}{2m_{\text{eff}}}$. Setting $E_k = \hbar^2k^2/(2m_{\text{eff}})$, we find the density of states

$$\begin{aligned} D_n^{\text{parabolic 3D}}(E) =& 2(\text{for spin}) \times \frac{1}{(2\pi)^3}\int_{1.\text{Bz}} \mathrm{d}^3k\, \delta\left(E - E_n - E_k\right) \\ =& \frac{1}{4\pi^3}\underbrace{\int_0^{2\pi}\mathrm{d}\varphi \int_0^{\pi}\mathrm{d}\vartheta\, \sin\theta}_{\to 4\pi} \underbrace{\int_0^{k_{max}}\mathrm{d}k\, k^2}_{\int_0^{E_{k\,max}}\mathrm{d}E_k \frac{m_{\text{eff}}\sqrt{2m_{\text{eff}}E_k}}{\hbar^3}} \delta\left(E - E_n - E_k\right) \\ =& \frac{m_{\text{eff}}\sqrt{2m_{\text{eff}}(E-E_n)}}{\pi^2\hbar^3}\Theta(E-E_n) \end{aligned} \tag{1.9}$$

Here $\Theta(x)$ is the Heaviside function with $\Theta(x) = 1$ for $x > 0$ and 0 for $x < 0$. In the same spirit we obtain

$$D_n^{\text{parabolic 2D}}(E) = 2(\text{for spin}) \times \frac{m_{\text{eff}}}{2\pi\hbar^2}\Theta(E-E_n) \tag{1.10}$$

in two dimensions [see Sec. 12.7 of Ibach and Lüth (2003) or Sec. 2.7.1 of Snoke (2008)].

If the states up to the Fermi energy are occupied, we find in the conventional three dimensional case the electron density

$$n_c = \int_{E_c}^{E_F}\mathrm{d}E D_n^{\text{parabolic 3D}}(E) = \frac{\left[2m_{\text{eff}}(E_F - E_c)\right]^{3/2}}{3\pi^2\hbar^3}\,. \tag{1.11}$$

This an be used to estimate the Fermi energy of metals. E.g., Aluminium has a nuclear charge of 5 protons and two electrons are tightly bound to the nucleus within the 1s shell. Thus charge neutrality requires 3 free electron per unit cell of volume 16.6 Å^3 (a forth of the cubic cell a^3 for the fcc lattice). Using the free electron mass, this provides

$$E_F - E_c = \frac{\hbar^2}{2m_e}\left(3\pi^2\frac{3}{16.6\text{Å}^3}\right)^{2/3} = 11.7\text{eV}$$

in good agreement with more detailed calculations displayed in Fig. 1.2.

1.3.2 General scheme to determine the Fermi level

For ionic crystals like KCl, it is good to start with the atomic orbitals of the isolated atoms/ions. Here the 3s and 3p states are entirely occupied both for the Cl^- and the K^+ ion. Combining these states to bands does not change the occupation. Thus, the resulting bands should all be occupied and the Fermi level is in the gap above the band dominated by the 3p states Cl^-, see Fig. 1.3.

A more general argument is the counting rule derived in Sec. 1.1.2. Here one first determines the number of electrons per unit cell required for the upper bands to achieve charge neutrality. Assuming spin degeneracy, this is twice the number of bands which need to be occupied. E.g., Aluminium requires 3 outer electrons per unit cell and thus 1.5 bands should be occupied in average. Indeed for any k-point, one or two bands lie below the Fermi energy in Fig. 1.2. The same argument applies for Cu, where 11 outer electrons per atom (in the 4s and 3d shell) require the occupation of 5.5 bands in average, see Fig. 1.4.

If there is more than one atom per unit cell, all charges have to be considered together. E.g. silicon crystallizes in the diamond lattice with two atoms per unit cell. As each Si atom has four electrons in the outer 3s/p shell, we need to populate 8 states per unit cell, i.e. 4 bands. Fig. 1.5 shows that these are just the four bands below the gap (all eight bands displayed result from the 3s/p levels), and the Fermi level is in the gap. The same argument holds for GaAs.

1.4 Properties of the band structure and Bloch functions

Most of the following properties are given without proof.[4]

1.4.1 Kramers degeneracy

As $\hat{H}$ is a hermitian operator and the eigenenergies are real, we find from $\hat{H}\Psi_{n,\mathbf{k}}(\mathbf{r}) = E_n(\mathbf{k})\Psi_{n,\mathbf{k}}(\mathbf{r})$ the relation

$$\hat{H}\Psi^*_{n,\mathbf{k}}(\mathbf{r}) = E_n(\mathbf{k})\Psi^*_{n,\mathbf{k}}(\mathbf{r})$$

Thus $\Psi^*_{n,\mathbf{k}}(\mathbf{r}) = \mathrm{e}^{-\mathrm{i}\mathbf{k}\cdot\mathbf{r}}u^*_{n,\mathbf{k}}(\mathbf{r}) \equiv \Psi_{n,-\mathbf{k}}(\mathbf{r})$ is an eigenfunction of the Hamilton-operator with Bloch vector $-\mathbf{k}$ and $E_n(-\mathbf{k}) = E_n(\mathbf{k})$.

The band structure satisfies the symmetry $E_n(-\mathbf{k}) = E_n(\mathbf{k})$.

If the band-structure depends on spin, the spin must be flipped as well.

1.4.2 Normalization

The lattice-periodic functions can be chosen such that

$$\int_{V_c} \mathrm{d}^3r\, u^*_{m,\mathbf{k}}(\mathbf{r})u_{n,\mathbf{k}}(\mathbf{r}) = V_c\delta_{m,n} \tag{1.12}$$

Furthermore they form a complete set of lattice periodic functions.

Then the Bloch functions can be normalized in two different ways:

- For infinite systems we have a continuous spectrum of $\mathbf{k}$ values and set

$$\varphi_{n,\mathbf{k}}(\mathbf{r}) = \frac{1}{(2\pi)^{3/2}}\mathrm{e}^{\mathrm{i}\mathbf{k}\cdot\mathbf{r}}u_{n,\mathbf{k}}(\mathbf{r}) \quad \Rightarrow \quad \int \mathrm{d}^3r\, \varphi^*_{m,\mathbf{k}'}(\mathbf{r})\varphi_{n,\mathbf{k}}(\mathbf{r}) = \delta_{m,n}\delta(\mathbf{k}-\mathbf{k}')$$

- For finite systems of volume V and Born-von Kármán boundary conditions we have a discrete set of $\mathbf{k}$ values and set

$$\varphi_{n,\mathbf{k}}(\mathbf{r}) = \frac{1}{\sqrt{V}}\mathrm{e}^{\mathrm{i}\mathbf{k}\cdot\mathbf{r}}u_{n,\mathbf{k}}(\mathbf{r}) \quad \Rightarrow \quad \int_V \mathrm{d}^3r\, \varphi^*_{m,\mathbf{k}'}(\mathbf{r})\varphi_{n,\mathbf{k}}(\mathbf{r}) = \delta_{m,n}\delta_{\mathbf{k},\mathbf{k}'}$$

1.4.3 Velocity and effective mass

The stationary Schrödinger equation for the electron in a crystal reads in spatial representation

$$\left(-\frac{\hbar^2}{2m_e}\Delta + V(\mathbf{r})\right)\Psi_{n,\mathbf{k}}(\mathbf{r}) = E_n(\mathbf{k})\Psi_{n,\mathbf{k}}(\mathbf{r})$$

[4] Details can be found in textbooks, such as Snoke (2008), Marder (2000), Czycholl (2004), or Kittel (1987).

Inserting the the Bloch functions $\Psi_{n,\mathbf{k}}(\mathbf{r}) = \mathrm{e}^{\mathrm{i}\mathbf{k}\cdot\mathbf{r}} u_{n\mathbf{k}}(\mathbf{r})$ can be expressed in terms of the lattice periodic functions $u_{n\mathbf{k}}(\mathbf{r})$ as

$$E_n(\mathbf{k}) u_{n\mathbf{k}}(\mathbf{r}) = \left(\frac{\hbar^2 k^2}{2m_e} + \frac{\hbar}{m_e}\mathbf{k}\cdot\frac{\hbar}{\mathrm{i}}\nabla - \frac{\hbar^2}{2m_e}\Delta + V(\mathbf{r}) \right) u_{n\mathbf{k}}(\mathbf{r})$$

Now we start with a solution $u_{n\mathbf{k}_0}(\mathbf{r})$ with energy $E_n(\mathbf{k}_0)$ and investigate small changes $\delta\mathbf{k}$:

$$\begin{aligned} E_n(\mathbf{k}_0+\delta\mathbf{k}) u_{n\mathbf{k}_0+\delta\mathbf{k}}(\mathbf{r}) =& \left(\hat{H}_0 + \frac{\hbar^2}{m_e}\mathbf{k}_0\cdot\delta\mathbf{k} + \frac{\hbar}{m_e}\delta\mathbf{k}\cdot\frac{\hbar}{\mathrm{i}}\nabla + \frac{\hbar^2}{2m_e}\delta\mathbf{k}^2 \right) u_{n\mathbf{k}_0+\delta\mathbf{k}}(\mathbf{r}) \\ \text{with } \hat{H}_0 =& \frac{\hbar^2 k_0^2}{2m_e} + \frac{\hbar}{m_e}\mathbf{k}_0\cdot\frac{\hbar}{\mathrm{i}}\nabla - \frac{\hbar^2}{2m_e}\Delta + V(\mathbf{r}) \end{aligned} \tag{1.13}$$

Using the Taylor expansion of $E_n(\mathbf{k})$, we can write

$$E_n(\mathbf{k}_0+\delta\mathbf{k}) = E_n(\mathbf{k}_0) + \frac{\partial E_n(\mathbf{k}_0)}{\partial\mathbf{k}}\cdot\delta\mathbf{k} + \sum_{i,j=x,y,z} \frac{\hbar^2}{2} \frac{1}{m_n(\mathbf{k}_0)}_{i,j} \delta k_i \delta k_j + \mathcal{O}(\delta k^3) \tag{1.14}$$

where we defined the

$$\textit{effective mass tensor} \quad \left(\frac{1}{m_n(\mathbf{k})}\right)_{i,j} = \frac{1}{\hbar^2}\frac{\partial^2 E_n(\mathbf{k})}{\partial k_i \partial k_j} \tag{1.15}$$

Now we want to relate the expansion coeficients in Eq. (1.14) to physical terms by considering Eq. (1.13) in the spirit of perturbation theory.

In first order perturbation theory, the change in energy is given by the expectation value of the perturbation $\propto \delta k$ with the unperturbed state:

$$\begin{aligned} E_n(\mathbf{k}_0+\delta\mathbf{k}) =& E_n(\mathbf{k}_0) + \frac{1}{V_c}\left\langle u_{n\mathbf{k}_0} \left| \frac{\hbar^2}{m_e}\mathbf{k}_0 + \frac{\hbar}{m_e}\frac{\hbar}{\mathrm{i}}\nabla \right| u_{n\mathbf{k}_0} \right\rangle \cdot\delta\mathbf{k} + \mathcal{O}(\delta k^2) \\ =& E_n(\mathbf{k}_0) + \frac{\hbar}{m_e}\mathbf{P}_{n,n}(\mathbf{k}_0)\cdot\delta\mathbf{k} + \mathcal{O}(\delta k^2) \end{aligned}$$

with the momentum matrix element

$$\mathbf{P}_{m,n}(\mathbf{k}) = \frac{\int_{V_c} \mathrm{d}^3 r\, \Psi^*_{m,\mathbf{k}}(\mathbf{r}) \frac{\hbar}{\mathrm{i}}\nabla \Psi_{n,\mathbf{k}}(\mathbf{r})}{\int_{V_c} \mathrm{d}^3 r\, |\Psi_{n,\mathbf{k}}(\mathbf{r})|^2}\,. \tag{1.16}$$

Comparing with Eq. (1.14) we can identify

$$\frac{\partial E_n(\mathbf{k})}{\partial\mathbf{k}} = \frac{\hbar}{m_e}\mathbf{P}_{n,n}$$

On the other hand, the quantum-mechanical current density of a Bloch electron is

$$\mathbf{J}(\mathbf{r}) = \frac{e}{m_e}\mathrm{Re}\left\{ \Psi^*_{n\mathbf{k}}(\mathbf{r}) \frac{\hbar}{\mathrm{i}}\nabla\Psi_{n\mathbf{k}}(\mathbf{r}) \right\}$$

and $\mathbf{P}_{n,n}(\mathbf{k})/m_e = \langle\mathbf{J}\rangle/e\langle n\rangle$ is just the average velocity in a unit cell. Thus we identify the

$$\textit{velocity of the Bloch state} \quad \mathbf{v}_n(\mathbf{k}) = \frac{1}{\hbar}\frac{\partial E_n(\mathbf{k})}{\partial\mathbf{k}} \tag{1.17}$$

The $\delta\mathbf{k}^2$ in Eq. (1.13) provides together with the second order perturbation theory for the terms $\propto \delta\mathbf{k}$

$$\left(\frac{1}{m_n(\mathbf{k})}\right)_{i,j} = \frac{1}{m_e}\delta_{i,j} + \frac{2}{m_e^2}\sum_{m(m\neq n)}\frac{P_{n,m;i}(\mathbf{k})P_{m,n;j}(\mathbf{k})}{E_n(\mathbf{k}) - E_m(\mathbf{k})}\,. \tag{1.18}$$

This shows that the effective mass deviates from the bare electron mass m_e due to the presence of neighboring bands. [5] We further see, that a small band gap of a semiconductor (e.g. InSb) is related to a small effective mass.

1.5 Envelope functions

1.5.1 The effective Hamiltonian

Now we want to investigate crystals with the lattice potential $V(\mathbf{r})$ and additional inhomogeneities, e.g. additional electro-magnetic fields with scalar potential $\phi(\mathbf{r},t)$ and vector potential $\mathbf{A}(\mathbf{r},t)$, which relate to the electric field $\mathbf{F}$ and the magnetic induction $\mathbf{B}$ via

$$\mathbf{F}(\mathbf{r},t) = -\nabla\phi(\mathbf{r},t) - \frac{\partial\mathbf{A}(\mathbf{r},t)}{\partial t} \qquad \mathbf{B}(\mathbf{r},t) = \nabla\times\mathbf{A}(\mathbf{r},t) \tag{1.19}$$

Then the single particle Schrödinger equation reads, see e.g. `http://www.teorfys.lu.se/staff/Andreas.Wacker/Scripts/quantMagnetField.pdf`

$$\mathrm{i}\hbar\frac{\partial}{\partial t}\Psi(\mathbf{r},t) = \left[\frac{(\hat{\mathbf{p}} + e\mathbf{A}(\mathbf{r},t))^2}{2m_e} + V(\mathbf{r}) - e\phi(\mathbf{r},t)\right]\Psi(\mathbf{r},t) \tag{1.20}$$

where $-e$ is the negative charge of the electron. For vanishing fields (i.e. $\mathbf{A}=0$ and $\phi=0$) Bloch's theorem provides the band structure $E_n(\mathbf{k})$ and the eigenstates $\Psi_{n\mathbf{k}}(\mathbf{r})$. As these eigenstates fopr a complete set of states, any wave functions $\Psi(\mathbf{r},t)$ can be expanded in terms of the Bloch functions. Now we assume that only the components of a single band with index n are of relevance, which is a good approximation if the energetical seperation between the bands is much larger than the terms in the Hamiltonian corresponding to the fields. Thus we can write

$$\Psi(\mathbf{r},t) = \int \mathrm{d}^3k\, c(\mathbf{k},t)\Psi_{n\mathbf{k}}(\mathbf{r}) \tag{1.21}$$

With the expansion coefficients $c(\mathbf{k},t)$ we can construct an *envelope function*[6]

$$f(\mathbf{r},t) = \int \mathrm{d}^3k\, c(\mathbf{k},t)\frac{1}{(2\pi)^{3/2}}e^{\mathrm{i}\mathbf{k}\cdot\mathbf{r}} \tag{1.22}$$

which does not contain the (strongly oscillating) lattice periodic functions $u_{n\mathbf{k}}(\mathbf{r})$. If $\mathbf{A}(\mathbf{r})$ and $\phi(\mathbf{r})$ are constant on the lattice scale (e.g. their Fourier components $A(q), \phi(q)$ are small unless $q \ll \mathbf{g}_i$) the envelope functions $f(\mathbf{r},t)$ satisfies the equation (to be motivated below)

$$\mathrm{i}\hbar\frac{\partial}{\partial t}f(\mathbf{r},t) = \left[E_n\left(-\mathrm{i}\nabla + \frac{e}{\hbar}\mathbf{A}(\mathbf{r},t)\right) - e\phi(\mathbf{r},t)\right]f(\mathbf{r},t) \tag{1.23}$$

where $[E_n\left(-\mathrm{i}\nabla - \frac{e}{\hbar}\mathbf{A}\right) + e\phi]$ is the *effective Hamiltonian*. Here one replaces the wavevector $\mathbf{k}$ in the dispersion relation $E_n(\mathbf{k})$ by an operator.

[5] This is used as a starting point for $\mathbf{k}\cdot\mathbf{p}$ theory, see, e.g., Chow and Koch (1999); Yu and Cardona (1999).

[6] This is the Wannier-Slater envelope function, see M.G. Burt, J. Phys.: Cond. Matter **11**, R53 (1999) for a wider class of envelope functions.

Close to an extremum in the band structure at $\mathbf{k}_0$ we find with Eq. (1.15)

$$\mathrm{i}\hbar\frac{\partial}{\partial t}f(\mathbf{r},t)=\left[E_n(\mathbf{k}_0)+\sum_{ij}\frac{1}{2}\left(\frac{\hbar}{\mathrm{i}}\frac{\partial}{\partial x_i}+eA_i\right)\left(\frac{1}{m_n(\mathbf{k}_0)}\right)_{i,j}\left(\frac{\hbar}{\mathrm{i}}\frac{\partial}{\partial x_j}+eA_j\right)-e\phi\right]f(\mathbf{r},t) \tag{1.24}$$

which is called *effective mass approximation*[7]. For crystals with high symmetry the mass tensor is diagonal for $\mathbf{k}_0$, and Eq. (1.24) has the form of a Schrödinger equation (1.20) with the electron mass replaced by the effective mass.

It is interesting to note, that Eq. (1.24) can also be derived for a slightly different envelope function $\tilde{f}_n(\mathbf{r},t)$, which is defined via the wave function as $\Psi(\mathbf{r},t)=\tilde{f}_n(\mathbf{r},t)u_{n\mathbf{k}_0}(\mathbf{r})$. Both definitions are equivalent close to the extremum of the band. The definition of Eqs. (1.21,1.22) has the advantage, that it holds in the entire band. On the other hand $\tilde{f}_n(\mathbf{r},t)$ allows for a multiband description, which is used in $\mathbf{k}\cdot\mathbf{p}$ theory.

1.5.2 Motivation of Eq. (1.23)*

Eq. (1.23) is difficult to proof.[8] Here we restrict us to $\mathbf{A}(\mathbf{r},t)=0$, i.e. without a magnetic field. For the electric potential we use the Fourier decomposition

$$\phi(\mathbf{r})=\int \mathrm{d}^3q\,\tilde{\phi}(\mathbf{q})e^{i\mathbf{q}\cdot\mathbf{r}}$$

and insert Eq. (1.21) into Eq. (1.20). Multiplying by $\Psi^*_{\mathbf{k}n}(\mathbf{r})$ and performing the integration $\int \mathrm{d}^3r$ provides us with the terms (omitting the band index):

$$\begin{aligned}\int \mathrm{d}^3r\,\Psi^*_{\mathbf{k}}(\mathbf{r})\mathrm{i}\hbar\int \mathrm{d}^3k'\,\dot{c}(\mathbf{k}',t)\Psi_{\mathbf{k}'}(\mathbf{r}) =&\mathrm{i}\hbar\dot{c}(\mathbf{k},t)\\ \int \mathrm{d}^3r\,\Psi^*_{\mathbf{k}}(\mathbf{r})\int \mathrm{d}^3k'\,c(\mathbf{k}',t)\left(\frac{p^2}{2m}+V(\mathbf{r})\right)\Psi_{\mathbf{k}'}(\mathbf{r}) =&E_n(\mathbf{k})c(\mathbf{k},t)\end{aligned}$$

Substituting $\mathbf{k}''=\mathbf{k}'+\mathbf{q}$ the potential part reads

$$\begin{aligned}&\int \mathrm{d}^3r\,\Psi^*_{\mathbf{k}}(\mathbf{r})(-e)\int \mathrm{d}^3q\,\tilde{\phi}(\mathbf{q})e^{i\mathbf{q}\cdot\mathbf{r}}\int \mathrm{d}^3k'\,c(\mathbf{k}',t)\frac{e^{i\mathbf{k}'\cdot\mathbf{r}}}{(2\pi)^{3/2}}u_{\mathbf{k}'}(\mathbf{r})\\ &\quad=\int \mathrm{d}^3r\,\Psi^*_{\mathbf{k}}(\mathbf{r})\int \mathrm{d}^3k''\frac{e^{i\mathbf{k}''\cdot\mathbf{r}}}{(2\pi)^{3/2}}u_{\mathbf{k}''-\mathbf{q}}(\mathbf{r})(-e)\int \mathrm{d}^3q\,\tilde{\phi}(\mathbf{q})c(\mathbf{k}''-\mathbf{q},t)\\ &\quad\overset{(u_{\mathbf{k}''-\mathbf{q}}\approx u_{\mathbf{k}''})\text{ for small }q}{\approx}(-e)\int \mathrm{d}^3q\,\tilde{\phi}(\mathbf{q})c(\mathbf{k}-\mathbf{q},t)\end{aligned}$$

Note that $u_{\mathbf{k}''-\mathbf{q}}\approx u_{\mathbf{k}''}$ requires an appropriate choice of phases, which is not always possible. Here the Berry phase becomes relevant. This provides us with

$$\mathrm{i}\hbar\dot{c}(\mathbf{k},t)\approx E_n(\mathbf{k})c(\mathbf{k},t)-e\int \mathrm{d}^3q\,\tilde{\phi}(\mathbf{q})c(\mathbf{k}-q,t) \tag{1.25}$$

[7] section 4.2.1 of Yu and Cardona (1999)

[8] See, e.g., the original article by Luttinger, Physical Review **84**, 814, (1951) using Wannier functions. A rigorous justification, as well as the range of validity is a subtle issue, see G. Nenciu, Reviews of Modern Physics **63**, 91 (1991).

Thus we find the following dynamics of the envelope function (1.22):

$$\begin{aligned} \mathrm{i}\hbar\frac{\partial}{\partial t}f(\mathbf{r},t) &= \int \mathrm{d}^3k\,\mathrm{i}\hbar\dot{c}(\mathbf{k},t)\frac{e^{\mathrm{i}\mathbf{k}\cdot\mathbf{r}}}{(2\pi)^{3/2}} \\ &\overset{(1.25)}{\approx} \int \mathrm{d}^3k\ \underbrace{E_n(\mathbf{k})}_{=E_n(-\mathrm{i}\nabla)}\ \frac{e^{\mathrm{i}\mathbf{k}\cdot\mathbf{r}}}{(2\pi)^{3/2}}c(\mathbf{k},t) - e\int \mathrm{d}^3k' \underbrace{\int \mathrm{d}^3q\,\tilde{\phi}(\mathbf{q})e^{\mathrm{i}\mathbf{q}\cdot\mathbf{r}}}_{=\phi(\mathbf{r})}\frac{e^{\mathrm{i}\mathbf{k}'\cdot\mathbf{r}}}{(2\pi)^{3/2}}c(\mathbf{k}',t) \end{aligned} \tag{1.26}$$

where we replaced $\mathbf{k}' = \mathbf{k} - \mathbf{q}$ in the last term. Thus Eq. (1.26) becomes Eq. (1.23).

1.5.3 Heterostructures

For semiconductor heterostructures, the band structure varies in space (more details can be found in section 12.7 of Ibach and Lüth (2003), e.g.). For several semiconductor materials like GaAs, InAs, or $Al_xGa_{1-x}As$ (for $x \lesssim 0.45$) the minimum of the conduction band is at the Γ-point and due to symmetry the effective mass equation (1.24) becomes

$$\mathrm{i}\hbar\frac{\partial}{\partial t}f_c(\mathbf{r},t) = \left[E_c(\mathbf{r}) - \nabla\frac{\hbar^2}{2m_c(\mathbf{r})}\nabla\right] f_c(\mathbf{r},t) \tag{1.27}$$

where we neglected external potentials here.[9] The derivatives are written in this peculiar way to guarantee the hermiticity of the effective Hamiltonian when the conduction band edge $E_c(\mathbf{r}) = E_{\text{conductionband}}(\mathbf{k}=0)$ and the effective mass $m_c(\mathbf{r})$ become spatially dependent.[10] At the interface located at $z = 0$ with material A at $z < 0$ and material B at $z > 0$ this implies the boundary connection rules

$$f_c(\vec{r})_{z\to 0^-} = f_c(\vec{r})_{z\to 0^+} \tag{1.28}$$

$$\frac{1}{m_c^A}\frac{\partial f_c(\vec{r})}{\partial z}_{z\to 0^-} = \frac{1}{m_c^B}\frac{\partial f_c(\vec{r})}{\partial z}_{z\to 0^+} \tag{1.29}$$

which allow for the study of the electron dynamics in the conduction band in semiconductor heterostructures. The valence band is more complicated as there are degenerate bands at $\mathbf{k} = 0$.[11]

As an example we consider a quantum well, i.e. a slap of material (e.g. GaAs) with thickness w embedded by regions of a different material with a higher energy E_c (e.g. $Al_{0.3}Ga_{0.7}As$)[12], see Fig. 1.6. For zero temperature and without impurities, charge neutrality implies that the valence bands of both materials are fully occupied and the conduction bands are empty. If additional electrons are provided (e.g. by doping) they will assemble in the region of lowest energy, i.e., in the range $0 < z < w$. If w is small with respect to the electron wavelength (typically several tens of nanometers at room temperature), quantization effects are important. They can be taken into account using Eq. (1.27). Here the conduction band edge $E_c(z)$ is

[9] A motivation is given in M.G. Burt, Phys. Rev. B **50**, 7518 (1994)

[10] This approach is due to D. J. Ben Daniel and C. B. Duke, Physical Review **152**, 683 (1966). While it is used by default, it is still under debate, see e.g. B. A. Foreman, Physical Review Letters **80**, 3823 (1998).

[11] Here $\mathbf{k}\cdot\mathbf{p}$ theory is used, see, e.g., chapters 5+6 of Chow and Koch (1999).

[12] Strictly speaking $Al_{0.3}Ga_{0.7}As$ is not a crystal but an alloy. However most physical properties, such as the bandstructure, can be well described by a weighted average of the GaAs and AlAs properties. A collection of relevant parameters can be found in I. Vurgaftman, J.R. Meyer, L.R. Ram-Mohan, J. Appl. Phys., **89**, 5815 (2001).

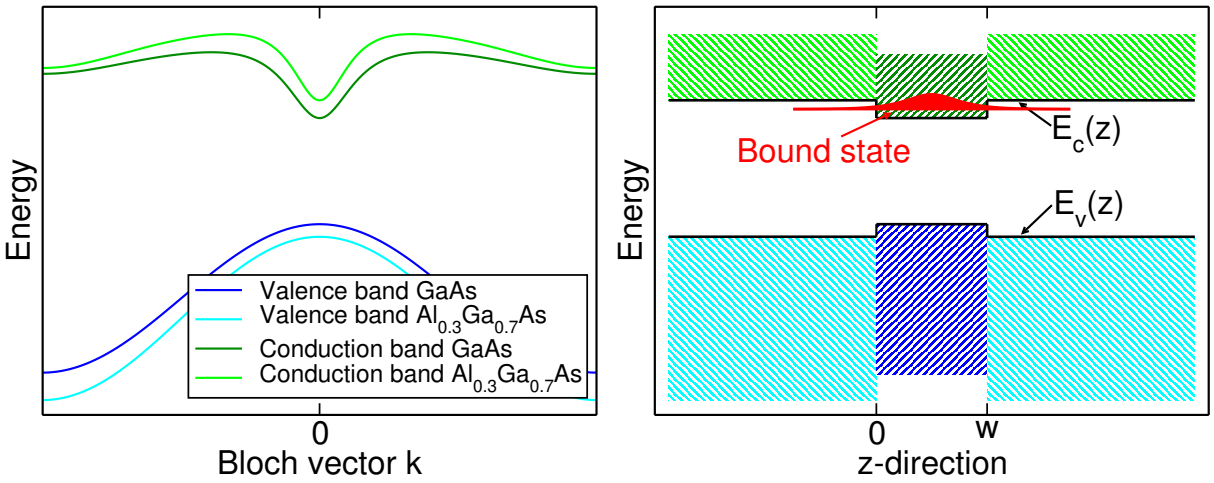

Figure 1.6: Band structure for two similar semiconductors and energy spectrum of a heterostructure together with a bound state in conduction band of the quantum well. Here the zero line for the wave function is put to the energy of the state, a common practice.

given by the upper black line in the right hand side of Fig. 1.6. As the system is translational invariant in x, y direction, the ansatz

$$f_c(\mathbf{r}) = \varphi_\nu(z)\mathrm{e}^{\mathrm{i}(k_x x + k_y y)} \tag{1.30}$$

is appropriate. For the z component we obtain the stationary Schrödinger equation for $k = 0$

$$E_\nu \varphi_\nu(z) = \left[-\frac{\partial}{\partial z}\frac{\hbar^2}{2m_c(z)}\frac{\partial}{\partial z} + E_c(z)\right]\varphi_\nu(z)$$

For $E_c(\mathrm{GaAs}) < E_\nu < E_c(\mathrm{Al_{0.3}Ga_{0.7}As})$ we obtain the solutions

$$\varphi_\nu(z) = \begin{cases} A\mathrm{e}^{\lambda z} & \text{for} \quad z < 0 \\ B\mathrm{e}^{\mathrm{i}qz} + C\mathrm{e}^{-\mathrm{i}qz} & \text{for} \quad 0 < z < w \\ D\mathrm{e}^{-\lambda z} & \text{for} \quad z > w \end{cases}$$

with $\lambda = \sqrt{2m_A(E_c(\mathrm{Al_{0.3}Ga_{0.7}As}) - E_\nu)}/\hbar$ and $q = \sqrt{2m_G(E_\nu - E_c(\mathrm{GaAs})}/\hbar$, where m_A and m_G are the effective masses at the Γ minimum of the conduction band of $\mathrm{Al_{0.3}Ga_{0.7}As}$ and GaAs, respectively. Now the boundary conditions (1.28,1.29) provide two equations at each interface, which can be subsumed in the matrix equation:

$$\underline{\underline{M}}(E_\nu)\begin{pmatrix} A \\ B \\ C \\ D \end{pmatrix} = 0 \quad \text{with} \quad \underline{\underline{M}}(E_\nu) = \begin{pmatrix} 1 & -1 & -1 & 0 \\ \lambda/m_A & -\mathrm{i}q/m_G & \mathrm{i}q/m_G & 0 \\ 0 & \mathrm{e}^{\mathrm{i}qw} & \mathrm{e}^{-\mathrm{i}qw} & -\mathrm{e}^{\lambda w} \\ 0 & \mathrm{i}q\mathrm{e}^{\mathrm{i}qw}/m_G & -\mathrm{i}q\mathrm{e}^{-\mathrm{i}qw}/m_G & \lambda\mathrm{e}^{\lambda w}/m_A \end{pmatrix}$$

where the E_ν-dependence arises by q and λ. The existence of nontrivial solutions requires $\det\underline{\underline{M}}(E_\nu) = 0$, which provides an equation to determine one or several discrete values E_ν. From the corresponding eigenstates $(A_\nu, B_\nu, C_\nu, D_\nu)^{\mathrm{tr}}$ the eigenfunctions $\varphi_\nu(z)$ can be directly constructed. An example is shown in red in Fig. (1.6). For finite k, we may use first order perturbation theory[13] and find the total energy of the state (1.30)

$$E_\nu(k_x, k_y) = E_\nu + \frac{\hbar^2(k_x^2 + k_y^2)}{2m_\nu} \quad \text{with} \quad \frac{1}{m_\nu} = \int \mathrm{d}z \frac{|\varphi_\nu(z)|^2}{m_c(z)}$$

This implies a parabolic dispersion in k in addition to the quantized energy E_ν, which is referred to as a subband.

[13] A correct solution would require to solve a different z-equation for each k_x, k_y, which seems however rarely be done in practice.

Chapter 2

Transport

2.1 Semiclassical equation of motion

Ehrenfest's theorem tells us that the classical limit of the quantum evolution is given by the equations of motion[1]

$$\dot{\mathbf{r}} = \frac{\partial H(\mathbf{r},\mathbf{p})}{\partial \mathbf{p}} \quad \text{and} \quad \dot{\mathbf{p}} = -\frac{\partial H(\mathbf{r},\mathbf{p})}{\partial \mathbf{r}}$$

where the classic canonical momentum $\mathbf{p}$ replaces $(\hbar/\mathrm{i})\nabla$ in the quantum mechanical Hamiltonian. From the effective Hamiltonian (1.23) we find with $\mathbf{k} = (\mathbf{p} + e\mathbf{A}(\mathbf{r},t))/\hbar$: (In the following $\downarrow$ indicates the quantity on which $\nabla = \partial/\partial\mathbf{r}$ operates in a product)

$$\begin{aligned}
\dot{\mathbf{r}} =& \frac{1}{\hbar}\frac{\partial E_n(\mathbf{k})}{\partial \mathbf{k}} = \mathbf{v}_n(\mathbf{k}) \\
\dot{\mathbf{p}} =& -e\underbrace{\frac{1}{\hbar}\nabla\left[\frac{\partial E_n(\mathbf{k})}{\partial \mathbf{k}}\cdot\overset{\downarrow}{\mathbf{A}}(\mathbf{r},t)\right]}_{\mathbf{v}_n(\mathbf{k})\times[\nabla\times\overset{\downarrow}{\mathbf{A}}]+\overset{\downarrow}{\mathbf{A}}(\mathbf{v}_n(\mathbf{k})\cdot\nabla)} + e\nabla\phi(\mathbf{r},t) \\
=& -e\mathbf{v}_n(\mathbf{k})\times\mathbf{B}(\mathbf{r},t) - e\mathbf{F}(\mathbf{r},t) - e\underbrace{\left[(\dot{\mathbf{r}}\cdot\nabla)\overset{\downarrow}{\mathbf{A}}(\mathbf{r},t) + \frac{\partial \mathbf{A}(\mathbf{r},t)}{\partial t}\right]}_{=\frac{\mathrm{d}\mathbf{A}(\mathbf{r},t)}{\mathrm{d}t}}
\end{aligned}$$

where the definitions of the electromagnetic potentials (1.19) are used. This provides the

semiclassical equation of motion

$$\dot{\mathbf{r}} = \mathbf{v}_n(\mathbf{k}) \tag{2.1}$$

$$\hbar\dot{\mathbf{k}} = -e\mathbf{v}_n(\mathbf{k})\times\mathbf{B}(\mathbf{r},t) - e\mathbf{F}(\mathbf{r},t) \tag{2.2}$$

for electrons in a band n.

Thus $\hbar\mathbf{k}$ follows the same acceleration law as the kinetic momentum $m\mathbf{v}$ of a classical particle. Accordingly, $\hbar\mathbf{k}$ is frequently referred to as crystal momentum. Such a classical description in terms of position and momentum is only valid on length scales larger than the wavelength of the electronic states. In a semiconductor with a parabolic band, we find $k = \sqrt{2m_{\mathrm{eff}}E(k)/\hbar^2} \approx 2\pi/25$ nm for an energy $E(k) \approx 25$ meV at room temperature and an effective mass of $m_{\mathrm{eff}} \approx 0.1m_e$. Thus the semiclassical model makes sense on the micron scale, but fails on the nanometer

[1] We follow Luttinger, Physical Review **84**, 814, (1951)

scale. Even if the treatment looks classical, the velocity $\mathbf{v}_n(k)$ contains the information of the energy bands, which is reflected by the term *semiclassical*.

One has to be aware, that the single-particle Bloch states considered here are an approximation where the interactions between the electrons are treated by an effective potential. This approximation has a certain justification for single-particle excitations from the ground sate of the interacting system. The properties of these excitations may however differ quite significantly from individual particles (e.g., their magnetic g-factor can differ essentially from $g \approx 2$ for individual electrons[2]) and thus one refers to them as *quasi-particles*. An important property is the acceleration in electric fields. Here the inertia of the quasiparticle is given by the direction-dependent effective mass tensor (1.15), as shown in the exercises.

2.2 General aspects of electron transport

Summing over all quasi-particles and performing the continuum limit, the current density is given by (see e.g., 9.2 of Ibach and Lüth (2003))

$$\mathbf{J} = \frac{2(\text{for spin})(-e)}{V} \sum_{n,\mathbf{k}} \mathbf{v}_n(\mathbf{k}) f_n(\mathbf{k}) = \frac{-2e}{(2\pi)^3} \sum_n \int_{1.\text{Bz}} \mathrm{d}^3k\, \mathbf{v}_n(\mathbf{k}) f_n(\mathbf{k}) \tag{2.3}$$

where $0 \le f_n(\mathbf{k}) \le 1$ is the occupation probability of the Bloch state $n\mathbf{k}$.

In thermal equilibrium the occupation probability is given by the *Fermi distribution*

$$f_n(\mathbf{k}) = \frac{1}{\exp\left(\frac{E_n(\mathbf{k})-\mu_{\text{int}}}{k_B T}\right)+1} = f_{\text{Fermi}}(E_n(\mathbf{k}))$$

where μ_{int} is the internal chemical potential[3]. Thus the current (2.3) vanishes due to Kramer's degeneracy. Therefore we only find an electric current, if the carriers change their crystal momentum due to acceleration by an electric field. For small fields the current is linear in the field strength $\mathbf{F}$, which is described by the *conductivity tensor* σ_{ij}

$$\mathbf{J} = \underline{\underline{\sigma}}\mathbf{F}$$

As the electric field (2.2) does not change the band index for weak fields, bands do not contribute to the current if they are either entirely occupied or entirely empty. Thus, we find:

Only partially occupied bands close to the Fermi energy contribute to the transport.

For metals, (e.g., Al in Fig. 1.2) the Fermi energy cuts through the energy bands, which are partially occupied and this provides a high conductivity. In contrast, semiconductors and insulators (e.g., Si and GaAs in Fig. 1.5) have an energy gap between the valence band and the conduction band. For an ideal crystal at zero temperature, the valence band is entirely occupied and the conduction band is entirely empty. Thus the conductivity is zero in this case. For semiconductors it is relatively easy to add electrons into the conduction band (by doping, heating, irradiation, or electrostatic induction), which allows to modify the conductivity in a wide range.

[2] E.g., $g \approx -0.4$ for conduction band electrons in GaAs, M. Oestreich and W.W. Rühle, Phys. Rev. Lett. **74**, 2315 (1995).

[3] I follow the notation of Kittel and Krömer (1980). μ_{int} can be understood as the chemical potential relative to a fixed point in the band structure. For given band structure μ_{int} is a function of temperature and electron density, but does not depend on the absolute electric potential.

In the same way one may remove electrons from the valence band (index v) of a semiconductor, which increases the conductivity as well. Now the excitation is a missing electron, and the corresponding quasi-particle is called a *hole*. The properties of holes (index h) can be extracted from the valence band $E_v(\mathbf{k})$ as follows [see Sec. 8 of Kittel (1996)]:

$$\begin{array}{cccc} q_h = e & \mathbf{k}_h = -\mathbf{k} & E_h(\mathbf{k}_h) = -E_v(\mathbf{k}) & \mu_{\text{int}}^{(h)} = -\mu_{\text{int}} \\ \mathbf{v}_h(\mathbf{k}_h) = \mathbf{v}_v(\mathbf{k}) & m_h(\mathbf{k}_h) = -m_v(\mathbf{k}) & f_h(\mathbf{k}_h) = 1 - f(\mathbf{k}) & \end{array} \tag{2.4}$$

and inserting into Eq. (2.3) provides the current

$$\mathbf{J} = \frac{2(\text{for spin})q_h}{(2\pi)^3} \int_{1.\text{Bz}} \mathrm{d}^3 k_h \, \mathbf{v}_h(\mathbf{k}_h) f_h(\mathbf{k})$$

while the acceleration law (2.2) becomes $\hbar \dot{\mathbf{k}}_h = q_h \mathbf{v}_h(\mathbf{k}_h) \times \mathbf{B}(\mathbf{r}, t) + q_h \mathbf{F}(\mathbf{r}, t)$. Note, that the hole mass m_h is positive at the maximum of the valence band, where the curvature is negative.

Taking a closer look at the acceleration law (2.2), we find that the Bloch vector $\mathbf{k}$ is continuously increasing in a constant electric field. If it reaches the boundary of the Brillouin zone (i.e. gets closer to a certain reciprocal lattice vector $\mathbf{G}_n$ than to the origin), it continues at the equivalent point $\mathbf{k} - \mathbf{G}_n$. In this way $\mathbf{k}$ performs a periodic motion through the Brillouin zone with zero average velocity.[4] This is, however, not the generic situation. Typically, scattering processes restore the equilibrium situation on a picosecond time scale. In a simplified description the average velocity $\mathbf{v}$ of the quasi-particle satisfies

$$\frac{\mathrm{d}\mathbf{v}}{\mathrm{d}t} = \frac{q\mathbf{F}}{m_{\text{eff}}} - \frac{\mathbf{v}}{\tau_m}$$

where τ_m is an average scattering time, m_{eff} the average effective mass, and $q = \pm e$ the charge of the relevant quasiparticles. The stationary solution for a constant electric field provides

$$\mathbf{v} = \text{sign}\{q\} \tilde{\mu} \mathbf{F} \quad \text{with the } \textit{mobility} \quad \tilde{\mu} = \frac{e\tau_m}{m_{\text{eff}}} \tag{2.5}$$

and the conductivity becomes $\sigma = e n_{QP} \tilde{\mu}_e$, where n_{QP} is the density of quasi-particles. In Sec. 2.4.1 a more detailed derivation will be given.

The key point is that electric conductivity is an interplay between acceleration of quasi-particles by an electric field and scattering events. While we defined the acceleration in Sec. 2.1, on the basis of the Bloch states of a perfect crystal, scattering is related to the deviations from ideality. In practice, no material is perfectly periodic due to the presence of impurities, lattice vacancies, lattice vibrations, etc. Their contribution can be considered as a perturbation potential to the crystal Hamiltonian studied so far. In the spirit of Fermi's golden rule, this provides transition rates between the Bloch states with different $\mathbf{k}$, as the Bloch vector is not a good quantum number of the total Hamiltonian any longer. Such transitions are generally referred to as scattering processes.

2.3 Phonon scattering

Similar to the electron Bloch states, the lattice vibrations of a crystal can be characterized by a wave vector $\mathbf{q}$ and the mode (e.g. acoustic/optical or longitudinal/transverse), described by

[4] This is called Bloch oscillation and can actually be observed in superlattices, C. Waschke et al., Phys. Rev. Lett. **70**, 3319 (1993), and systems of cold atoms, H Keßler et al., New J. Phys. **18**, 102001 (2016)

an index j. The corresponding angular frequency is $\omega_j(\mathbf{q})$. Like any harmonic oscillation the energy of the lattice vibrations is quantized in portions $\hbar\omega_j(\mathbf{q})$, which are called *phonons*. Using the standard raising ($b_j^\dagger$) and lowering (b_j) operators (see, e.g., `www.teorfys.lu.se/staff/Andreas.Wacker/Scripts/oscilquant.pdf`), the Hamiltonian for the lattice vibrations reads

$$\hat{H}_{\rm phon} = \sum_{j,\mathbf{q}} \hbar\omega_j(\mathbf{q}) \left[b_j^\dagger(\mathbf{q}) b_j(\mathbf{q}) + \frac{1}{2} \right] \tag{2.6}$$

The eigenvalues of the number operator $b_j^\dagger(\mathbf{q})b_j(\mathbf{q})$ are the integer phonon occupation numbers $n_j(\mathbf{q}) \geq 0$.

In thermal equilibrium the expectation value of the phonon occupations is given by the *Bose distribution*.

$$\langle n_j(\mathbf{q})\rangle = \frac{1}{{\rm e}^{\hbar\omega_j(\mathbf{q})/k_BT} - 1} = f_{\rm Bose}(\hbar\omega_j(\mathbf{q})) \tag{2.7}$$

The elongation of the ions follows

$$s(\mathbf{R},t) \propto {\rm e}^{{\rm i}\mathbf{q}\cdot\mathbf{R}} \left(b_j(\mathbf{q}){\rm e}^{-{\rm i}\omega_j(\mathbf{q})t} + b_j^\dagger(-\mathbf{q}){\rm e}^{{\rm i}\omega_j(\mathbf{q})t} \right)$$

where the use of $(-\mathbf{q})$ in the raising operator guarantees that the operator is hermitian. See subsection 2.5.1 for details.

These lattice oscillations couple to the electronic states due to different mechanisms, such as the deformation potential (subsection 2.5.2) or the lattice polarization for optical phonons in polar crystals (subsection 2.5.3). The essence is that lattice vibrations distort the crystal periodicity and constitute the perturbation potential

$$V(\mathbf{r},t) = \sum_{\mathbf{q}j} U^{(\mathbf{q},j)}(\mathbf{r}){\rm e}^{{\rm i}\mathbf{q}\cdot\mathbf{r}} \left[b_j(\mathbf{q}){\rm e}^{-{\rm i}\omega_j(\mathbf{q})t} + b_j^\dagger(-\mathbf{q}){\rm e}^{{\rm i}\omega_j(\mathbf{q})t} \right] \tag{2.8}$$

Here $U^{(\mathbf{q}j)}(\mathbf{r}+\mathbf{R}) = U^{(\mathbf{q}j)}(\mathbf{r})$ is a lattice periodic function, describing the local details of the microscopic interaction mechanism[5] In order to provide a Hermitian operator, $\left[U^{(\mathbf{q},j)}(\mathbf{r})\right]^* = U^{(-\mathbf{q},j)}(\mathbf{r})$ holds.

2.3.1 Scattering Probability

Fermi's golden rule (see, e.g., `www.teorfys.lu.se/staff/Andreas.Wacker/Scripts/fermiGR.pdf`) gives us the *transition probability per time*[6] between Bloch states $\Psi_{n,\mathbf{k}}$ and $\Psi_{n',\mathbf{k}'}$.

$$\begin{aligned} W_{n\mathbf{k}\to n'\mathbf{k}'} = {} & \frac{2\pi}{\hbar} \sum_{\mathbf{q}j} \\ & \times \Big[\underbrace{\left|\langle \Psi_{n',\mathbf{k}'}, n_j(\mathbf{q})-1 | U_{\mathbf{q}j}(\mathbf{r}){\rm e}^{{\rm i}\mathbf{q}\cdot\mathbf{r}} \hat{b}_j(\mathbf{q}) | \Psi_{n,\mathbf{k}}, n_j(\mathbf{q})\rangle\right|^2 \delta\left(E_{n'}(\mathbf{k}') - E_n(\mathbf{k}) - \hbar\omega_j(\mathbf{q})\right)}_{\text{Phonon absorption}} \\ & + \underbrace{\left|\langle \Psi_{n',\mathbf{k}'}, n_j(-\mathbf{q})+1 | U_{\mathbf{q}j}(\mathbf{r}){\rm e}^{{\rm i}\mathbf{q}\cdot\mathbf{r}} \hat{b}_j^\dagger(-\mathbf{q}) | \Psi_{n,\mathbf{k}}, n_j(-\mathbf{q})\rangle\right|^2 \delta\left(E_{n'}(\mathbf{k}') - E_n(\mathbf{k}) + \hbar\omega_j(\mathbf{q})\right)}_{\text{Phonon emission}} \Big] \end{aligned} \tag{2.9}$$

[5] $U_{\mathbf{q}j}(\mathbf{r})$ is constant for the deformation potential of acoustic phonons. It has a spatial dependence for scattering at polar phonons, which is however neglected in the averaging procedure applied in Sec. 2.5.3.

[6] sometimes called *scattering probability*, which is unfortunate as this suggests a dimensionless quantity.

Here the presence of the phonon lowering and raising operators requires that the occupation $n_j(\mathbf{q})$ of the phonon mode involved in the transition must change together with the electron state. This is indicated by combining the phonon occupation with the electron state. We find, that the first term relates to absorption of a phonon by the electron from the phonon mode $(\mathbf{q}, j)$, while the second relates to phonon emission into the mode $(-\mathbf{q}, j)$. Concomitantly, the δ-function tells us, that the energy of the final state $E_{n'}(\mathbf{k}')$ is enlarged/decreased by $\hbar\omega_j(\mathbf{q})$ compared to $E_n(\mathbf{k})$. Let us now analyze the matrix elements:

From quantum mechanics we know $\hat{b}_j(\mathbf{q})|n_j(\mathbf{q})\rangle = \sqrt{n_j(\mathbf{q})}|n_j(\mathbf{q})-1\rangle$ and $\hat{b}_j^\dagger(\mathbf{q})|n_j(\mathbf{q})\rangle = \sqrt{n_j(\mathbf{q})+1}|n_j(\mathbf{q})+1\rangle$. Therefore the phonon part gives us a pre-factor $n_j(\mathbf{q})$ in the absorption $[n_j(-\mathbf{q})+1]$ in the emission term. This shows that phonon absorption vanishes for $T \to 0$ when the phonons are not excited, while there is always a finite probability for phonon emission.

The spatial part can be treated as follows for a general function $F(\hat{\mathbf{p}}, \hat{\mathbf{r}})$, which is lattice-periodic in $\mathbf{r}$.

$$\begin{aligned}\langle\Psi_{n',\mathbf{k}'}|F(\hat{\mathbf{p}},\hat{\mathbf{r}})\mathrm{e}^{\mathrm{i}\mathbf{q}\cdot\mathbf{r}}|\Psi_{n,\mathbf{k}}\rangle &= \frac{1}{V}\int_V \mathrm{d}^3r\,\mathrm{e}^{-\mathrm{i}\mathbf{k}'\cdot\mathbf{r}}u^*_{n'\mathbf{k}'}(\mathbf{r})F(\hat{\mathbf{p}},\hat{\mathbf{r}})\mathrm{e}^{\mathrm{i}\mathbf{q}\cdot\mathbf{r}}\mathrm{e}^{\mathrm{i}\mathbf{k}\cdot\mathbf{r}}u_{n\mathbf{k}}(\mathbf{r}) \\ &= \underbrace{\frac{1}{N_c}\sum_{\mathbf{R}}\mathrm{e}^{\mathrm{i}(\mathbf{q}+\mathbf{k}-\mathbf{k}')\cdot\mathbf{R}}}_{\sum_{\mathbf{G}}\delta_{\mathbf{q}+\mathbf{k}-\mathbf{k}',\mathbf{G}}}\underbrace{\frac{1}{V_c}\int_{V_c}\mathrm{d}^3\tilde{r}\,\mathrm{e}^{-\mathrm{i}\mathbf{k}'\cdot\tilde{\mathbf{r}}}u_{n'\mathbf{k}'}(\tilde{\mathbf{r}})F(\hat{\mathbf{p}},\hat{\mathbf{r}})u_{n\mathbf{k}}(\tilde{\mathbf{r}})\mathrm{e}^{\mathrm{i}(\mathbf{q}+\mathbf{k})\cdot\tilde{\mathbf{r}}}}_{=F_{n'\mathbf{k}',n\mathbf{k}}} \qquad (2.10)\end{aligned}$$

where we used the decomposition $\mathbf{r} = \mathbf{R} + \tilde{\mathbf{r}}$, where $\tilde{\mathbf{r}}$ is within the unit cell V_c. Together we find the

Electron-phonon transition probability per time

$$\begin{aligned}W_{n\mathbf{k}\to n'\mathbf{k}'} = \frac{2\pi}{\hbar}\sum_{\mathbf{q}j}\sum_{\mathbf{G}}\delta_{\mathbf{k}',\mathbf{q}+\mathbf{k}+\mathbf{G}}|U^{(\mathbf{q},j)}_{n'\mathbf{k}',n\mathbf{k}}|^2\Big[&n_j(\mathbf{q})\delta\left(E_{n'}(\mathbf{k}')-E_n(\mathbf{k})-\hbar\omega_j(\mathbf{q})\right) \\ &+(n_j(-\mathbf{q})+1)\delta\left(E_{n'}(\mathbf{k}')-E_n(\mathbf{k})+\hbar\omega_j(-\mathbf{q})\right)\Big] \qquad (2.11)\end{aligned}$$

Here processes employing a finite vector $\mathbf{G}$ of the reciprocal lattice are called Umklapp processes (from the German word for flip), while normal processes restrict to $\mathbf{G} = 0$. As $\mathbf{k}' - \mathbf{k}$ can be uniquely decomposed into a vector $-\mathbf{G}$ of the reciprocal lattice and a vector $\mathbf{q}$ within the Brillouin zone, one finds that Umklapp processes allow for transitions with a rather large momentum transfer $\mathbf{k}'-\mathbf{k}$. On the other hand only normal process are of relevance if the physical processes are limited to a small region of the Brillouin zone, such as a single energy minimum in a semiconductor. Frequently, Umklapp processes are entirely neglected for simplicity.

2.3.2 Thermalization

Consider two states $1 = (n_1\mathbf{k}_1)$ and $2 = (n_2\mathbf{k}_2)$ with occupations f_1, f_2 and energies $E_2 = E_1 + \Delta E$ where $\Delta E = \hbar\omega_\alpha(\mathbf{k}_2-\mathbf{k}_1) > 0$ matches a photon energy with wavevector $\mathbf{q}_0 = \mathbf{k}_2-\mathbf{k}_1$. Then the net transition rate from 1 to 2 is given by

$$\begin{aligned}&f_1(1-f_2)W_{1\to2} - f_2(1-f_1)W_{2\to1} \\ &\quad= f_1(1-f_2)\frac{2\pi}{\hbar}\sum_{\mathbf{q}j}\sum_{\mathbf{G}}\delta_{\mathbf{k}_2,\mathbf{q}+\mathbf{k}_1-\mathbf{G}}|U^{(\mathbf{q},j)}_{n_2\mathbf{k}_2,n_1\mathbf{k}_1}|^2\langle n_j(\mathbf{q})\rangle\delta\left(\Delta E-\hbar\omega_j(\mathbf{q})\right) \\ &\quad- f_2(1-f_1)\frac{2\pi}{\hbar}\sum_{\mathbf{q}j}\sum_{\mathbf{G}}\delta_{\mathbf{k}_1,\mathbf{q}+\mathbf{k}_2-\mathbf{G}}|U^{(\mathbf{q},j)}_{n_1\mathbf{k}_1,n_2\mathbf{k}_2}|^2[\langle n_j(-\mathbf{q})\rangle+1]\delta\left(-\Delta E+\hbar\omega_j(-\mathbf{q})\right)\end{aligned}$$

where Pauli blocking has been taken into account by the $(1-f_i)$ terms. Now the $\delta_{\mathbf{k}',\mathbf{k}}$ picks $\mathbf{q}=\mathbf{q}_0$ in the first line and $\mathbf{q}=-\mathbf{q}_0$ in the second line. Furthermore, only the phonon mode $j=\alpha$ remains due to energy conservation. As $(U^{(\mathbf{q},\alpha)}_{n_2\mathbf{k}_2,n_1\mathbf{k}_1})^* = U^{(-\mathbf{q},\alpha)}_{n_1\mathbf{k}_1,n_2\mathbf{k}_2}$ the squares of the matrix elements are identical. Assuming that the phonon system is in thermal equilibrium with the lattice temperature T, $\langle n_j(\mathbf{q}_0)\rangle$ is given by the Bose distribution (2.7) and we find

$$\begin{aligned} f_1(1-f_2)W_{1\to 2} - f_2(1-f_1)W_{2\to 1} &\propto f_1(1-f_2)\frac{1}{\mathrm{e}^{\Delta E/k_BT}-1} - f_2(1-f_1)\left(\frac{1}{\mathrm{e}^{\Delta E/k_BT}-1}+1\right) \\ &= \frac{(1-f_2)(1-f_1)}{\mathrm{e}^{\Delta E/k_BT}-1}\left(\frac{f_1}{1-f_1}-\frac{f_2}{1-f_2}\mathrm{e}^{\Delta E/k_BT}\right) \end{aligned}$$

This net transition vanishes if $\frac{f_i}{1-f_i} = A\mathrm{e}^{-E_i/k_BT}$. Relating the proportionality constant A to the chemical potential μ_{int} via $A=\mathrm{e}^{\mu_{\mathrm{int}}/k_BT}$, we obtain $f_i = f_{\mathrm{Fermi}}(E_i)$. Thus the net transition rate vanishes if the electron system is in thermal equilibrium with the temperature of the phonon bath.

Phonon scattering establishes the thermal equilibrium in the electron distribution.

2.4 Boltzmann Equation

In the following we restrict us to a single band and omit the band index n. We define the distribution function $f(\mathbf{r},\mathbf{k},t)$ by $f(\mathbf{r},\mathbf{k},t)\mathrm{d}^3r\mathrm{d}^3k/(2\pi)^3$ to be the probability to find an electron in the volume d^3r around $\mathbf{r}$ and d^3k around $\mathbf{k}$. If $f(\mathbf{r},\mathbf{k},t)$ is only varying on large scales $\Delta r\Delta k \gg 1$ its temporal evolution is based on the semiclassical motion (2.1,2.2) leading to the

Boltzmann equation

$$\frac{\partial}{\partial t}f(\mathbf{r},\mathbf{k},t) + \mathbf{v}(\mathbf{k})\frac{\partial}{\partial \mathbf{r}}f(\mathbf{r},\mathbf{k},t) + \frac{(-e)}{\hbar}(\mathbf{F}+\mathbf{v}(\mathbf{k})\times\mathbf{B})\frac{\partial}{\partial \mathbf{k}}f(\mathbf{r},\mathbf{k},t) = \left(\frac{\partial f}{\partial t}\right)_{\mathrm{scattering}} \tag{2.12}$$

Read section 5.9 of Snoke (2008) or sections 9.4+5 of Ibach and Lüth (2003) for detailed information. The scattering term has the form

$$\left(\frac{\partial f(\mathbf{r},\mathbf{k},t)}{\partial t}\right)_{\mathrm{scattering}} = \sum_{\mathbf{k}'} W_{\mathbf{k}'\to\mathbf{k}} f(\mathbf{r},\mathbf{k}',t)[1-f(\mathbf{r},\mathbf{k},t)] - W_{\mathbf{k}\to\mathbf{k}'} f(\mathbf{r},\mathbf{k},t)[1-f(\mathbf{r},\mathbf{k}',t)]$$

for phonon (or impurity) scattering. Note that the scattering term is local in time and space. An overview on different scattering mechanisms can be found in chapter 5 of Snoke (2008) or section 9.3 of Ibach and Lüth (2003).

In section (2.3.2) it was discussed that on the long run scattering processes restore thermal equilibrium. This suggests the *relaxation time approximation*

$$\left(\frac{\partial f}{\partial t}\right)_{\mathrm{scattering}} = \frac{-\delta f(\mathbf{r},\mathbf{k},t)}{\tau_m(\mathbf{k})} \quad \text{with} \quad \delta f(\mathbf{r},\mathbf{k},t) = f(\mathbf{r},\mathbf{k},t) - f_{\mathrm{Fermi}}(E(\mathbf{k}))$$

where the variety of complicated scattering processes is subsumed in a scattering time $\tau_m(\mathbf{k})$, which is typically somewhat shorter than a picosecond[7].

[7] The time introduced here is actually the momentum scattering time, which is larger than the total scattering time, as forward scattering is less effective.

2.4.1 Electrical conductivity

Now we want to consider the current caused by a weak electric field $\mathbf{F}$ (and vanishing magnetic field). As the distribution function becomes thermal for zero field, we may write $f(\mathbf{r},\mathbf{k},t) = f_{\text{Fermi}}(E(\mathbf{k})) + \mathcal{O}(F)$. In *linear response* (i.e., only terms linear in F are considered) only the zeroth order of $\frac{\partial}{\partial \mathbf{k}} f(\mathbf{r},\mathbf{k},t)$ enters, as this term is multiplied by $\mathbf{F}$ in the Boltzmann equation (2.12). Specifically, we use

$$\frac{\partial}{\partial \mathbf{k}} f(\mathbf{r},\mathbf{k},t) \approx \frac{\partial}{\partial \mathbf{k}} f_{\text{Fermi}}(E(\mathbf{k})) = \frac{\mathrm{d}f_{\text{Fermi}}(E(\mathbf{k}))}{\mathrm{d}E} \hbar \mathbf{v}(\mathbf{k})\,. \tag{2.13}$$

Then the stationary (i.e. $\frac{\partial}{\partial t} f(\mathbf{r},\mathbf{k},t) = 0$) and spatially homogeneous (i.e. $\frac{\partial}{\partial \mathbf{r}} f(\mathbf{r},\mathbf{k},t) = 0$) Boltzmann equation in relaxation time approximation reduces to

$$\delta f(\mathbf{r},\mathbf{k},t) = \tau_m(\mathbf{k}) e\mathbf{F}\cdot\mathbf{v} \frac{\mathrm{d}f_{\text{Fermi}}(E(\mathbf{k}))}{\mathrm{d}E}$$

Thus we find for stationary transport in a homogeneous systems

$$\begin{aligned} \mathbf{J} &= \frac{2(\text{for spin})(-e)}{(2\pi)^3} \int_{1.\text{Bz}} \mathrm{d}^3k\, \mathbf{v}(\mathbf{k}) \delta f(\mathbf{k}) && (2.14)\\ &= \underbrace{\frac{e^2}{4\pi^3} \int_{1.\text{Bz}} \mathrm{d}^3k\, \mathbf{v}(\mathbf{k}) \left(-\frac{\mathrm{d}f_{\text{Fermi}}(E(\mathbf{k}))}{\mathrm{d}E}\right) \tau_m(\mathbf{k}) \mathbf{v}(\mathbf{k})}_{=\underline{\underline{\sigma}}} \cdot \mathbf{F} && (2.15) \end{aligned}$$

providing us with the tensor of the electrical conductivity $\underline{\underline{\sigma}}$.

The conductivity becomes rather simple for an isotropic, parabolic band structures $E(k) = \hbar^2 k^2/2m_{\text{eff}}$ with $\tau_m(\mathbf{k}) = \tau_m(E(k))$. Here the density of states is given by $D(E) = D_0\sqrt{E}$, see Eq. (1.9). Using $\mathbf{k} = \mathbf{n}k$ with the unit vector $\mathbf{n}$ we find

$$\underline{\underline{\sigma}} = e^2 \int_0^\infty \mathrm{d}E D(E) \frac{2E}{m_{\text{eff}}} \tau_m(E) \left(-\frac{\mathrm{d}f_{\text{Fermi}}(E)}{\mathrm{d}E}\right) \underbrace{\frac{1}{4\pi} \int_0^{2\pi} \mathrm{d}\varphi \int_{-1}^{1} \mathrm{d}(\cos\theta)\, \mathbf{nn}}_{=\underline{\underline{\mathcal{T}}}}$$

The elements of the tensor $\underline{\underline{\mathcal{T}}}$ are given by $\mathcal{T}_{zz} = \frac{1}{4\pi}\int \mathrm{d}\varphi \int \mathrm{d}(\cos\theta)\, \cos^2\theta = \frac{1}{3}$ and $\mathcal{T}_{xz} = \frac{1}{4\pi}\int \mathrm{d}\varphi \int \mathrm{d}(\cos\theta)\, \sin\theta\cos\varphi\cos\theta = 0$. Altogether we find $\underline{\underline{\mathcal{T}}} = \frac{1}{3}\underline{\underline{1}}$. Thus the conductivity is a scalar and the current is parallel to the field. For metals we have $-\mathrm{d}f_{\text{Fermi}}/\mathrm{d}E \approx \delta(E - E_F)$ and we find

$$\sigma = e^2 \frac{\tau_m(E_F)}{m_{\text{eff}}} n \qquad \text{which gives the mobility} \quad \tilde{\mu} = \frac{e\tau_m(E_F)}{m_{\text{eff}}}$$

in accordance with the simple model (2.5). The same expression holds for larger temperatures $k_B T \gtrsim E_F$ (typical for semiconductors), if τ_m is constant[8].

2.4.2 Transport in inhomogeneous systems

Now we assume that there are spatial variations of the density [or correspondingly the internal chemical potential $\mu_{\text{int}}(\mathbf{r})$] and the temperature $T(\mathbf{r})$ in addition to the electric field. This is

[8]For non-degenerate systems, this can be generalized to $\tau_m \propto E^r$ and an r-dependent pre-factor appears in the mobility. In this is case the Hall mobility differs from the transport mobility, see chapter 4.2 of Seeger (1989).

approximated by the local equilibrium

$$f_0(E(\mathbf{k}),\mathbf{r}) = \frac{1}{\exp\left(\frac{E(\mathbf{k})-\mu_{\rm int}(\mathbf{r})}{k_B T(\mathbf{r})}\right)+1}$$

which replaces the Fermi function in the relaxation time approximation. In the left hand side of the Boltzmann equation (2.12) we use in lowest order for the spatial variations of $\mu_{\rm int}(\mathbf{r})$ and $T(\mathbf{r})$

$$\frac{\partial}{\partial \mathbf{r}} f(\mathbf{r},\mathbf{k},t) \approx \frac{\partial}{\partial \mathbf{r}} f_0(E(\mathbf{k}),\mathbf{r}) = -\frac{\partial f_0(E(\mathbf{k}),\mathbf{r})}{\partial E}\left(\nabla\mu_{\rm int}(\mathbf{r}) + \frac{E(\mathbf{k})-\mu_{\rm int}(\mathbf{r})}{T(\mathbf{r})}\nabla T(\mathbf{r})\right)$$

and find together with Eq. (2.13)

$$\delta f(\mathbf{r},\mathbf{k},t) = -\tau_m(\mathbf{k})\frac{\partial f_0(E(\mathbf{k}),\mathbf{r})}{\partial E}\mathbf{v}(\mathbf{k})\cdot\left(e\mathbf{F} + \nabla\mu_{\rm int}(\mathbf{r}) + \frac{E(\mathbf{k})-\mu_{\rm int}(\mathbf{r})}{T(\mathbf{r})}\nabla T(\mathbf{r})\right) \tag{2.16}$$

to be inserted into Eq. (2.14).

2.4.3 Diffusion and chemical potential

At first we neglect temperature gradients. Using Eq. (2.15), we find

$$\mathbf{J} = \underline{\underline{\sigma}}\mathbf{F} + \frac{1}{e}\underline{\underline{\sigma}}\nabla\mu_{\rm int}(\mathbf{r}) \tag{2.17}$$

As the internal chemical potential is a function of the density, the second term provides the

electron *diffusion*

$$\mathbf{J} = eD\nabla n \quad \text{with the } \textit{Einstein relation} \quad D = \frac{\sigma}{e^2}\frac{{\rm d}\mu_{\rm int}}{{\rm d}n}$$

Note that the right-hand side of Eq. (2.17) can be written as $\frac{1}{e}\underline{\underline{\sigma}}\nabla\mu(\mathbf{r})$ with the

chemical potential $\mu = \mu_{\rm int} - e\phi(\mathbf{r})$

Thus (for constant temperature) there is no current flow for a constant chemical potential. We follow here the notation of Kittel and Krömer (1980). Our chemical potential is frequently referred to as electrochemical potential ζ or, in particular for semiconductors, as Fermi level E_F.

For inhomogeneous systems (e.g. pn diodes or semiconductor heterostructures) it is convenient to plot the band edge $E_c - e\phi(\mathbf{r})$ in combination with μ. Then, spatial variations of μ imply current flow and the difference between μ and the shifted band edge provides $\mu_{\rm int}$, i.e. the actual electron density. The underlying idea is demonstrated in Fig. 2.1. It can be directly extended to different band edges (such as conduction and valence band) as well as to heterostructures with a spatial dependence $E_c(\mathbf{r})$, see Fig. 2.2.

2.4.4 Thermoelectric effects*

The heat-current density is given by (see sections 9.6+7 of Ibach and Lüth (2003) for details!)

$$\mathbf{J}_Q = \frac{1}{4\pi^3}\int_{1.{\rm Bz}} {\rm d}^3k\ [E(\mathbf{k})-\mu_{\rm int}]\,\mathbf{v}(\mathbf{k})\delta f(\mathbf{k})$$

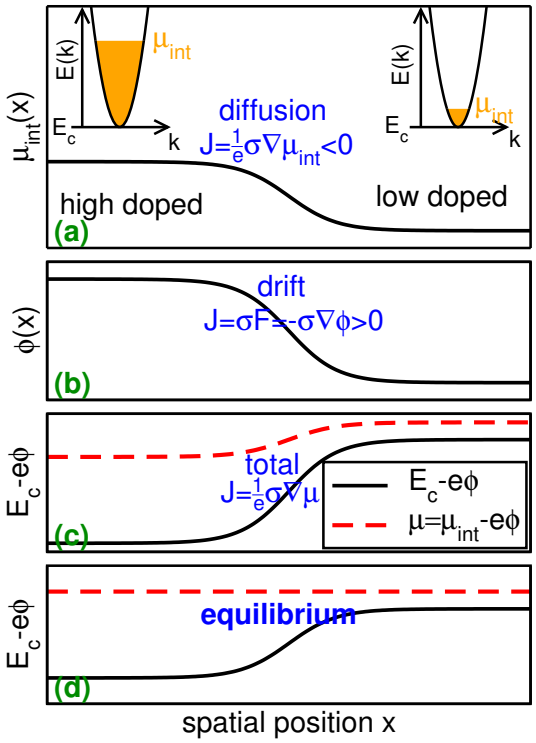

Figure 2.1: (a) Internal chemical potential in a junction between a high-doped and a low-doped semiconductor. (b) Electrical potential, which provides a drift current via the electric field. (c) (Electro-)Chemical potential $\mu = \mu_{\rm int} - e\phi$, which drives the total current. Note that the difference between the curves for μ and $E_c - e\phi(\mathbf{r})$ is a measure for the local charge density. (d) same as (c) for a different electric potential, so that there is no net current.

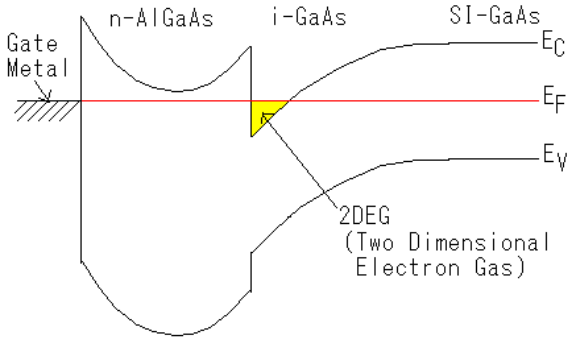

Figure 2.2: Spatial variation of the band alignment $E_c - e\phi(\mathbf{r})$ in a high-electron-mobility-transistor (HEMT) which is determined by the uniformity of the chemical potential μ (here denoted as E_F). SI stands for semi-insulating, where the chemical potential is in the middle of the gap. i and n stand for intrinsic (undoped) and n-doped regions respectively. The ionized donors in n-$Al_xGa_{1-x}As$ provide a positive space charge with a positive curvature of $-e\phi(\mathbf{r})$. The electrons in the 2DEG provide a negative curvature. (From Wikipedia Commons)

This provides us with transport coefficients [using $\mathbf{F}' = \mathbf{F} + \nabla\mu_{\rm int}(\mathbf{r})/e = \nabla\mu/e$ in Eq. (2.16)]

$$\mathbf{J} = \mathcal{L}^{11}\mathbf{F}' + \mathcal{L}^{12}(-\nabla T) \tag{2.18}$$

$$\mathbf{J}_Q = \mathcal{L}^{21}\mathbf{F}' + \mathcal{L}^{22}(-\nabla T) \tag{2.19}$$

These equations describe electrical conductance, heat conductance as well as thermoelectric effects, such as (see chapter 13 of Ashcroft and Mermin (1979) for details)

Peltier effect: An electric current implies heat current $\mathbf{J}_Q = \Pi\mathbf{J}$ for constant temperature with the Peltier constant $\Pi = \mathcal{L}^{21}/\mathcal{L}^{11}$

Seebeck effect: A temperature difference is associated with a bias for vanishing electric current: $\mathbf{F}' = S\nabla T$ with the thermoelectric constant (thermopower) $S = \mathcal{L}^{12}/\mathcal{L}^{11}$

thermal conductivity: A temperature difference causes a heat current $\mathbf{J}_Q = -\kappa\nabla T$ for vanishing electric current with the thermal conductivity $\kappa = \mathcal{L}^{22} - \mathcal{L}^{21}\mathcal{L}^{12}/\mathcal{L}^{11}$.

$\mathcal{L}^{11}$ and $\mathcal{L}^{22}$ are positive, while $\mathcal{L}^{12}$ and $\mathcal{L}^{21}$ are typically (e.g., for parabolic band structure) negative for electron transport and positive for hole transport. Thus:

Particles flow from high to low density and from high to low temperature.

The coefficients $\mathcal{L}^{ij}$ are not independent: One finds $T\mathcal{L}^{12} = \mathcal{L}^{21}$, and consequently $\Pi = TS$, which reflects the general Onsager relation[9]. For metals with $E_F \gg k_B T$ one obtains $\mathcal{L}^{22}/\mathcal{L}^{11} = T\pi^2 k_B^2/3e^2$. Approximating the thermal conductivity $K \approx \mathcal{L}^{22}$, this provides the *Wiedemann-Franz law* $K/T\sigma$ =const, which was found experimentally already in 1853.

2.5 Details for Phonon quantization and scattering*

See also Sections 4.1+2 of Snoke (2008) for an overview.

2.5.1 Quantized phonon spectrum

We consider a crystal with ions at the equilibrium positions $\mathbf{R} + \mathbf{r}_\alpha$, where $\mathbf{R}$ is the lattice vector of the Bravais lattice and α the atom index, which counts the atoms of mass m_α in each unit cell. The potential energy of the lattice has a minimum for the equilibrium positions and thus the potential is approximately quadratic in the elongations $\mathbf{s}(\mathbf{R}, \alpha)$ from the equilibrium positions

$$V(\{\mathbf{s}(\mathbf{R},\alpha)\}) = \frac{1}{2}\sum_{\mathbf{R},\Delta\mathbf{R}\alpha\alpha'} \mathbf{s}(\mathbf{R},\alpha)^\dagger \underline{\underline{\tilde{D}}}^{\Delta\mathbf{R}}_{\alpha,\alpha'} \mathbf{s}(\mathbf{R}+\Delta\mathbf{R},\alpha')$$

We want to solve the $3NN_\alpha$ coupled equations of motion

$$m_\alpha \frac{\mathrm{d}^2\mathbf{s}(\mathbf{R},\alpha,t)}{\mathrm{d}^2 t} = -\frac{\partial V(\{\mathbf{s}(\mathbf{R},\alpha,t)\})}{\partial \mathbf{s}(\mathbf{R},\alpha)} = -\sum_{\Delta\mathbf{R}\alpha'} \underline{\underline{\tilde{D}}}^{\Delta\mathbf{R}}_{\alpha,\alpha'} \mathbf{s}(\mathbf{R}+\Delta\mathbf{R},\alpha',t)\,.$$

Due to the translational invariance of the lattice, the Ansatz

$$\mathbf{s}(\mathbf{R},\alpha,t) = \frac{1}{\sqrt{Nm_\alpha}} \sum_{j,\mathbf{q}} \mathrm{e}^{\mathrm{i}\mathbf{q}\cdot\mathbf{R}} \mathbf{e}^{(j)}_\alpha(\mathbf{q}) Q_j(\mathbf{q},t)$$

gives us $3NN_\alpha$ uncoupled oscillators (see chap 4.2 of Ibach and Lüth (2003))

$$\frac{\mathrm{d}^2 Q_j(\mathbf{q},t)}{\mathrm{d}^2 t} = -\omega_j^2(\mathbf{q}) Q_j(\mathbf{q},t) \tag{2.20}$$

where the frequencies $\omega_j(\mathbf{q})$ are obtained from the eigenvalue problem

$$\sum_{\alpha'} \left(\sum_{\Delta\mathbf{R}} \mathrm{e}^{i\mathbf{q}\cdot\Delta\mathbf{R}} \underline{\underline{\tilde{D}}}^{\Delta\mathbf{R}}_{\alpha,\alpha'} \frac{1}{\sqrt{m_\alpha m_{\alpha'}}} \right) \mathbf{e}^{(j)}_{\alpha'}(\mathbf{q}) = \omega_j^2(\mathbf{q}) \mathbf{e}^{(j)}_\alpha(\mathbf{q})$$

[9] We consider the particle current $\mathbf{J}_P = \mathbf{J}/(-e)$ and the energy current $\mathbf{J}_U = \mathbf{J}_Q + \mu \mathbf{J}_P$ as functions of their respective conjugate forces $\nabla\frac{1}{T}$ and $-\nabla\frac{\mu}{T}$, see, e.g., Kittel and Krömer (1980):

$$\begin{aligned}
\mathbf{J}_P &= \frac{\mathcal{L}^{11}}{e^2}\left(-\nabla\frac{\mu}{T}\right) - \left(\frac{\mathcal{L}^{12}T^2}{e} + \frac{\mathcal{L}^{11}\mu T}{e^2}\right)\nabla\frac{1}{T} \\
\mathbf{J}_U &= -\left(\frac{\mathcal{L}^{21}T}{e} + \frac{\mathcal{L}^{11}T\mu}{e^2}\right)\left(-\nabla\frac{\mu}{T}\right) + \left(\frac{\mathcal{L}^{11}\mu^2 T}{e^2} - \frac{\mathcal{L}^{21}\mu T}{e} - \frac{\mathcal{L}^{12}\mu T^2}{e} + \mathcal{L}^{22}T^2\right)\nabla\frac{1}{T}
\end{aligned}$$

The Onsager relation states that this coefficient matrix is symmetric, requiring $T\mathcal{L}^{12} = \mathcal{L}^{21}$.

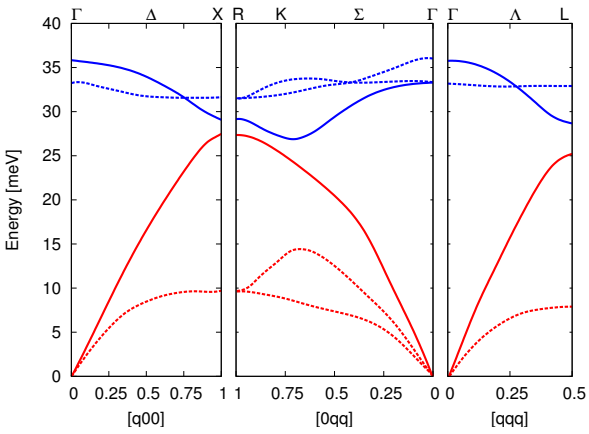

Figure 2.3: Phonon spectrum of GaAs with optical (blue) and acoustic (red) phonons. The full lines refer to longitudinal and the dashed lines the transversal phonons. [After J.S. Blakemore J. Appl. Phys **53**, R123 (1982)]

For each $\mathbf{q}$ we have $3N_\alpha$ eigenmodes (label j) satisfying $\sum_\alpha [\mathbf{e}_\alpha^{(i)}(\mathbf{q})]^* \cdot \mathbf{e}_\alpha^{(j)}(\mathbf{q}) = \delta_{ij}$, $\mathbf{e}_\alpha^{(i)}(-\mathbf{q}) = [\mathbf{e}_\alpha^{(i)}(\mathbf{q})]^*$ and $\omega_j(-\mathbf{q}) = \omega_j(\mathbf{q})$. As the elongations $\mathbf{s}$ are real we have $Q_j(\mathbf{q},t) = Q_j^*(-\mathbf{q},t)$. An example for such a phonon spectrum is shown in Fig. 2.3.

The Hamilton operator corresponding to the classical equation of motion reads[10]:

$$\hat{H}_{\text{phon}} = \sum_{j,\mathbf{q}} \frac{1}{2}\hat{\Pi}_j^\dagger(\mathbf{q})\hat{\Pi}_j(\mathbf{q}) + \frac{1}{2}\omega_j^2(\mathbf{q})\hat{Q}_j^\dagger(\mathbf{q})\hat{Q}_j(\mathbf{q})$$

with the operators

$$\hat{Q}_j(\mathbf{q}) = \sum_{\alpha,\mathbf{R}} \sqrt{\frac{m_\alpha}{N}} \mathrm{e}^{-i\mathbf{q}\cdot\mathbf{R}} \mathbf{e}_\alpha^{(j)*}(\mathbf{q}) \cdot \hat{\mathbf{s}}(\mathbf{R},\alpha) \qquad \hat{\Pi}_j(\mathbf{q}) = \sum_{\alpha,\mathbf{R}} \frac{1}{\sqrt{N m_\alpha}} \mathrm{e}^{-i\mathbf{q}\cdot\mathbf{R}} \mathbf{e}_\alpha^{(j)*}(\mathbf{q}) \cdot \hat{\mathbf{p}}(\mathbf{R},\alpha)$$

We define the lowering operator as usual

$$b_j(\mathbf{q}) = \frac{1}{\sqrt{2\hbar\omega_j(\mathbf{q})}} \left[\omega_j(\mathbf{q})\hat{Q}_j(\mathbf{q}) + \mathrm{i}\hat{\Pi}_j(\mathbf{q})\right]$$

As the operators $\hat{Q}_j^\dagger(\mathbf{q}) = \hat{Q}_j(-\mathbf{q})$ and $\hat{\Pi}_j^\dagger(\mathbf{q}) = \hat{\Pi}_j(-\mathbf{q})$ are non-hermitian, we have the corresponding raising operator

$$b_j^\dagger(\mathbf{q}) = \frac{1}{\sqrt{2\hbar\omega_j(\mathbf{q})}} \left[\omega_j(\mathbf{q})\hat{Q}_j(-\mathbf{q}) - \mathrm{i}\hat{\Pi}_j(-\mathbf{q})\right]$$

which can be inverted by

$$\hat{Q}_j(\mathbf{q}) = \sqrt{\frac{\hbar}{2\omega_j(\mathbf{q})}}[b_j(\mathbf{q}) + b_j^\dagger(-\mathbf{q})] \qquad \hat{\Pi}_j(\mathbf{q}) = -\mathrm{i}\sqrt{\frac{\hbar\omega_j(\mathbf{q})}{2}}[b_j(\mathbf{q}) - b_j^\dagger(-\mathbf{q})] \tag{2.21}$$

Due to the commutation relation $[\hat{\Pi}_j(\mathbf{q}), \hat{Q}_i(\mathbf{q}')] = \hbar/\mathrm{i}\,\delta_{ij}\delta_{\mathbf{q},-\mathbf{q}'}$ we find the standard relations $[b_j(\mathbf{q}), b_j^\dagger(\mathbf{q}')] = \delta_{ij}\delta_{\mathbf{q},\mathbf{q}'}$ and $[b_j(\mathbf{q}), b_i(\mathbf{q}')] = [b_j^\dagger(\mathbf{q}), b_i^\dagger(\mathbf{q}')] = 0$ as well as Eq. (2.6).

From quantum mechanics we know the eigenstates and –energies $E_n = \hbar\omega_j(\mathbf{q})(n_j(\mathbf{q}) + 1/2)$ for each phonon mode. Thus the set of numbers $\{n_j(\mathbf{q})\}$ describes the state of the lattice vibrations. The time dependence of the operators is given by

$$b_j(\mathbf{q},t) = b_j(\mathbf{q})\mathrm{e}^{-\mathrm{i}\omega_j(\mathbf{q})t} \qquad b_j^\dagger(\mathbf{q},t) = b_j^\dagger(\mathbf{q})\mathrm{e}^{\mathrm{i}\omega_j(\mathbf{q})t} \tag{2.22}$$

in the Heisenberg picture.

[10] We follow R. Feynman *Statistical Mechanics*; G. Mahan *Many Particle physics* uses $\hat{P} = \hat{\Pi}^\dagger$

2.5.2 Deformation potential interaction with longitudinal acoustic phonons

This is a common scattering process present in all materials. We follow Ferry (1991) here. For acoustic phonons the elongations satisfy $\mathbf{s}(\mathbf{R},\alpha) \approx \mathbf{s}(\mathbf{R})$. Thus

$$\mathbf{e}_\alpha^{(j)}(\mathbf{q}) \approx \sqrt{\frac{m_\alpha}{\sum_\beta m_\beta}}\mathbf{e}^{(j)}(\mathbf{q}) = \sqrt{\frac{Nm_\alpha}{\rho_m V}}\mathbf{e}^{(j)}(\mathbf{q})$$

Here $\rho_m = \sum_\alpha m_\alpha/V_c$ is the mass density. We can rewrite the elongations as a continuous field

$$\mathbf{S}(\mathbf{r}) = \frac{1}{\sqrt{\rho_m V}}\mathbf{e}^{(j)}(\mathbf{q})\mathrm{e}^{\mathrm{i}\mathbf{q}\cdot\mathbf{r}}Q_j(\mathbf{q})$$

Now the band structure changes, when the crystal is compressed, which can be approximated by an energy shift $\delta E_n = \Xi_n \delta V/V$ for each band n. The local compression due to the phonon mode is given by

$$\frac{\delta V}{V} = \operatorname{div}\mathbf{S}(\mathbf{r}) = \frac{1}{\sqrt{\rho_m V}}\mathrm{i}\mathbf{q}\cdot\mathbf{e}^{(j)}(\mathbf{q})\mathrm{e}^{\mathrm{i}\mathbf{q}\cdot\mathbf{r}}Q_j(\mathbf{q},t)$$

and it becomes obvious that only longitudinal acoustic phonons contribute, i.e., $j = LA$. Thus we find the effective electron potential

$$V_{Def.Pot.}(\mathbf{r},t) = \sum_{\mathbf{q}} \Xi_n \sqrt{\frac{\hbar}{2\rho_m V\omega_{LA}(\mathbf{q})}}\left[\mathrm{i}\mathbf{q}\cdot\mathbf{e}^{(LA)}(\mathbf{q})\right]\mathrm{e}^{\mathrm{i}\mathbf{q}\cdot\mathbf{r}}\left[b_{LA}(\mathbf{q})\mathrm{e}^{-\mathrm{i}\omega_{LA}(\mathbf{q})t} + b_{LA}^\dagger(-\mathbf{q})\mathrm{e}^{\mathrm{i}\omega_{LA}(\mathbf{q})t}\right] \tag{2.23}$$

2.5.3 Polar interaction with longitudinal optical phonons

Polar scattering at optical phonons is the dominant phonon scattering mechanism in III/V semiconductors. For longitudinal optical phonons the average polarization of a unit cell is given by

$$\mathbf{P}(\mathbf{R},t) = \frac{1}{V_c}\sum_\alpha q_\alpha \mathbf{s}(\mathbf{R},\alpha) = \frac{\tilde{q}}{V_c}\tilde{\mathbf{s}}(\mathbf{R})$$

where

$$\tilde{\mathbf{s}}(\mathbf{R}) = \frac{1}{\sqrt{N\rho_m V_c}}\sum_{\mathbf{q}} \mathrm{e}^{\mathrm{i}\mathbf{q}\cdot\mathbf{R}}\tilde{\mathbf{e}}(\mathbf{q})Q_{\mathrm{LO}}(\mathbf{q})\,.$$

Here $\tilde{\mathbf{e}}(\mathbf{q})$ and $\tilde{q}$ are defined via $\tilde{q}\tilde{\mathbf{e}}(\mathbf{q})/\sqrt{\rho_m V_c} = \sum_\alpha q_\alpha \mathbf{e}_\alpha(\mathbf{q})/\sqrt{m_\alpha}$ and $|\tilde{\mathbf{e}}(\mathbf{q})| = 1$. As there is no macroscopic charge we have $\epsilon_0\mathbf{F} + \mathbf{P} = 0$ and obtain the mechanical potential of an electron

$$V(\mathbf{r},t) = -e\phi(\mathbf{r},t) = \frac{e}{\epsilon_0}\int \mathrm{d}\mathbf{r}\cdot\mathbf{P}(\mathbf{r},t) = \frac{e\tilde{q}}{\mathrm{i}\epsilon_0 V_c}\frac{\tilde{\mathbf{s}}(\mathbf{R})\cdot\mathbf{q}}{q^2}$$

where we used $\tilde{\mathbf{e}}(\mathbf{q}) \parallel \mathbf{q}$. This results in the potential

$$V_{\text{Polar optical phonon}}(\mathbf{r},t) = \sum_{\mathbf{q}} g(\mathbf{q})\mathrm{e}^{\mathrm{i}\mathbf{q}\cdot\mathbf{r}}\left[b_{LO}(\mathbf{q})\mathrm{e}^{-\mathrm{i}\omega_{LO}(\mathbf{q})t} + b_{LO}^\dagger(-\mathbf{q})\mathrm{e}^{\mathrm{i}\omega_{LO}(-\mathbf{q})t}\right] \tag{2.24}$$

with the Fröhlich-coupling

$$g(\mathbf{q}) = \frac{1}{\sqrt{V}}\mathrm{i}e\sqrt{\frac{\hbar\omega_{LO}(\mathbf{q})}{2\epsilon_0}\left(\frac{1}{\epsilon(\infty)} - \frac{1}{\epsilon(0)}\right)}\underbrace{\frac{(-\mathrm{i})\tilde{\mathbf{e}}(\mathbf{q})\cdot\mathbf{q}}{q^2}}_{\to 1/|\mathbf{q}|} \tag{2.25}$$

satisfying $g(-\mathbf{q}) = g(\mathbf{q})^*$. Here $\epsilon(0)$ and $\epsilon(\infty)$ are the dielectric constants for zero frequency and for frequencies well above the optical phonon resonance, respectively. We used

$$\frac{\tilde{q}}{\epsilon_0 V_c} = \omega_{LO}\sqrt{\left(\frac{1}{\epsilon(\infty)} - \frac{1}{\epsilon(0)}\right)\frac{\rho_m}{\epsilon_0}} \tag{2.26}$$

resulting from the dielectric properties[11].

[11]See, e.g., section 6.8 of Seeger (1989). A similar treatment is found in Ferry (1991)

Chapter 3

Magnetism

Electrodynamics of continua tells us, that the *magnetic field* $\mathbf{B}$ is related to the field $\mathbf{H}$ by $\mathbf{B} = \mu_0(\mathbf{H} + \mathbf{M})$ where the magnetization $\mathbf{M}$ (density of magnetic moments $\boldsymbol{\mu}$) is a material property and $\mu_0 = 4\pi \times 10^{-7}\mathrm{Vs/Am}$ is the vacuum permeability. In this chapter we want to provide a physical basis of $\mathbf{M}$. Frequently, we have a linear relation

$$\mathbf{M} = \frac{\chi}{\mu_0}\mathbf{B} \tag{3.1}$$

defining the magnetic susceptibility χ.[1] Materials with $\chi > 0$ are called *paramagnetic*, while materials with $\chi < 0$ are called *diamagnetic*. In addition, $\mathbf{M} \neq 0$ is possible even for a vanishing magnetic induction. Such materials are called *ferromagnetic*.

3.1 Classical magnetic moments

In classical electrodynamics the magnetic moment of a current distribution is defined by

$$\boldsymbol{\mu} = \frac{1}{2}\int \mathrm{d}^3 r\, \mathbf{r} \times \mathbf{j}(\mathbf{r})$$

E.g., for an annual current I surrounding the oriented area $\mathbf{A}$ we find $\boldsymbol{\mu} = I\mathbf{A}$.

Now we consider a rotating body with a total mass m and a total charge q. We assume that the charge and the mass follow the same normalized spatial distribution $P(\mathbf{r})$ (corresponding to $|\Psi(\mathbf{r})|^2$ in quantum mechanics) resulting in the charge distribution $\rho(\mathbf{r}) = qP(\mathbf{r})$ and the mass distribution $\rho_m(\mathbf{r}) = mP(\mathbf{r})$. Using the relation[2] $m\mathbf{v} = \mathbf{p} - q\mathbf{A}$ in the presence of a vector potential, we find

$$\boldsymbol{\mu} = \frac{1}{2}\int \mathrm{d}^3 r\, \mathbf{r} \times \rho(\mathbf{r})\mathbf{v}(\mathbf{r}) = \frac{q}{2m}\int \mathrm{d}^3 r\, \mathbf{r} \times P(\mathbf{r}) m\mathbf{v}(\mathbf{r}) = \frac{q}{2m}\mathbf{L} - \frac{q}{2m}\int \mathrm{d}^3 r\, \mathbf{r} \times \rho(\mathbf{r})\mathbf{A}(\mathbf{r}) \tag{3.2}$$

Thus magnetic moments are intrinsically connected to the angular momentum $\mathbf{L} = \mathbf{r} \times \mathbf{p}$ with a ratio $\frac{q}{2m}$. Qauntum mechanics provides the quantization of the angular momentum in (half-integer) units of $\hbar$. Thus the *Bohr magneton* $\mu_B = \frac{e\hbar}{2m_e} = 5.788 \times 10^{-5}\mathrm{eV/T}$ is a typical unit.

[1] We treat $\mathbf{B}$ as the primary magnetic field as it appears in the Lorentz force. Traditionally, $\mathbf{H}$ was denoted as magnetic field, as it is directly related to measurable free currents, and $\mathbf{B}$ was called magnetic induction. In the same spirit, the susceptibility is traditionally defined as $\mathbf{M} = \chi'\mathbf{H}$ providing $\chi' = \chi/(1-\chi)$, which in practice does not make a difference, as typically $|\chi| \ll 1$. See Chap. 11 of Purcell and Morin *Electricity and Magnetism* (Cambridge University Press, 2013) for an enlightening discussion.

[2] See, e.g., `http://www.teorfys.lu.se/staff/Andreas.Wacker/Scripts/quantMagnetField.pdf`

In addition there is a term $\propto \mathbf{A}$, which vanishes for point-like particles and is frequently not mentioned in the literature.

The interaction of a magnetic moment with an external magnetic field $\mathbf{B}$ is described by the energy

$$E = -\boldsymbol{\mu} \cdot \mathbf{B} \tag{3.3}$$

which can be proven by evaluating the force on a magnetic dipole in an inhomogeneous external magnetic field

$$\mathbf{F} = \int \mathrm{d}^3 r\, \mathbf{j}(\mathbf{r}) \times \mathbf{B}(\mathbf{r}) \overset{\text{difficult}}{=} \nabla[\boldsymbol{\mu} \cdot \mathbf{B}(\mathbf{r})] \tag{3.4}$$

as well as the torque on the magnetic moment in a constant external magnetic field

$$\boldsymbol{\tau} = \int \mathrm{d}^3 r\, \mathbf{r} \times (\mathbf{j}(\mathbf{r}) \times \mathbf{B}) \overset{\text{difficult}}{=} \boldsymbol{\mu} \times \mathbf{B}$$

where in both cases the current distribution does not change in its own frame, if the magnetic moment is moved or rotated. For details see section 5.7 of Jackson (1998).

3.2 Magnetic susceptibilities from independent electrons

To simplify the notation, we redefine in this chapter both the orbital angular momentum $\hat{\mathbf{l}} = \hat{\mathbf{r}} \times \hat{\mathbf{p}}/\hbar$ and the spin $\hat{\mathbf{s}}$ by dividing by $\hbar$, yielding dimensionless quantities.

For a homogeneous constant magnetic field we can use the vector potential $\mathbf{A}(\mathbf{r}) = \frac{1}{2}\mathbf{B} \times \mathbf{r}$ and the Hamilton operator (1.20) becomes

$$\hat{H} = \frac{\hat{\mathbf{p}}^2}{2m} + V(\mathbf{r}) \underbrace{+ \frac{e\hbar}{2m_e} \mathbf{B} \cdot \hat{\mathbf{l}}}_{=\mu_B \mathbf{B} \cdot \hat{\mathbf{l}}} + \frac{e^2}{8m_e} B^2 r_\perp^2 \tag{3.5}$$

where $B = |\mathbf{B}|$ and $\mathbf{r}_\perp$ is the projection of $\mathbf{r}$ onto the plane perpendicular to $\mathbf{B}$. (Technically one has $B^2 r_\perp^2 = (\mathbf{B} \times \mathbf{r})^2$)

In addition, the electron has an intrinsic property, the spin, which can be described by a *spinor wave function* $(\Psi(\uparrow, t), \Psi(\downarrow, t))^{tr}$ with an angular momentum, the spin, of 1/2. The *Spin operator* is given by $\hat{\mathbf{s}} = \frac{1}{2}\boldsymbol{\sigma}$ where

$$\sigma_x = \begin{pmatrix} 0 & 1 \\ 1 & 0 \end{pmatrix} \sigma_y = \begin{pmatrix} 0 & -i \\ i & 0 \end{pmatrix} \sigma_z = \begin{pmatrix} 1 & 0 \\ 0 & -1 \end{pmatrix}$$

are the Pauli matrices. The interaction with the magnetic induction is given by

$$\hat{H}_{\text{spin}} = g_e \frac{e\hbar}{2m_e} \hat{\mathbf{s}} \cdot \mathbf{B} \tag{3.6}$$

where $g_e = 2.0023\ldots$ is the Landé factor of the free electron.[3] Thus the corresponding magnetic moment is $\boldsymbol{\mu} = -g\mu_B \mathbf{s}$.

The total Hamiltonian (3.5) provides the expectation value of the energy

$$\langle \hat{H} + \hat{H}_{\text{spin}} \rangle = \left\langle \frac{\hat{\mathbf{p}}^2}{2m} + V(\mathbf{r}) \right\rangle + \mu_B \mathbf{B} \cdot \langle \hat{\mathbf{l}} + g_e \hat{\mathbf{s}} \rangle + \left\langle \frac{e^2}{8m_e} B^2 r_\perp^2 \right\rangle$$

[3] This quantity could recently be measured with a remarkable accuracy of 7.6 parts in 10^{13}, B. Odom *et al.*, Phys. Rev. Lett. **97** 030801 (2006) and agrees well with calculations based on relativistic quantum electrodynamics

Physical origin	formula	magnitude
Thermal orientation of localized magnetic moments, *paramagnetism*	$\chi = n\mu_0 \frac{(g\mu_B)^2 J(J+1)}{3k_B T}$	$+3 \times 10^{-3}$ at 300 K
A^2 term for bound orbitals, *Larmor diamagnetism*	$\chi = -n\mu_0 \frac{e^2}{6m_e} Z_a \langle r_a^2 \rangle$	-6×10^{-5}
Second order perturbation theory for bound orbitals, *Van Vleck paramagnetism**	$\chi = 2n\mu_0\mu_B^2 \sum_n \frac{\lvert\langle n\rvert \hat{L}_z + g_e \hat{S}_z \lvert 0\rangle\rvert^2}{E_n - E_0}$	$+2 \times 10^{-5}$
Spin splitting for band electrons *Pauli paramagnetism*	$\chi = \mu_0 \frac{(g\mu_B)^2}{4} D(E_F)$	$+10^{-5}$
A further term for Bloch states in a magnetic field *Landau diamagnetism**	$\chi = -\chi_{Pauli} \times \frac{1}{3} \left(\frac{m_e}{m_{\text{eff}}} \right)^2$	-3×10^{-6}

Table 3.1: Overview for the different contribution to the susceptibility within the single electron model. For the numerical values the density $n = 10^{29}/\text{m}^3$, $g = 2$, $J = 0.5$, $Z_a \langle r_a^2 \rangle \approx 10\text{Å}^2$, $\sum_n |\langle n|\hat{L}_z + g_e \hat{S}_z|0\rangle|^2/(E_n - E_0) \approx (5\text{eV})^{-1}$, and $D(E_F) = (3\pi^2 n)^{1/3} m_{\text{eff}}/(\pi^2\hbar^2)$ where $m_{\text{eff}} = m_e$ are used. Read your textbook for details! [Detailed information for Van Vleck paramagnetism as well as Landau diamagnetism can be found in Marder (2000) and Czycholl (2004).]

Now the magnetic moment can be defined as $-\partial\langle\hat{H}\rangle/\partial B$ providing

$$\langle \boldsymbol{\mu} \rangle = -\mu_B \langle \hat{\mathbf{l}} + g_e \hat{\mathbf{s}} \rangle - \frac{e^2 \langle r_\perp^2 \rangle}{4m_e} \mathbf{B} \tag{3.7}$$

Except for the g_e-factor of the electron spin, this is just the classical relation (3.2) with $\mathbf{A}(\mathbf{r}) = \frac{1}{2}\mathbf{B} \times \mathbf{r}$ as considered here.

As discussed in the following subsections, the first term $-\mu_B \langle \hat{\mathbf{l}} + g_e \hat{\mathbf{s}} \rangle$ causes paramagnetism and the second $-\frac{e^2 \langle r_\perp^2 \rangle}{4m_e} \mathbf{B}$ brings about diamagnetism. A summary of the different contributions to the susceptibility in the independent electron model is given in Table 3.1. The main general trend is that paramagnetism dominates if there are magnetic moments, which can align with the magnetic field. Otherwise, the diamagnetic contribution takes over. In particular, many molecules including water ($\chi = -9.1 \times 10^{-6}$) are diamagnetic (but oxygen O_2 is paramagnetic).

3.2.1 Larmor Diamagnetism

The second term in Eq. (3.7) provides the susceptibility $\chi = -n\mu_0 e^2 \langle r_\perp^2 \rangle/(4m_e)$, which is negative, thus describing *diamagnetism*. Frequently one replaces $\langle r_\perp^2 \rangle = 2\langle r^2 \rangle/3$ which is appropriate

for isotropic systems. [4]

As energy is needed to establish a magnetic field in a diamagnetic substance, they experience a force at gradients of the magnetic field, see also Eq. (3.4). This may be used to levitate bodies, such as living frogs, see `http://www.ru.nl/hfml/research/levitation/diamagnetic/`.[5]

3.2.2 Paramagnetism by thermal orientation of spins

We consider $\mathbf{B} = B\mathbf{e}_z$ and assume that $\langle \boldsymbol{\mu} \rangle = -\mu_B \langle \hat{l}_z + g_e \hat{s}_z \rangle \mathbf{e}_z$ also points in z direction. A finite magnetic moment is thus related to the system occupying a state with a finite z-component of the angular momentum operator. For a symmetric system such states are part of multiplet which has the same energy for vanishing magnetic field. Thus, in thermal equilibrium all states of the multiplet have equal probability and there is no resulting magnetic moment.

The situation is different for a finite magnetic field, which is studied for a spin-1/2 system here: For $B > 0$ the spin state with lowest energy, is the spin state $|\downarrow\rangle = (0,1)^{tr}$ which satisfies $\hat{s}_z|\downarrow\rangle = m|\downarrow\rangle$ with $m = -1/2$. However, at finite temperature, the state with $m = 1/2$ can be occupied as well. From the Boltzmann distribution (canonical distribution) we find

$$\langle m \rangle = \frac{\frac{1}{2}\exp\left(\frac{-g\mu_B B}{2k_B T}\right) - \frac{1}{2}\exp\left(\frac{g\mu_B B}{2k_B T}\right)}{\exp\left(\frac{-g\mu_B B}{2k_B T}\right) + \exp\left(\frac{g\mu_B B}{2k_B T}\right)} = -\frac{1}{2}\tanh\left(\frac{g\mu_B B}{2k_B T}\right) \approx -\frac{g\mu_B B}{4k_B T} \tag{3.8}$$

Thus we find the magnetic moment $\langle \boldsymbol{\mu} \rangle = -g\mu_B \langle m \rangle \mathbf{e}_z = \frac{g^2\mu_B^2}{4k_B T}\mathbf{B}$ and for a density n of spins, the susceptibility becomes $\chi = n\mu_0 g^2 \mu_B^2/(4k_B T)$ (the Curie law[6]), which is the dominant paramagnetic contribution.

More generally, the total angular momentum $\mathbf{J} = \mathbf{L} + \mathbf{S}$ of an atom containing several valence electrons is related to its magnetic moment via $-ge\hbar\mathbf{J}/(2m_e)$ where g is the general Landé factor[7]. Again, only the z-component (defined by the direction of $\mathbf{B}$) of the angular momentum $\hat{J}_z$ is of relevance, which has the eigenvalues M_J with $M_J = J, J-1, \ldots, -J$. Correspondingly, the z-component of the magnetic momentum is $\mu_z = -g\mu_B M_J$. (See exercises and Table 3.1).

3.2.3 Pauli paramagnetism

Now we consider metallic substances, where the Fermi energy is within a band. In a classical picture, the spin of the conduction electrons could be easily oriented to follow the magnetic field and one would expect a large paramagnetic contribution as discussed in section 3.2.2. However the Pauli principle does not allow for such an easy spin flip as both spins directions

[4] This Larmor diamagnetism can be understood in a classical picture: Consider an electron oscillating in the potential of the nucleus. The Lorentz force $(-e)\mathbf{v} \times \mathbf{B}$ induces a rotation of the oscillation direction around $\mathbf{B}$. Comparison with the Coriolis force $2m\mathbf{v} \times \boldsymbol{\omega}_0$ is a system which rotates with ω_0, shows that the presence of the magnetic field has the same implication as the pseudo force in a system rotating with the Larmor frequency $\boldsymbol{\omega}_0 = (-e)\mathbf{B}/2m$. Thus the pendulum will rotate with $-\boldsymbol{\omega}_0$ (like the Foucault pendulum) creating a magnetic moment $\boldsymbol{\mu} = e\boldsymbol{\omega}_0\langle r_\perp^2 \rangle/2 = -e^2\langle r_\perp^2 \rangle \mathbf{B}/4m$ in agreement with the result given above. Note however that the classical interpretation of magnetic effects is questionable as pointed out already in the PhD Thesis of N. Bohr, Copenhagen, 1911. See also S.L. O'Dell and R.K.P. Zia, Am. J. Phys. **54**, 32 (1986)

[5] See also M.D. Simon and A.K. Geim: Journal of Applied Physics **87**, 1600 (2000).

[6] after Pierre Curie, who is even better known for the work on radioactivity together with his wife Marie Curie

[7] One finds $g = \frac{3}{2} + \frac{1}{2}\left[\frac{S(S+1)-L(L+1)}{J(J+1)}\right]$, interpolating between $g = 1$ for the total angular momentum $\mathbf{L}$ and $g = 2$ for the total spin $\mathbf{S}$, see chapter 31 of Ashcroft and Mermin (1979).

are occupied far below the Fermi energy. In contrast only the states close to the Fermi energy may contribute as outlined below.

In metals, the Fermi energy is located within an electronic band, with density of state $D(E)$ (for both spin directions). A finite magnetic field $\mathbf{B} = B\mathbf{e}_z$ changes the energy $E^0(\mathbf{k})$ of spin up/down states by $\pm g_e\mu_B B/2$. Thus we obtain a spin resolved density of state

$$\begin{aligned} D_{\uparrow/\downarrow}(E) =& \frac{1}{(2\pi)^3}\int_{1.\mathrm{Bz}} \mathrm{d}^3k\,\delta\left(E - E^0(\mathbf{k}) \mp \frac{g_e\mu_B B}{2}\right) \\ =& \frac{1}{2}D\left(E \mp \frac{g_e\mu_B B}{2}\right) \end{aligned} \tag{3.9}$$

Filling up to the Fermi level, the total density of occupied spin-down states increases by $\approx D(E_F)g_e\mu_B B/4$ while the number of spin-up states decreases by the same amount, see Fig. 3.1. The difference in occupation gives the magnetization $\mathbf{M} = g_e^2\mu_B^2 D(E_F)\mathbf{B}/4$ providing a parametric contribution $\chi = \mu_0 g_e^2\mu_B^2 D(E_F)/4$.

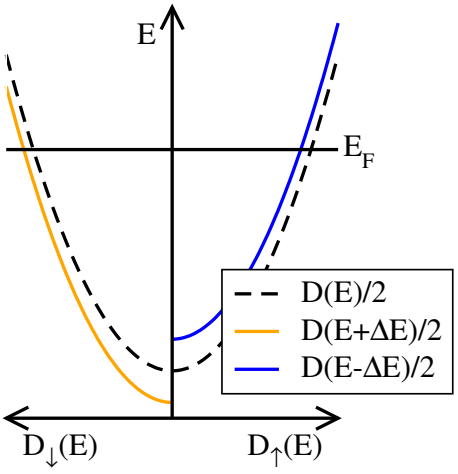

Figure 3.1: Spin-resolved density of states for $\Delta E = g_e\mu_B B/2 > 0$.

Indeed many metals such as sodium and aluminium are paramagnetic. However others such as copper and silver are diamagnetic. In particular bismuth has an extremely large value of $\chi = -16.6 \times 10^{-5}$

3.3 Ferromagnetism by interaction

The interaction between magnetic moments can favor situations where all moments are aligned. The magnetic dipole-dipole interaction gives the energy

$$E_{DD} = -\frac{\mu_0}{4\pi}\frac{\boldsymbol{\mu}_1 \cdot \boldsymbol{\mu}_2}{r^3} \sim 50\mu\mathrm{eV} \quad \text{for} \quad r = 1\text{Å}, \mu_i = \mu_B$$

which is far below the thermal energy ($k_B T = 25$ meV at room temperature). It is found that an effective interaction in a quantum many-particle system, the exchange interaction, provides a strong interaction, which can favor parallel spin configurations.

3.3.1 Many-Particle Schrödinger equation

The concept of many-particle wave functions can be introduced as a generalization of single particle states.

- Single particle wave function without spin: $\Psi(\mathbf{r})$, where $|\Psi(\mathbf{r})|^2$ is the probability density to find the particle at $\mathbf{r}$. Thus the normalization $\int \mathrm{d}^3r|\Psi(\mathbf{r})|^2 = 1$ is needed.
- Single particle state with spin function

$$\Psi(\mathbf{r})\begin{pmatrix} a \\ b \end{pmatrix} \quad \text{with } |a|^2 + |b|^2 = 1. \quad \text{generalize: } \begin{pmatrix} \Psi(\mathbf{r},\uparrow) \\ \Psi(\mathbf{r},\downarrow) \end{pmatrix} \text{ with } \int \mathrm{d}^3r \sum_{s=\uparrow,\downarrow} |\Psi(\mathbf{r},s)|^2 = 1$$

  Here $|\Psi(\mathbf{r},\uparrow)|^2$ is the probability density to find the particle at $\mathbf{r}$ with spin $\uparrow$.

- Two particle state $\Psi(\mathbf{r}_1, s_1, \mathbf{r}_2, s_2)$, where $|\Psi(\mathbf{r}_1, s_1, \mathbf{r}_2, s_2)|^2$ is the probability density to find the first particle at $\mathbf{r}_1$ with spin s_1 *and* the second particle at $\mathbf{r}_2$ with spin s_2. The normalization reads $\int \mathrm{d}^3 r_1 \sum_{s_1=\uparrow,\downarrow} \int \mathrm{d}^3 r_2 \sum_{s_2=\uparrow,\downarrow} |\Psi(\mathbf{r}_1, s_1; \mathbf{r}_2, s_2)|^2 = 1$
- The dynamics is given by the Schrödinger equation:

$$\mathrm{i}\hbar \frac{\partial}{\partial t} \Psi(\mathbf{r}_1, s_1; \mathbf{r}_2, s_2, t) = \left[-\frac{\hbar^2}{2m_A} \Delta_1 + V_A(\mathbf{r}_1, \hat{\mathbf{s}}_1) - \frac{\hbar^2}{2m_B} \Delta_2 + V_B(\mathbf{r}_2, \hat{\mathbf{s}}_2) + V_{AB}(\mathbf{r}_1; \mathbf{r}_2) \right] \Psi$$

  where particle 1 is of sort A and particle 2 is of sort B and may have different masses, interaction parameters etc.

It is often reasonable to consider *product functions* where also the spin function factorizes:

$$\Psi_{\mathrm{Product}}(\mathbf{r}_1, s_1; \mathbf{r}_2, s_2) = \phi_a(\mathbf{r}_1) \chi_\alpha(s_1) \phi_b(\mathbf{r}_2) \chi_\beta(s_2)$$

where a, b denote the quantum state (e.g. quantum numbers). Note that only very few two-particle wave function can be written in this way.

For identical particles ($A = B$), the Hamilton operator is symmetric with respect to an exchange in the particle indices $1 \leftrightarrow 2$. This symmetry allows for a classification of the wave functions. Here all observed phenomena agree with the following

Symmetry Postulate:
For identical particles with half-integer spin (*Fermions*, e.g., electrons) the states must be antisymmetric in the particle indices, i.e.,

$$\Psi(\mathbf{r}_1, s_1; \mathbf{r}_2, s_2, t) = -\Psi(\mathbf{r}_2, s_2; \mathbf{r}_1, s_1, t)$$

For more than two particles the same holds for all index combinations i, j.

Product states can easily be anti-symmetrized as

$$\begin{aligned} \Psi_{\mathrm{Slater}}(\mathbf{r}_1, s_1; \mathbf{r}_2, s_2) =& \frac{1}{\sqrt{2}} \left[\phi_a(\mathbf{r}_1) \chi_\alpha(s_1) \phi_b(\mathbf{r}_2) \chi_\beta(s_2) - \phi_b(\mathbf{r}_1) \chi_\beta(s_1) \phi_a(\mathbf{r}_2) \chi_\alpha(s_2) \right] \\ =& \frac{1}{\sqrt{2!}} \left| \begin{pmatrix} \phi_a(\mathbf{r}_1) \chi_\alpha(s_1) & \phi_b(\mathbf{r}_1) \chi_\beta(s_1) \\ \phi_a(\mathbf{r}_2) \chi_\alpha(s_2) & \phi_b(\mathbf{r}_2) \chi_\beta(s_2) \end{pmatrix} \right| \end{aligned} \tag{3.10}$$

where the *Slater determinant* of dimension $N \times N$ with pre-factor $1/\sqrt{N!}$ can be used for N-particle systems[8]. We find directly that the function vanishes if $a = b$ and $\alpha = \beta$, i.e., two particle are put into the identical single-particle state. This is the *Pauli principle*.

3.3.2 The band model for ferromagnetism

Now we study the joint probability density $P(\mathbf{r}_1, \mathbf{r}_2) = \sum_{s_1 s_2} |\Psi(\mathbf{r}_1, s_1; \mathbf{r}_2, s_2)|^2$ for two plane waves $\mathrm{e}^{\mathrm{i}\mathbf{k}\cdot\mathbf{r}}/\sqrt{V}, \mathrm{e}^{\mathrm{i}\mathbf{k}'\cdot\mathbf{r}}/\sqrt{V}$. We find from Eq. (3.10)

$$P(\mathbf{r}_1, \mathbf{r}_2) = \frac{1}{2V^2} \left[2 - \left(\mathrm{e}^{\mathrm{i}(\mathbf{k}-\mathbf{k}')\cdot(\mathbf{r}_1-\mathbf{r}_2)} + \mathrm{e}^{-\mathrm{i}(\mathbf{k}-\mathbf{k}')\cdot(\mathbf{r}_1-\mathbf{r}_2)} \right) \left| \sum_{s_1} \chi_\alpha(s_1) \chi^*_\beta(s_1) \right|^2 \right]$$

For $\alpha = \beta$, e.g., both spins are $\uparrow$, we find

$$P(\mathbf{r}_1, \mathbf{r}_2) = \frac{1 - \cos\left[(\mathbf{k} - \mathbf{k}') \cdot (\mathbf{r}_1 - \mathbf{r}_2)\right]}{V^2}$$

[8] We tacitly assume the orthonormality $\langle \phi_a | \phi_b \rangle = \delta_{ab}$, $\langle \chi_\alpha | \chi_\beta \rangle = \delta_{\alpha\beta}$ for the normalization properties here.

and the probability to find both particles at the same place vanishes. In contrast, for $\alpha =\uparrow$ and $\beta =\downarrow$ we find $P(\mathbf{r}_1, \mathbf{r}_2) = \frac{1}{V^2}$. As the Coulomb interaction between electrons is repulsive and decreases as $1/|\mathbf{r}_1 - \mathbf{r}_2|$ we find

The state with aligned spins has a reduced Coulomb interaction. The difference compared to the case with opposed spins is called *exchange interaction*.

We approximate

$$\langle\Psi|\tfrac{e^2}{4\pi\epsilon_0|\mathbf{r}_1-\mathbf{r}_2|}|\Psi\rangle = \int \mathrm{d}^3 r_1 \int \mathrm{d}^3 r_2 \, P(\mathbf{r}_1, \mathbf{r}_2) \frac{e^2}{4\pi\epsilon_0|\mathbf{r}_1 - \mathbf{r}_2|} = \frac{UV_c}{V} - \frac{IV_c}{V}\delta_{\alpha\beta}$$

where I is the Stoner parameter which is of the order of 1 eV.[9] Now we regard a Bloch state $\mathbf{k}$ with spin $\uparrow$. The energy $E^0(\mathbf{k})$ resulting from the periodic potential of the core ions does not dependent on the spin. Summing over the Coulomb interaction with all other valence electrons $\mathbf{k}'$ (where $n_{\uparrow/\downarrow}V$ is the number of electrons with spin up/down, respectively) we obtain an estimate for the total energy of the Bloch state

$$E_\uparrow(\mathbf{k}) = E^0(\mathbf{k}) + UV_c(n_\uparrow + n_\downarrow) - IV_c n_\uparrow$$

As the total electron density $n = n_\uparrow + n_\downarrow$ is fixed by the condition of charge neutrality, the corresponding term is a constant contribution to the energy and can be incorporated into $E^0(\mathbf{k})$. The corresponding expression with $\uparrow\leftrightarrow\downarrow$ holds for $E_\downarrow(\mathbf{k})$. In the exercises we show, that ferromagnetism occurs if $ID(E_F)V_c/2 > 1$, which is the *Stoner criterion*. Thus, metals with a particular high density of states at the Fermi energy are ferromagnetic. This is the case for iron, cobalt, and nickel, where the localized d-shells are partially filled.[10]

3.3.3 Singlet and Triplet states

Alternatively one can symmetrize the spin-part and the spatial-part separately by

$$\Psi_{\text{Singlet}} = \frac{1}{N_{ab}} \left(\phi_a(\mathbf{r}_1)\phi_b(\mathbf{r}_2) + \phi_b(\mathbf{r}_1)\phi_a(\mathbf{r}_2)\right) \frac{1}{\sqrt{2}} \left(\chi_\alpha(s_1)\chi_\beta(s_2) - \chi_\beta(s_1)\chi_\alpha(s_2)\right) \quad (3.11)$$

$$\Psi_{\text{Triplet}} = \frac{1}{\sqrt{2}} \left(\phi_a(\mathbf{r}_1)\phi_b(\mathbf{r}_2) - \phi_b(\mathbf{r}_1)\phi_a(\mathbf{r}_2)\right) \frac{1}{N_{\alpha\beta}} \left(\chi_\alpha(s_1)\chi_\beta(s_2) + \chi_\beta(s_1)\chi_\alpha(s_2)\right) \quad (3.12)$$

where $N_{ab} = 2$ for $a = b$ and $N_{ab} = \sqrt{2}$ for $a \neq b$ to ensure the normalization.

It is obvious that the triplet state has a reduced probability to find both particles at the same place. Thus we expect a lower energy of the triplet state due to the repulsive electron-electron interaction between the particles, which is quantified by a parameter $J = E_{\text{Singlet}} - E_{\text{Triplet}}$.[11]

Now $\hat{\mathbf{s}}_1 + \hat{\mathbf{s}}_2$ is the operator for the total spin of both states and $(\hat{\mathbf{s}}_1 + \hat{\mathbf{s}}_2)^2$ has the eigenvalue 2 for the triplet state and 0 for the singlet state. Thus the effective Hamiltonian describing the interaction between the spins reads

$$\hat{H}_{\text{eff}} = E_{\text{Singlet}} - \frac{J}{2}(\hat{\mathbf{s}}_1 + \hat{\mathbf{s}}_2)^2 = E_{\text{Singlet}} - \frac{J}{2}(\hat{\mathbf{s}}_1^2 + 2\hat{\mathbf{s}}_1 \cdot \hat{\mathbf{s}}_2 + \hat{\mathbf{s}}_2^2) = E_{\text{Singlet}} - \frac{3J}{4} - J\hat{\mathbf{s}}_1 \cdot \hat{\mathbf{s}}_2 \quad (3.13)$$

as the single electron states are eigenstates of $\hat{\mathbf{s}}_i^2$ with eigenvalue 3/4.

[9] See, e.g., J.F. Janak, Phys. Rev. B **16**, 255 (1977) for calculated values.

[10] A detailed discussion including finite temperature can be found in section 8.4 of Ibach and Lüth (2003).

[11] Concomitant, probability density is shifted away from the original states, where an external potential is low. This is a competing effect which can cause the singlet state to be lower is energy as well. Indeed, for a system of two particles, the ground state has always spin zero according to the Lieb-Mattis theorem, see Marder (2000).

3.3.4 Heisenberg model

For a lattice of localized magnetic moments (e.g., Mn atoms in a host material) with total angular momentum $\hat{\mathbf{S}}_n$ at lattice site n, Eq. (3.13) suggests the generalization

$$\hat{H}_{\text{Heisenberg}} = \sum_{(n,m)} -\frac{J}{2}\hat{\mathbf{S}}_n \cdot \hat{\mathbf{S}}_m + g\mu_B \mathbf{B} \cdot \sum_n \hat{\mathbf{S}}_n \tag{3.14}$$

where (n,m) restricts the sums over n,m to those combinations of lattice sites forming next neighbors. Hereby each pair is counted twice.[12] An extension to longer range interaction (describing ferrimagnetism, e.g.) is straightforward.

In order to find a simple solution we rewrite

$$\hat{\mathbf{S}}_n \cdot \hat{\mathbf{S}}_m = (\hat{\mathbf{S}}_n - \langle\hat{\mathbf{S}}_n\rangle)\cdot(\hat{\mathbf{S}}_m - \langle\hat{\mathbf{S}}_m\rangle) + \hat{\mathbf{S}}_n \cdot \langle\hat{\mathbf{S}}_m\rangle + \langle\hat{\mathbf{S}}_n\rangle \cdot \hat{\mathbf{S}}_m - \langle\hat{\mathbf{S}}_n\rangle \cdot \langle\hat{\mathbf{S}}_m\rangle \tag{3.15}$$

Neglecting *correlations* of the form $(\hat{\mathbf{S}}_n - \langle\hat{\mathbf{S}}_n\rangle)\cdot(\hat{\mathbf{S}}_m - \langle\hat{\mathbf{S}}_m\rangle)$ we receive the[13]

Heisenberg model in *Mean-Field approximation*

$$\hat{H}^{\text{MF}}_{\text{Heis}} = \sum_n g\mu_B \hat{\mathbf{S}}_n \cdot (\mathbf{B} + \mathbf{B}^{\text{MF}}_n) + \sum_{(n,m)} \frac{J}{2}\langle\hat{\mathbf{S}}_n\rangle \cdot \langle\hat{\mathbf{S}}_m\rangle \quad \text{with} \quad \mathbf{B}^{\text{MF}}_n = -\sum_\delta \frac{J}{g\mu_B}\langle\hat{\mathbf{S}}_{n+\delta}\rangle \tag{3.16}$$

where each spin at position n is subjected to an additional effective magnetic field B^{MF} (called *mean field*) resulting from the average spins of its neighboring lattice sites $n+\delta$.

Now we assume that $\mathbf{B} = B\mathbf{e}_z$ and $\langle\hat{\mathbf{S}}_n\rangle = \langle\hat{\mathbf{S}}\rangle = \langle\hat{S}^z\rangle\mathbf{e}_z$ is independent of the lattice site. Assuming ν neighboring spins, we have $B^{\text{MF}} = -\nu J\langle\hat{S}^z\rangle/g\mu_B$. Then we find from Eq. (3.8) for $S = 1/2$:

$$\langle\hat{S}^z\rangle = -\frac{1}{2}\tanh\left(\frac{g\mu_B B - \nu J\langle\hat{S}^z\rangle}{2k_B T}\right)$$

At $T = 0$ all spins are aligned and $\mathbf{M} = -g\mu_B\langle\hat{S}^z\rangle/V_c = \pm g\mu_B/(2V_c) = \pm M_0$ even for $\mathbf{B} = 0$. Note that in the latter case the direction of $\mathbf{M}$ is not defined and depends on the history of the system. This is accompanied by hysteresis effects.

For higher temperatures and small values of $\langle\hat{S}^z\rangle$ and B we may expand $\tanh x \approx x - x^3/3$ providing

$$\langle\hat{S}^z\rangle \approx -\frac{1}{2}\left(\frac{g\mu_B B - \nu J\langle\hat{S}^z\rangle}{2k_B T}\right) + \frac{1}{6}\left(\frac{g\mu_B B - \nu J\langle\hat{S}^z\rangle}{2k_B T}\right)^3$$

This provides us with a finite magnetization $|\mathbf{M}| = g\mu_B\langle\hat{S}^z\rangle/V_c$ for $B = 0$ below a *critical temperature* $T_c = \nu J/(4k_B)$. Close to T_c we find

$$|\mathbf{M}(T)| \sim \frac{g\mu_B}{2V_c}\sqrt{3}\left(\frac{T_c - T}{T_c}\right)^\beta \quad \text{for} \quad \begin{matrix} T < T_c \\ T \to T_c \end{matrix}$$

[12] Our definition of J agrees with Ashcroft and Mermin (1979) and Marder (2000). In contrast Ibach and Lüth (2003); Kittel (1996); Czycholl (2004) use $\tilde{J} = J/2$. Snoke (2008) uses effectively $\tilde{J} = J/8$ as he represents spin 1/2 by the variable $s_i = \pm 1$.

[13] I follow Ashcroft and Mermin (1979) which is also consistent with Kittel (1996). There is a different (in my opinion incorrect) argumentation providing $B_{\text{eff}} = -\sum_\delta J/2\langle\hat{\mathbf{S}}_{n+\delta}\rangle/g\mu_B$ used in Ibach and Lüth (2003); Czycholl (2004). The conceptual difference is partially hidden by different definitions of J!

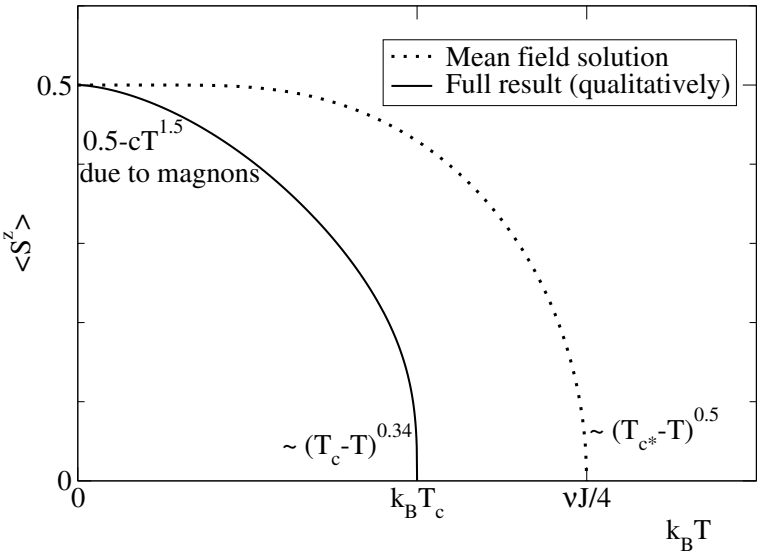

Figure 3.2: Spin polarization for the Heisenberg model for $\mathbf{B} = 0$. The mean-field solution provides a qualitative understanding of the temperature dependence. However, correlations in the fluctuations reduce the impact of the local field, and lead to a lower critical temperature and different critical exponents. This feature can be seen in the low temperature behavior, where the magnons (spin waves) reduce the polarization, see Eq. (3.17).

with $\beta = 1/2$. For $T > T_c$ the susceptibility reads

$$\chi(T) \sim \mu_0 \frac{(g\mu_B)^2}{4V_c k_B T_c} \left(\frac{T_c}{T - T_c}\right)^{\gamma} \quad \text{for} \quad \begin{array}{l} T > T_c \\ T \to T_c \end{array}$$

with $\gamma = 1$. Thus χ diverges for $T \to T_c$. While this behavior is qualitatively right, the critical exponents are replaced by $\beta = 0.34$ and $\gamma = 1.38$, if the fluctuations are properly taken into account[14]. In the same way the critical temperature T_c and the pre-factors change, see Fig. 3.2.

The magnetization vanishes above the critical temperature T_c, where the susceptibility shows a divergence $\chi(T) \propto |T - T_c|^{-\gamma}$

3.3.5 Spin waves*

The ground state $|0\rangle$ of the Heisenberg-Hamiltonian (for $J > 0$) is the state where all spins are aligned (in z-direction) with the magnetization $|\mathbf{M}| = M_0 = g\mu_B S/V_c$. The flip of a single spin costs an energy of $\sim S\nu J$. The resulting state is $|n\rangle = \hat{S}_n^-|0\rangle/\sqrt{2S}$ where $\hat{S}_n^{\pm} = \hat{S}_n^x \pm \mathrm{i}\hat{S}_n^y$ raises/lowers the z-component of the spin at site n by 1. This state is not an eigenstate of the Hamiltonian as

$$\hat{H}_{\text{Heis}}|n\rangle = \frac{1}{\sqrt{2S}}[\hat{H}_{\text{Heis}}, \hat{S}_n^-]|0\rangle + \frac{1}{\sqrt{2S}}\hat{S}_n^- \hat{H}_{\text{Heis}}|0\rangle = \frac{1}{\sqrt{2S}}[\hat{H}_{\text{Heis}}, \hat{S}_n^-]|0\rangle + E_0|n\rangle$$

Now the spin operators at different sites commute with each other and using the identity $\hat{\mathbf{S}}_{n+\delta}\hat{\mathbf{S}}_n = \hat{S}_{n+\delta}^z\hat{S}_n^z + \frac{1}{2}\hat{S}_{n+\delta}^-\hat{S}_n^+ + \frac{1}{2}\hat{S}_{n+\delta}^+\hat{S}_n^-$ we find

$$[\hat{H}_{\text{Heis}}, \hat{S}_n^-] = -J\sum_{\delta}\left(\hat{S}_{n+\delta}^z[\hat{S}_n^z, \hat{S}_n^-] + \frac{1}{2}\hat{S}_{n+\delta}^-[\hat{S}_n^+, \hat{S}_n^-] + \frac{1}{2}\hat{S}_{n+\delta}^+[\hat{S}_n^-, \hat{S}_n^-]\right)$$

Using the commutation relations $[\hat{S}^z, \hat{S}^-] = -\hat{S}^-$, $[\hat{S}^+, \hat{S}^-] = 2\hat{S}^z$, provides us with

$$[\hat{H}_{\text{Heis}}, \hat{S}_n^-] = -J\sum_{\delta}\left(-\hat{S}_{n+\delta}^z\hat{S}_n^- + \hat{S}_{n+\delta}^-\hat{S}_n^z\right) .$$

[14]This is done by renormalization group theory. The exponents are according to page 7 of D. Amit *Field theory, the renormalization group, and critical phenomena.*

Then we find

$$\hat{H}_{\text{Heis}}|n\rangle = E_0|n\rangle + JS\sum_\delta (|n\rangle - |n+\delta\rangle)\,.$$

However we can construct eigenstates in form of a *spin wave*

$$|\mathbf{k}\rangle = \frac{1}{\sqrt{2SN}}\sum_n \mathrm{e}^{\mathrm{i}\mathbf{k}\cdot\mathbf{R}_n}\hat{S}_n^-|0\rangle$$

with energies

$$E_k = E_0 + JS \underbrace{\sum_\delta \left(1-\mathrm{e}^{-\mathrm{i}\mathbf{k}\cdot\mathbf{R}_\delta}\right)}_{\approx k^2a^2 \text{ for small } k \text{ and a cubic 3 dim. lattice}}$$

which dominate the excitation spectrum at low energies. These excitations can be approximately treated as independently from each other. In this sense they are similar to the phonons in the lattice and are called *magnons*. Thus their excitation probability follows the Bose distribution

$$f_k = \frac{1}{\exp\left(\frac{E_k-E_0}{k_BT}\right)-1}$$

and we find in quadratic approximation the total excitation

$$\sum_k f_k = \frac{V}{(2\pi)^2}\int_0^\infty \mathrm{d}k\, 4\pi k^2 \frac{1}{\exp\left(\frac{JSk^2a^2}{k_BT}\right)-1} = V\left(\frac{k_BT}{JSa^2}\right)^{3/2} \underbrace{\frac{1}{2\pi^2}\int_0^\infty \mathrm{d}x \frac{1}{\mathrm{e}^{x^2}-1}}_{\approx 0.0586\ldots}\,.$$

As each magnon reduces the total magnetization by $g\mu_B/V$ and we find for simple cubic lattices with $V_c = a^3$

$$|\mathbf{M}| = \frac{g\mu_B S}{V_c}\left[1 - \frac{0.0586}{S^{5/2}}\left(\frac{k_BT}{J}\right)^{3/2}\right] \tag{3.17}$$

Thus the magnetization drops as $M(t) = M_0 - \text{const}T^{3/2}$, which constitutes a significant deviation from the mean field result, see Fig. 3.2. Similarly, the magnons contribute to the specific heat[15] $\propto T^{3/2}$.

[15] See Czycholl (2004)

Chapter 4

Introduction to dielectric function and semiconductor lasers

4.1 The dielectric function

In this section physical quantities such as the frequency or electric fields are frequently allowed to be complex in order to simplify calculations. In this case I denote quantities which are complex by an additional tilde (such as $\tilde{\omega}$).

Maxwell's equations in material

$$\begin{aligned} \operatorname{div} \mathbf{D}(\mathbf{r},t) &= \rho_{\text{free}}(\mathbf{r},t) && (4.1)\\ \operatorname{div} \mathbf{B}(\mathbf{r},t) &= 0 && (4.2)\\ \operatorname{rot} \mathbf{F}(\mathbf{r},t) &= -\frac{\partial}{\partial t}\mathbf{B}(\mathbf{r},t) && (4.3)\\ \operatorname{rot} \mathbf{H}(\mathbf{r},t) &= \mathbf{j}_{\text{free}}(\mathbf{r},t) + \frac{\partial}{\partial t}\mathbf{D}(\mathbf{r},t) && (4.4) \end{aligned}$$

together with the material relations

$$\mathbf{B}(\mathbf{r},t) = \mu_0\big(\mathbf{H}(\mathbf{r},t) + \mathbf{M}(\mathbf{r},t)\big) \quad \text{and} \quad \mathbf{D}(\mathbf{r},t) = \epsilon_0\mathbf{F}(\mathbf{r},t) + \mathbf{P}(\mathbf{r},t) \tag{4.5}$$

Here $\mathbf{F}$ is the electric field averaged over the atomic scale and ρ_{free}, $\mathbf{j}_{\text{free}}$ refer to macroscopic charges/currents, respectively.

In this chapter we concentrate on the polarization $\mathbf{P}(t)$ which is related to the electric field via

$$\mathbf{P}(t) = \int_{-\infty}^{t} \mathrm{d}t' \chi(t-t')\epsilon_0\mathbf{F}(t')$$

with the *susceptibility* function $\chi(t-t')$ which takes into account the history[1]. *It is important to realize, that the time argument in $\chi(t)$ refers to the time difference between field and polarization and not to a change of material properties with time.* A possible spatial dependence is ignored here and we assume that the response is local in space. We also assume an isotropic material, otherwise $\chi(t-t')$ becomes a tensor. We use the following convention for Fourier-transforms in time:

$$h(\omega) = \int_{-\infty}^{\infty} \mathrm{d}t\, h(t)\mathrm{e}^{\mathrm{i}\omega t} \quad \text{and} \quad h(t) = \frac{1}{2\pi}\int_{-\infty}^{\infty} \mathrm{d}\omega\, h(\omega)\mathrm{e}^{-\mathrm{i}\omega t}$$

[1] The conventional static susceptibility is given by $\chi = \chi(\omega) = const$ leading to $\chi(t) = \chi\delta(t)$.

If we define $\chi(t) = 0$ for $t < 0$ we find $\mathbf{P}(\omega) = \chi(\omega)\epsilon_0\mathbf{F}(\omega)$. Furthermore we define the *dielectric function* $\epsilon(\omega) = 1 + \chi(\omega)$ such that $\mathbf{D}(\omega) = \epsilon(\omega)\epsilon_0\mathbf{F}(\omega)$. In materials the dielectric function is essentially determined by four different effects:

1. The interaction with lattice vibrations, associated with elongations of the ionic charges. See Section 4.2.
2. Interaction of light with free carriers in the conduction band. See Section 4.3.
3. Electron-transitions between the bands, see Section 4.4.
4. Electron-electron interactions, see the discussion in Chapter 6.

4.1.1 Kramers-Kronig relation

While $\chi(t)$ is a real quantity by definition (both $\mathbf{P}(t)$ and $\mathbf{F}(t)$ physical quantities) its Fourier transform $\chi(\omega)$ can be complex. Causality implies that $\chi(t)$ vanishes for negative times. This provides a relation between imaginary and real part of $\chi(\omega)$, which is derived in the following.

Considering complex frequencies $\tilde{\omega}$ the Fourier transformation $\chi(\tilde{\omega}) = \int_0^\infty \mathrm{d}t\, \chi(t)\mathrm{e}^{\mathrm{i}\tilde{\omega}t}$ of the susceptibility converges for all $\tilde{\omega}$ with $\mathrm{Im}\{\tilde{\omega}\} > 0$ if $|\chi(t)|$ is bounded. Therefore the complex function $\chi(\tilde{\omega})$ is analytical in the upper half of the complex plane. The theory of complex functions tells us that this implies for real ω_0

$$0 = \oint_{\text{upper half plane}} \mathrm{d}\tilde{\omega} \frac{\chi(\tilde{\omega})}{\tilde{\omega} - \omega_0 + \mathrm{i}0^+} = \int_{-\infty}^{\infty} \mathrm{d}\omega \frac{\chi(\omega)}{\omega - \omega_0 + \mathrm{i}0^+} = \int_{-\infty}^{\infty} \mathrm{d}\omega \mathcal{P}\left\{\frac{\chi(\omega)}{\omega - \omega_0}\right\} - \mathrm{i}\pi\chi(\omega_0)$$

as $\omega_0 - \mathrm{i}0^+$ is outside the closed path of integration, where we used the relation (sometimes called Sokhotski-Weierstrass theorem)

$$\frac{1}{x - x_0 \pm \mathrm{i}0^+} = \mathcal{P}\left\{\frac{1}{x - x_0}\right\} \mp \mathrm{i}\pi\delta(x - x_0) \tag{4.6}$$

Separating imaginary and real part we obtain the *Kramers-Kronig Relations*

$$\mathrm{Re}\{\chi(\omega_0)\} = \frac{1}{\pi}\int_{-\infty}^{\infty} \mathrm{d}\omega \mathcal{P}\left\{\frac{\mathrm{Im}\{\chi(\omega)\}}{\omega - \omega_0}\right\}, \quad \mathrm{Im}\{\chi(\omega_0)\} = -\frac{1}{\pi}\int_{-\infty}^{\infty} \mathrm{d}\omega \mathcal{P}\left\{\frac{\mathrm{Re}\{\chi(\omega)\}}{\omega - \omega_0}\right\} \tag{4.7}$$

relating the imaginary part to the real part for any dielectric function satisfying causality.

Math used for Eq. (4.6): Lets consider the function

$$\frac{1}{x - x_0 + \mathrm{i}\epsilon} = \frac{x - x_0}{(x - x_0)^2 + \epsilon^2} - \mathrm{i}\frac{\epsilon}{(x - x_0)^2 + \epsilon^2}$$

For $\epsilon \to 0$, the real and imaginary part both develop a singularity at x_0. This singularity can often be cured by using the expression in an integral for finite $\epsilon > 0$ and performing the limit $\epsilon \to 0$ at a later stage. This procedure defines the principal value and the delta function as

$$\mathcal{P}\left\{\frac{1}{x - x_0}\right\} = \lim_{\epsilon\to 0} \frac{x - x_0}{(x - x_0)^2 + \epsilon^2} \qquad \delta(x - x_0) = \lim_{\epsilon\to 0} \frac{1}{\pi}\frac{\epsilon}{(x - x_0)^2 + \epsilon^2}$$

This limit $\lim_{\epsilon\to 0}$ for $\epsilon > 0$ (which has to be taken after an integration over one of the variables x, x_0) is specified by the notation $\epsilon \to 0^+$ providing Eq. (4.6)

4.1.2 Connection to oscillating fields

Assuming a homogeneous and isotropic material without macroscopic charges of currents, Maxwell's equations[2] give us for a plane wave

$$\mathbf{F}(\mathbf{r},t) = \mathrm{Re}\left\{\tilde{\mathbf{F}}_0 \mathrm{e}^{\mathrm{i}(\tilde{k}\mathbf{e}_k\cdot\mathbf{r}-\omega t)}\right\} \quad \text{and} \quad \mathbf{B}(\mathbf{r},t) = \mathrm{Re}\left\{\tilde{\mathbf{B}}_0 \mathrm{e}^{\mathrm{i}(\tilde{k}\mathbf{e}_k\cdot\mathbf{r}-\omega t)}\right\}$$

the relations

$$\mathbf{e}_k\cdot\tilde{\mathbf{B}}_0 = 0\,, \quad \tilde{\mathbf{B}}_0 = \frac{\tilde{k}}{\omega}\mathbf{e}_k\times\tilde{\mathbf{F}}_0\,, \quad \epsilon(\omega)\mathbf{e}_k\cdot\tilde{\mathbf{F}}_0 = 0 \quad \text{and} \quad \tilde{k}^2\left[\tilde{\mathbf{F}}_0 - \mathbf{e}_k(\mathbf{e}_k\cdot\tilde{\mathbf{F}}_0)\right] = \frac{\omega^2}{c^2}\epsilon(\omega)\tilde{\mathbf{F}}_0\,. \tag{4.8}$$

For *transversal fields* ($\mathbf{e}_k\cdot\tilde{\mathbf{F}}_0 = 0$), we find the common electromagnetic waves with the dispersion

$$\tilde{k} = \frac{\omega\tilde{n}}{c} = k + \mathrm{i}\frac{\alpha}{2} \quad \text{with} \quad \tilde{n} = \sqrt{\epsilon(\omega)} \tag{4.9}$$

where α is the absorption coefficient (in unit 1/length) for the radiation intensity I given by temporal average of the Poynting vector over one oscillation period

$$I(\mathbf{r}) = \langle\mathbf{F}(\mathbf{r},t)\times\mathbf{H}(\mathbf{r},t)\rangle = \left|\tilde{\mathbf{F}}_0\mathrm{e}^{\mathrm{i}\tilde{k}\mathbf{e}_k\cdot\mathbf{r}}\right|^2\frac{\mathrm{Re}\{\tilde{k}\}}{2\mu_0\omega} = |\tilde{\mathbf{F}}_0|^2\mathrm{e}^{-\alpha\mathbf{e}_k\cdot\mathbf{r}}\frac{nc\epsilon_0}{2}\mathbf{e}_k \tag{4.10}$$

where $n = \mathrm{Re}\{\tilde{n}\}$ is the *refractive index*, which describes the change in wavelength in the material.

Here α can be measured by the absorption of light with increasing thickness of a sample. The refractive index is commonly determined by the reflection of the light intensity given by

$$R = \left|\frac{\tilde{n}-1}{\tilde{n}+1}\right|^2 \tag{4.11}$$

for normal incidence from vacuum(air), see section 7.3 of D. Jackson *Electrodynamics*.[3] Inspecting Eqs. (4.10,4.11), we find:

This radiation intensity is zero if $\mathrm{Re}\{\tilde{n}\} = 0$, i.e. $\epsilon(\omega) \le 0$ and no radiation can propagate in the material. This is accompanied with total reflection $R = 1$ at the surface of the material.

For the *longitudinal fields* ($\mathbf{e}_k \parallel \mathbf{F}_0$), Eq. (4.8) provides the condition $\epsilon(\omega) = 0$, which may be satisfied at a discrete frequency ω_0. As $\mathbf{D}(\omega) = \epsilon(\omega)\epsilon_0\mathbf{F}(\omega)$ this allows for the presence of a finite electric field $F(t) \sim \mathrm{e}^{-\mathrm{i}\omega_0 t}$ with zero displacement $D(t)$. Eq. (4.5) shows that the polarization $\mathbf{P}(t) = -\mathbf{F}(t)/\epsilon_0$ oscillates in antiphase with the field providing a natural oscillation of the system at ω_0.

The zeros of $\epsilon(\omega)$ determine natural oscillations of the system, where the electric field is longitudinal and the magnetic field vanishes.

In most cases, however, n is positive and the situation becomes particularly simple, if we consider a small change in the dielectric properties in a host material with real ϵ_{host}. Then it is convenient to redefine [see, e.g., Sec 1.8 of Chow and Koch (1999)]

$$\mathbf{P}_{\mathrm{change}}(\omega) = \chi^{\mathrm{rel}}(\omega)\epsilon_{\mathrm{host}}\epsilon_0\mathbf{F}(\omega)$$

[2] As the magnetic susceptibility is small for most materials we neglect all magnetic properties and set in the following $\mu_r = 1$ for simplicity. This does not hold for specially designed metamaterials, where even $\mu_r < 0$ can be realized, see R.A. Shelby, D.R. Smith, and S. Schultz, Science **292**, 77 (2001).

[3] In practice one considers incidence under an oblique angle, where the polarization changes (ellipsometry), see chapter 6 of Yu and Cardona (1999).

Assuming $|\chi^{\rm rel}| \lesssim 1/2$ the change in refractive index is given by

$$\delta\tilde{n} = \sqrt{(1+\chi^{\rm rel}(\omega))\epsilon_{\rm host}} - \sqrt{\epsilon_{\rm host}} \approx \sqrt{\epsilon_{\rm host}}\chi^{\rm rel}(\omega)/2 \tag{4.12}$$

where we used the Taylor expansion $\sqrt{1+x} \approx 1 + x/2 - x^2/8 \ldots$. With $k_{\rm host} = \omega\sqrt{\epsilon_{\rm host}}/c$ we find from Eq. (4.9)

$$\begin{aligned} \delta k = k - k_{\rm host} &\approx k_{\rm host}\left(\frac{{\rm Re}\{\chi^{\rm rel}(\omega)\}}{2} + \mathcal{O}\left\{\frac{|\chi^{\rm rel}|^2}{8}\right\}\right) \\ \alpha &\approx k_{\rm host}{\rm Im}\{\chi^{\rm rel}(\omega)\}\left(1 + \mathcal{O}\left\{\frac{|\chi^{\rm rel}(\omega)|}{2}\right\}\right) \end{aligned} \tag{4.13}$$

Thus the imaginary part of $\chi^{\rm rel}(\omega)$ provides absorption and the real part a change in the refractive index (or, equivalently, the wavelength).

If ${\rm Im}\{\chi^{\rm rel}(\omega)\} < 0$, the absorption coefficient becomes negative, i.e., the radiation intensity increases while transversing the medium, which is called *gain* associated with the gain coefficient $G = -\alpha$.

4.2 Interaction with lattice vibrations

The lattice is formed by ions. Thus lattice vibration can be associated with local charge transfer on the atomic scale resulting in a polarization, which is of particular significance for optical phonons

As a model system we consider an harmonic oscillator with mass m_c effective charge $\tilde{q}$, frequency ω_0 and damping γ. For a given electric field $\mathbf{F}(t)$ we obtain the equation of motion for the elongations $\mathbf{s}$

$$m_c\ddot{\mathbf{s}}(t) + m_c\gamma\dot{\mathbf{s}}(t) + m_c\omega_0^2\mathbf{s}(t) = \tilde{q}\mathbf{F}(t) \quad \Leftrightarrow \quad \mathbf{s}(\omega)(\omega_0^2 - \omega^2 - {\rm i}\gamma\omega) = \frac{\tilde{q}}{m_c}\mathbf{F}(\omega)$$

Here we neglect the retroaction of the polarization on the electric field for simplicity.[4] The electric dipole moment $\mathbf{p} = \tilde{q}\mathbf{s}(t)$ is proportional to the elongation and thus, the dielectric function has the form

$$\epsilon(\omega) = \epsilon(\infty) + \frac{A}{\omega_0^2 - \omega^2 - {\rm i}\gamma\omega}$$

where $\epsilon(\infty)$ is the dielectric constant well above the phonon resonance, and A describes the strength of the interaction. We obtain the static dielectric constant $\epsilon(0) = \epsilon(\infty) + A/\omega_0^2$.[5] Thus we may write

$$\frac{\epsilon(\omega)}{\epsilon(\infty)} = 1 + \omega_0^2\left(\frac{\epsilon(0)}{\epsilon(\infty)} - 1\right)\left[\frac{\omega_0^2 - \omega^2}{(\omega_0^2-\omega^2)^2 + (\gamma\omega)^2} + {\rm i}\frac{\gamma\omega}{(\omega_0^2-\omega^2)^2 + (\gamma\omega)^2}\right] \tag{4.14}$$

We find that the imaginary part of $\epsilon(\omega)$ is positive and has a pole at the resonance frequency, while the real part exhibits a dramatic drop there, see Fig. 4.1.

[4] For a full treatment, see Ashcroft and Mermin (1979).

[5] This allows for a quantitative determination of $\tilde{q}$, as used in Eq. (2.26) for the matrix element of polar optical phonon scattering, which however, requires a more detailed treatment, see section 22.3.2 of Marder (2000).

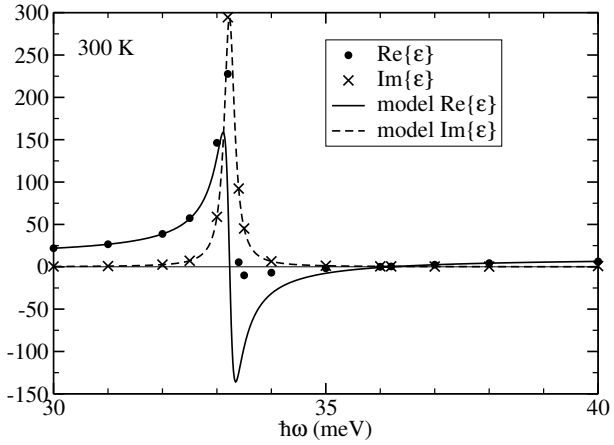

Figure 4.1: Dielectric function of GaAs from Eq. (4.14) with experimental data [from *Properties of GaAs*, edited by M.R. Brozel and G. E. Stillman (Inspec, 1995)]. We use $\epsilon(\infty) = 10.88$, $\epsilon(0) = 12.92$, and $\hbar\omega_0 = 33.23$ meV.

For $\gamma = 0$ the dielectric function becomes zero for $\omega = \omega_1$ with $\omega_1^2 = \omega_0^2 \frac{\epsilon(0)}{\epsilon(\infty)}$. As discussed in Sec. 4.1.2, this constitutes an oscillation mode with frequency ω_1 where the vibration of the ions is modified by the polarization field. For a finite phonon vector $\mathbf{q}$, we find the microscopic polarization charge $-\nabla\cdot\mathbf{P} \sim -\mathrm{i}\mathbf{q}\cdot\mathbf{P}$. Thus, the retroaction of the polarization on the oscillation is only possible for longitudinal phonon modes $\mathbf{q} \parallel \mathbf{s}$. Therefore $\omega_1 = \omega_{\mathrm{LO}}$ can be identified as the frequency of the longitudinal optical phonons. If the ionic elongations $\mathbf{s}$ are perpendicular to $\mathbf{q}$, there is no polarization charge with the same spatial behavior $\mathrm{e}^{\mathrm{i}\mathbf{q}\cdot\mathbf{r}}$ and $\omega_0 = \omega_{\mathrm{TO}}$ can be identified as the frequency of the transverse optical phonons.[6] This provides us with the Lyddane-Sachs-Teller relation

$$\frac{\omega_{\mathrm{LO}}^2}{\omega_{\mathrm{TO}}^2} = \frac{\epsilon(0)}{\epsilon(\infty)}$$

Further note, that the real part of $\epsilon(\omega)$ is negative for $\omega_{\mathrm{TO}} < \omega < \omega_{\mathrm{LO}}$, which is causing total reflectance at the surface of the material.

The imaginary part of the dielectric function has a pronounced peak at the frequency of the transversal optical phonons, ω_{TO}, while vanishing of the real part defines the longitudinal optical phonon frequency ω_{LO}.

Transverse polar optical phonons couple to the electromagnetic radiation, which is of particular significance for $q \approx \omega_{\mathrm{TO}}/c$. The coupled modes are called *polaritons*. Please consult your textbook for details!

4.3 Interaction with free carriers

The Drude model (2.5) provides a frequency dependent conductivity for the electrons in the conduction band with density n_c and effective mass m_{eff}

$$\sigma(\omega) = \frac{n_c e^2}{m_{\mathrm{eff}}} \frac{1}{\frac{1}{\tau} - \mathrm{i}\omega} .$$

Now the polarization changes by microscopic currents transferring charge by $\dot{\mathbf{P}} = \mathbf{J}$, thus $-\mathrm{i}\omega\mathbf{P}(\omega) = \mathbf{J}(\omega) = \sigma(\omega)\mathbf{F}(\omega)$ and we find $\chi^{\mathrm{rel}}(\omega) = \mathrm{i}\sigma(\omega)/(\omega\epsilon_{\mathrm{host}}\epsilon_0)$. This yields

$$\chi^{\mathrm{rel}}(\omega) = -\frac{n_c e^2}{m_{\mathrm{eff}}\epsilon_{\mathrm{host}}\epsilon_0} \frac{1}{\omega^2 + \mathrm{i}\frac{\omega}{\tau}} \tag{4.15}$$

[6] This is only true for $|\mathbf{q}| \gg \omega_0/c$ – otherwise one has to include the formation of polaritons due to the interaction of transverse phonons with the light field, which is always of transverse character. At $\mathbf{q} = 0$, where one cannot distinguish between transverse and longitudinal character, the transverse phonons appear indeed with the frequency ω_{LO}.

Adding the host contribution, this provides the dielectric function

$$\tilde{\epsilon}(\omega) = \epsilon_{\text{host}} \left[1 - \frac{\omega_{\text{pl}}^2 \tau^2}{\omega^2\tau^2+1} \left(1 - \mathrm{i}\frac{1}{\omega\tau} \right) \right] \quad \text{with the plasma frequency} \quad \omega_{\text{pl}}^2 = \frac{n_c e^2}{m_{\text{eff}} \epsilon_{\text{host}} \epsilon_0}$$

For $\omega_{\text{pl}}\tau < 1$ (moderately doped semiconductors), the real part is always positive and we find absorption due to the positive imaginary part. This is the free carrier absorption

$$\alpha_{\text{free carrier}} = \frac{\sigma(0)}{c\sqrt{\epsilon_{\text{host}}}\epsilon_0} \frac{1}{\omega^2\tau^2+1}$$

which is of importance for the THz physics in doped semiconductors, see Yu and Cardona (1999) for details.

If, on the other hand, $\omega_{\text{pl}}\tau \gg 1$ (metals), we find a zero of $\epsilon(\omega)$ at the plasma frequency ω_{pl}, which is a self-sustained longitudinal oscillation, as discussed in the exercise. Note, that for $1/\tau \ll \omega < \omega_{\text{pl}}$ we observe a negative $\tilde{\epsilon}(\omega)$, which implies total reflection. As $\hbar\omega_{\text{pl}} \sim 10\text{eV}$ for metals ($n \sim 10^{23}/\text{cm}^3, m_{\text{eff}} \approx m_e, \epsilon_{\text{host}} \approx 1$), this implies that metals reflect visible light.

4.4 Optical transitions

The electromagnetic field is given in Coulomb gauge by

$$\mathbf{A}(\mathbf{r},t) = \frac{1}{2\mathrm{i}\omega} \left(\mathbf{F}_0 \mathrm{e}^{\mathrm{i}\mathbf{q}\cdot\mathbf{r}-\mathrm{i}\omega t} - \mathbf{F}_0^* \mathrm{e}^{-\mathrm{i}\mathbf{q}\cdot\mathbf{r}+\mathrm{i}\omega t} \right) \quad \text{with} \quad q = n\omega/c \quad \text{and} \quad \mathbf{A}_0 \cdot \mathbf{q} = 0 \tag{4.16}$$

where n is the refractive index ($n \approx 3.6$ for GaAs for $\hbar\omega \approx E_{\text{gap}} = 1.43$ eV). Using Eq. (1.20) this gives us the perturbation potential[7]

$$\hat{V}(t) = \hat{F}\mathrm{e}^{-\mathrm{i}\omega t} + \hat{F}^\dagger \mathrm{e}^{\mathrm{i}\omega t} + \mathcal{O}(F_0^2) \quad \text{with} \quad \hat{F} = \frac{e}{2\mathrm{i}\omega m_e} \mathrm{e}^{\mathrm{i}\mathbf{q}\cdot\mathbf{r}} \mathbf{F}_0 \cdot \hat{\mathbf{p}}$$

providing the scattering matrix element

$$\begin{aligned} \langle \Psi_{n'\mathbf{k}'} | \hat{F} | \Psi_{n\mathbf{k}} \rangle =& \frac{e\mathbf{F}_0}{2\mathrm{i}\omega m_e} \cdot \frac{1}{V_c} \int_{V_c} \mathrm{d}^3 r \underbrace{\frac{1}{N} \sum_{\mathbf{R}} \mathrm{e}^{\mathrm{i}(\mathbf{q}+\mathbf{k}-\mathbf{k}')\cdot\mathbf{R}}}_{=\delta_{\mathbf{k}',\mathbf{q}+\mathbf{k}} \approx \delta_{\mathbf{k}',\mathbf{k}}} \mathrm{e}^{-\mathrm{i}(\mathbf{k}'-\mathbf{q})\cdot\mathbf{r}} u_{n'\mathbf{k}'}^*(\mathbf{r}) \hat{\mathbf{p}} \mathrm{e}^{\mathrm{i}\mathbf{k}\cdot\mathbf{r}} u_{n\mathbf{k}}(\mathbf{r}) \\ \approx& \frac{e}{2\mathrm{i}\omega m_e} \delta_{\mathbf{k}',\mathbf{k}} \mathbf{F}_0 \cdot \mathbf{P}_{n'n}(\mathbf{k}) \end{aligned} \tag{4.17}$$

with the momentum matrix element from Eq. (1.16). Here we used the fact that the q-vector of the photon ($\sim 1/\mu\text{m}$) is negligible with respect to the extension of the Brillouin zone, which implies that $\mathbf{k} \approx \mathbf{k}'$ holds. Using $\hat{\mathbf{p}} = \mathrm{i}m_e[\hat{H}_0, \hat{\mathbf{r}}]/\hbar$, we find for normalizable (i.e. localized) eigenstates $|a\rangle, |b\rangle$ of $\hat{H}_0$ the electric dipole moment:

$$\boldsymbol{\mu}_{ab} = -e\langle a|\mathbf{r}|b\rangle = -\frac{e}{E_a - E_b}\langle a|[\hat{H}_0, \hat{\mathbf{r}}]|b\rangle = \frac{\mathrm{i}e\hbar}{m_e(E_a-E_b)}\langle a|\hat{\mathbf{p}}|b\rangle$$

In the same spirit, we define the transition dipole-moment as

$$\boldsymbol{\mu}_{n'n}(\mathbf{k}) = \frac{\mathrm{i}e\hbar}{m_e} \frac{1}{E_{n'}(\mathbf{k}) - E_n(\mathbf{k})} \mathbf{P}_{n'n}(\mathbf{k}) \tag{4.18}$$

[7] Notation as in `http://www.teorfys.lu.se/Staff/Andreas.Wacker/Scripts/fermiGR.pdf`

albeit the Bloch states $|n\mathbf{k}\rangle$ are not-normalizable and the expression $\langle n'\mathbf{k}|\mathbf{r}|n\mathbf{k}\rangle$ is ill defined.[8] However, this comparison suggests, that $\boldsymbol{\mu}_{n'n}(\mathbf{k})$ is of the order of elementary charge times lattice constant. Putting things together and taking into account that the energy-conserving δ-function implies $E_{n'}(\mathbf{k}) - E_n(\mathbf{k}) = \pm\hbar\omega$ we find the total transition rate from Fermi's golden rule

$$W_{n\mathbf{k}\to n'\mathbf{k}} = \frac{2\pi}{\hbar}\left|\frac{1}{2}\mathbf{F}_0\cdot\boldsymbol{\mu}_{n'n}(\mathbf{k})\right|^2 \left[\delta(E_{n'}(\mathbf{k}) - E_n(\mathbf{k}) - \hbar\omega) + \delta(E_{n'}(\mathbf{k}) - E_n(\mathbf{k}) + \hbar\omega)\right]$$

Now we investigate transitions between the valence and the conduction band in a semiconductor and we find the net transition rate

$$R_{v\to c} = \frac{2\pi}{\hbar}\sum_{\mathbf{k}}\left|\frac{1}{2}\mathbf{F}_0\cdot\boldsymbol{\mu}_{cv}(\mathbf{k})\right|^2 \delta(E_c(\mathbf{k}) - E_v(\mathbf{k}) - \hbar\omega)\left[f_v(\mathbf{k}) - f_c(\mathbf{k})\right] \tag{4.19}$$

where the transition $c \to v$ are due to stimulated emission and $v \to c$ are due to stimulated absorption of a photon. Both processes are related to a change of the number of photons which can be quantified as follows: The decrease in energy density of the radiation field is $R_{v\to c}\hbar\omega/V$, while the average energy flux density is given by Eq. (4.10). The ratio gives the absorption coefficient

$$\alpha(\omega) = \frac{R_{v\to c}\hbar\omega}{VI} = \frac{\pi\omega}{c\epsilon_0 n}\frac{1}{V}\sum_{\mathbf{k}}\left|\mu_{cv}(\mathbf{k})\right|^2\delta(E_c(\mathbf{k}) - E_v(\mathbf{k}) - \hbar\omega)\left[f_v(\mathbf{k}) - f_c(\mathbf{k})\right] \tag{4.20}$$

which describes the decrease of radiation intensity by length (unit 1/cm). Here μ_{cv} is the component of the electric dipole matrix element in the direction of the electric field.

Using parabolic bands with $E_c(\mathbf{k}) = E_c + \hbar^2k^2/2m_c$ and $E_v(\mathbf{k}) = E_v - \hbar^2k^2/2m_h$, a transition at $\mathbf{k}$ corresponds to the frequency

$$\hbar\omega = E_c(\mathbf{k}) - E_v(\mathbf{k}) = E_{\text{gap}} + \frac{\hbar^2k^2}{2m_r} \quad \text{with} \quad m_r = \frac{m_cm_h}{m_c+m_h}$$

In order to simplify Eq. (4.20) we assume a constant dipole matrix element and that $f_{c/v}(\mathbf{k})$ only depends on the respective energy $E_{c/v}(\mathbf{k})$. Then we set $E_k = \hbar^2k^2/2m_r$ and use

$$\frac{1}{V}\sum_{\mathbf{k}} \to \int \mathrm{d}E_k D_{\text{joint}}(E_k) \quad \text{with the joint density of states} \quad D_{\text{joint}}(E_k) = \frac{m_r^{3/2}\sqrt{2E_k}}{\pi^2\hbar^3}\Theta(E_k)$$

in the continuum limit (spin is contained in the $\mathbf{k}$-sum) and obtain

$$\begin{aligned}\alpha(\omega) =& \frac{\pi\omega\left|\mu_{cv}\right|^2}{c\epsilon_0 n}D_{\text{joint}}(\hbar\omega - E_{\text{gap}}) \\ &\times\left[f_v\left(E_v - (\hbar\omega - E_{\text{gap}})\frac{m_r}{m_h}\right) - f_c\left(E_c + (\hbar\omega - E_{\text{gap}})\frac{m_r}{m_c}\right)\right]\end{aligned} \tag{4.21}$$

For a semiconductor in the ground state with $f_c \approx 0$ and $f_v \approx 1$ we thus find the

absorption for a pure semiconductor $\alpha \propto \Theta(\hbar\omega - E_{\text{gap}})\sqrt{\hbar\omega - E_{\text{gap}}}$

as shown in Fig. (4.2). For conversion to wavelength (in vacuum/air, the wavelength in the semiconductor is reduced by the factor $1/n$) we have $\lambda = 2\pi c/\omega = 1.24\mu\text{m}/E$, where the energy is in eV. One can memorize that green light is approximately 550 nm, 550 THz or 2.3 eV. A collection of data for the band gap of different semiconductors is shown in Fig. 4.3.

[8] See M.G. Burt, J. Phys. Condensed Matter **5**, 4091 (1993)

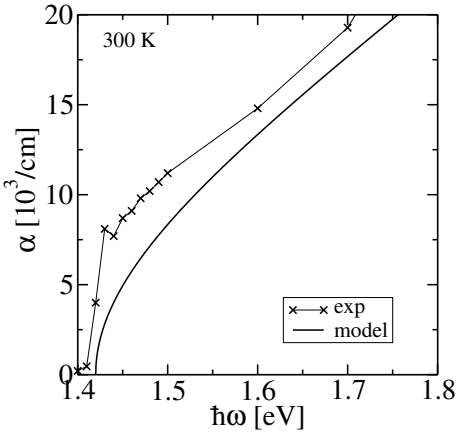

Figure 4.2: Absorption of GaAs from Eq. (4.21) using $E_{\rm gap} = 1.42$eV, $m_r = 0.06$, $\mu_{cv} = e \times 0.5$nm in comparison with experimental data [from *Properties of GaAs*, edited by M.R. Brozel and G. E. Stillman (Inspec, 1995)]. The strong deviation between experiment and theory around $E_{\rm gap}$ is due to the exciton peak discussed in section 6.1.3.

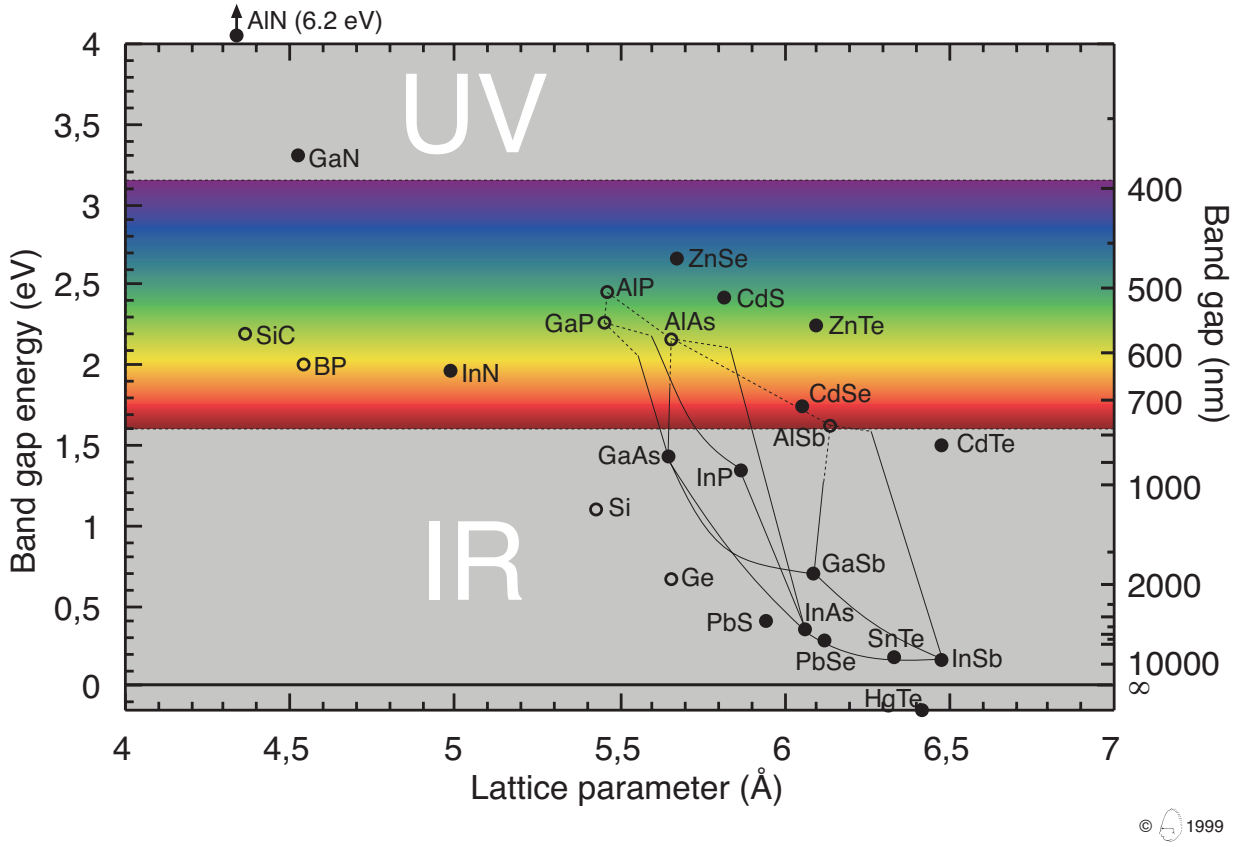

Figure 4.3: Band gap and lattice constant of different semiconductors, full/open circles indicate direct/indirect gaps, respectively. (At indirect gaps the minimum of the conduction band is at a different position in the Brillouin zone than the maximum of the valance band, which does not allow for direct optical transitions.) @ Martin H. Magnusson, Lund University

4.5 The semiconductor laser

In thermal equilibrium we have $f_c(\mathbf{k}) \ll f_v(\mathbf{k})$ and Eq. (4.20) shows that there is only absorption of radiation. However, in the vicinity of a *pn-junction in forward bias*, there is a strong injection of conduction band electrons from the n region and of holes from the p-region, see Fig. 4.4. This allows for *inversion* $f_c(\mathbf{k}) > f_v(\mathbf{k})$, in particular for those $\mathbf{k}$-values close to the band edge. This provides negative $\alpha(\omega)$, i.e. gain, for frequencies close to $E_{\rm gap}/\hbar$. The occurrence of gain in such a pn-diode can be used to fabricate semiconductor lasers. In practice, one combines the pn-

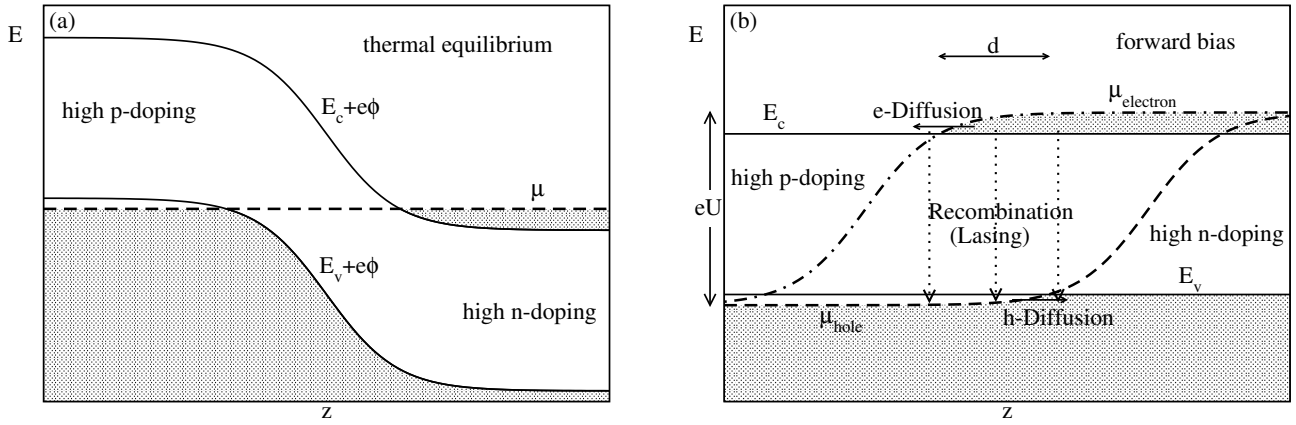

Figure 4.4: Scheme of a semiconductor laser: a) pn-diode in equilibrium. b) pn-diode under forward bias $eU = \mu_{\rm el} - \mu_{\rm hole} \approx E_{\rm gap}$. There is inversion within the recombination zone.

junction with a semiconductor heterostructure (the advantage is quantified in Sects. 4.5.1,4.5.2, see Fig. 4.5. If the confinement is smaller than the thermal wavelength of the carriers (typically 20 nm), one speaks about quantum well lasers.

4.5.1 Phenomenological description of gain*

The occupation $f_c(\mathbf{k})$ in the active region depends on the carrier density N in the conduction band, which is determined by a rate equation[9]

$$\frac{{\rm d}N(t)}{{\rm d}t} = \frac{J\eta}{ed} - N\gamma_{\rm eff} - \frac{1}{V}R_{c\to v} \tag{4.22}$$

where η is the efficiency, with which the carriers reach the active region of thickness d. $\gamma_{\rm eff}$ is the effective recombination rate. Gain, the increase of the radiation intensity per length, can be expressed in the active region by

$$G = A_g(N - N_g) \tag{4.23}$$

where N_g is the density, where stimulated emission and absorption compensate each other.

For small optical fields, $R_{c\to v}$ can be neglected in Eq. (4.22) and we have the stationary solution

$$N = N_0 = \frac{J\eta}{e\gamma_{\rm eff}d}, \quad G = G_0 = A_g(N_0 - N_g) \tag{4.24}$$

In contrast, for large intensities I of the optical field Eq. (4.22) gives us

$$N = N_g + \frac{N_0 - N_g}{1 + \frac{I}{I_{\rm sat}}}, \quad G = \frac{G_0}{1 + \frac{I}{I_{\rm sat}}} \quad \text{with} \quad I_{\rm sat} = \frac{\hbar\omega\gamma_{\rm eff}}{A_g}$$

where $R_{c\to v}\hbar\omega = VGI$ has been used[10]. Thus the *gain saturates* at high lasing intensities.

[9] I follow chapter 1 of Chow and Koch (1999) here.

[10] Note that $\gamma_{\rm eff}$ comprehends non-radiative recombination γ_{nr} as well as radiative recombination by spontaneous optical transitions. The latter give a rate which is $\propto N^2$ or $\propto N^{3/2}$ (see, e.g., Fig. 2.3 of Chow and Koch (1999)). Thus $\gamma_{\rm eff}(N)$ depends on density and $\gamma_{\rm eff}(N_0)$ should be used in Eq. (4.24) to determine N_0. while $\gamma_{\rm eff}(N_g) \approx \gamma_{nr}$ is more appropriate for $I_{\rm sat}$.

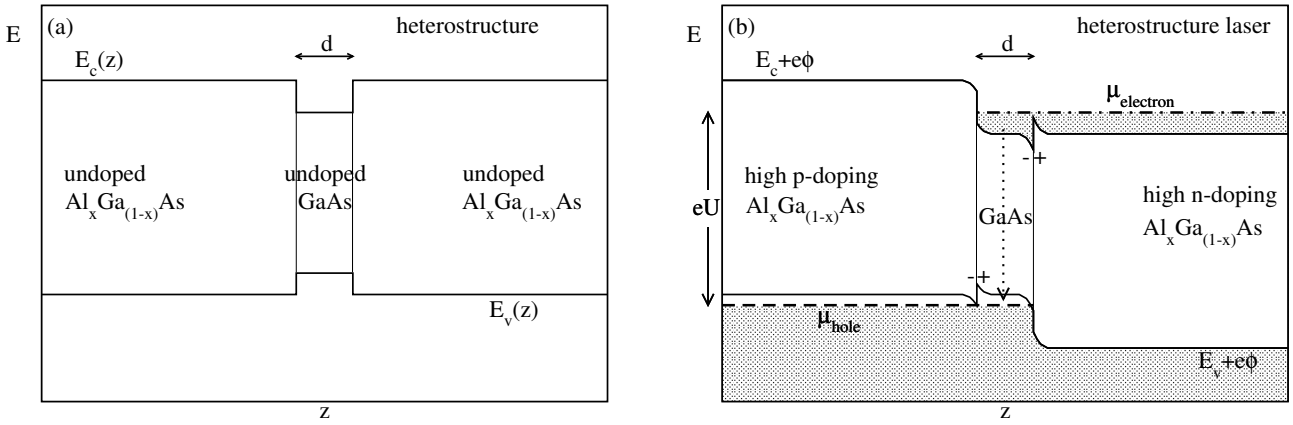

Figure 4.5: Scheme of a heterostructure laser

4.5.2 Threshold current*

A laser combines gain material with a resonator cavity of length L, with reflectivity R_1, R_2. Here one may use the (parallel!) facets of the semiconductor crystal, exploiting Fresnel reflection. The condition for lasing is that the radiation is enhanced during a round-trip in the cavity, i.e.

$$R_1 R_2 \mathrm{e}^{2(\Gamma G - \alpha_{\mathrm{abs}})L} > 1$$

where the confinement factor $\Gamma < 1$ is the overlap of the optical mode with the active region and α_{abs} denotes the absorption in the material. This provides us with

$$J > J_{\mathrm{th}} = \frac{e\gamma_{\mathrm{eff}} d}{\eta} \left\{ N_g + \frac{1}{A_g \Gamma} \left[\alpha_{\mathrm{abs}} - \frac{1}{2L} \log(R_1 R_2) \right] \right\}$$

where the threshold current density J_{th} is a key figure of merit. In order to minimize power consumption and lattice heating a low value is desirable. This implies

- Low recombination rate γ_{eff}. As non-radiative recombination occurs at lattice imperfections, this implies a good crystal quality.
- High capture efficiency $\eta \approx 1$ of the injected carriers to the active zone.
- Small thickness d of active region. For standard pn-junctions the active region is of the order of the diffusion length[11], which is typically several μm. Therefore a crucial improvement was the use of semiconductors heterostructures (Nobel prize for Alferov and Kroemer, 2000) in the late 60ies, which confine the carriers to a smaller region, see Fig. 4.5.
- Small N_g, and large A_g, describing the gain properties of the material. As the carriers are spread over a wider k-range for increasing temperature, N_g increases with temperature. The temperature dependence is often written as $J_{\mathrm{th}} \sim \mathrm{e}^{T/T_0}$ where T_0 is the characteristic temperature of the laser.[12]
- Good confinement of the optical mode around the active region by a waveguide resulting in large values of Γ.

[11] See section 12.7 of Ibach and Lüth (2003)

[12] I do not know the origin of the exponential behavior.

Chapter 5

Quantum kinetics of many-particle systems

5.1 Occupation number formalism

The occupation number formalism (also called second quantization) is the central tool for describing the quantum mechanics of many-particle systems. Here I give a short summary. Detailed proofs are given in the textbooks Schrieffer (1983); Kittel (1987); Czycholl (2004).

If we treat a system of many identical particles, it is extremely cumbersome to work with many-particle wave functions as in section 3.3.1. In particular it is difficult to keep track of the antisymmetry. Furthermore, this formulation is only appropriate for a fixed number of particles.

To overcome these problems, the occupation number representation is a convenient way, which is the standard tool of many-particle physics.

5.1.1 Definitions

Here we start with a fixed basis set of orthonormal single-particle states $\varphi_n(\mathbf{r})$ where $n = 1, 2, \ldots$ labels the states. For a crystal one typically uses the Bloch states and the addition of spin is straightforward.

For an N-particle state we write the Slater determinant (3.10) formed by the states with indices $n_1, n_2 \ldots n_N$ (with $n_1 < n_2 \ldots < n_N$) as an abstract state

$$|\underset{n=1}{0}, 0, \underset{n=n_1}{1}, 0, 0, \underset{n=n_2}{1}, \underset{n=n_3}{1}, 0, \ldots\rangle = |o_1, o_2, \ldots o_n, \ldots\rangle\,.$$

Here the numbers o_n are 1 if $n \in \{n_1, n_2 \ldots n_N\}$ and 0 otherwise. They give the occupations of the states $|\varphi_n\rangle$ in the many-particle state. Two such states differ unless all occupations are identical, and we have the orthonormality relation

$$\langle o_1', o_2', \ldots | o_1, o_2, \ldots\rangle = \delta_{o_1', o_1}\delta_{o_2', o_2}\ldots$$

which can be verified by using the corresponding Slater determinants. Furthermore we define creation $\hat{a}_n^\dagger$ and annihilation operators $\hat{a}_n$ of a particle in state n by their action on our states via

$$\hat{a}_n^\dagger |o_1, o_2, \ldots o_n, \ldots\rangle = \delta_{o_n,0}(-1)^{S_n}|o_1, o_2, \ldots o_n + 1, \ldots\rangle \quad (5.1)$$

$$\hat{a}_n |o_1, o_2, \ldots o_n, \ldots\rangle = \delta_{o_n,1}(-1)^{S_n}|o_1, o_2, \ldots o_n - 1, \ldots\rangle \quad (5.2)$$

where $S_n = \sum_{n'=1}^{n-1} o_{n'}$. The notation indicates, that the creation operator is the adjoint of the annihilation operator. This is indeed true as $\langle o|\hat{a}_n^\dagger|o'\rangle = (-1)^{S'_n}\delta_{o'_n,0}\delta_{o_n,1}\prod_{i\neq n}\delta_{o'_i,o_i} = \langle o'|\hat{a}_n|o\rangle^*$ holds for arbitrary states $|o\rangle = |o_1, o_2, \ldots\rangle$ and $|o'\rangle = |o'_1, o'_2, \ldots\rangle$.

Now we define the

$$\textbf{vacuum state} \quad |0\rangle = |0, 0, 0, \ldots\rangle \tag{5.3}$$

which does not contain any particles. Note that this state is a physical state with norm one, i.e. $\langle 0|0\rangle = 1$ in contrast to the null-element $|\text{null}\rangle$ of the space, which has $\langle\text{null}|\text{null}\rangle = 0$. For example this null-element is obtained by annihilating a state which is not there, $\hat{a}_1|0, o_2, \ldots\rangle = |\text{null}\rangle$, or by multiplying an arbitrary state with zero, $0|\Psi\rangle = |\text{null}\rangle$. The difference between $|\text{null}\rangle$ and $|0\rangle$ becomes particularly clear for the action of a creation operator:

$$\hat{a}_1^\dagger|0\rangle = |1, 0, 0, \ldots\rangle \quad \text{while} \quad \hat{a}_1^\dagger|\text{null}\rangle = |\text{null}\rangle$$

In this spirit any many-particle Slater state formed by the states with indices $n_1, n_2 \ldots n_N$ can be written as

$$|\underset{n=1}{0}, 0, \underset{n=n_1}{1}, 0, 0, \underset{n=n_2}{1}, \underset{n=n_3}{1}, 0, \ldots\rangle = \hat{a}_{n_1}^\dagger \hat{a}_{n_2}^\dagger \ldots \hat{a}_{n_N}^\dagger|0\rangle$$

which provides a very easy notation. Note that the exchange of two indices gives a factor -1 due to the definition (5.1) as appropriate for fermions.

Example: The singlet state (3.11) reads for $a \neq b$:

$$\begin{aligned}\Psi_{\text{Singlet}}(\mathbf{r}_1, s_1; \mathbf{r}_2, s_2) = \frac{1}{\sqrt{2}}\Big[&\frac{1}{\sqrt{2}}\left(\varphi_a(\mathbf{r}_1)\chi_\alpha(s_1)\varphi_b(\mathbf{r}_2)\chi_\beta(s_2) - \varphi_b(\mathbf{r}_1)\chi_\beta(s_1)\varphi_a(\mathbf{r}_2)\chi_\alpha(s_2)\right)\\ &+ \frac{1}{\sqrt{2}}\left(\varphi_b(\mathbf{r}_1)\chi_\alpha(s_1)\varphi_a(\mathbf{r}_2)\chi_\beta(s_2) - \varphi_a(\mathbf{r}_1)\chi_\beta(s_1)\varphi_b(\mathbf{r}_2)\chi_\alpha(s_2)\right)\Big]\end{aligned}$$

and thus can be written as

$$|\Psi_{\text{Singlet}}\rangle = \frac{1}{\sqrt{2}}\left[\hat{a}_{a\alpha}^\dagger\hat{a}_{b\beta}^\dagger|0\rangle + \hat{a}_{b\alpha}^\dagger\hat{a}_{a\beta}^\dagger|0\rangle\right]$$

in occupation number representation.

5.1.2 Anti-commutation rules

The fermionic creation and annihilation operators satisfy the

Anti-commutation rules

$$\left\{\hat{a}_n^\dagger, \hat{a}_{n'}^\dagger\right\} = 0 \quad \{\hat{a}_n, \hat{a}_{n'}\} = 0 \quad \left\{\hat{a}_n, \hat{a}_{n'}^\dagger\right\} = \delta_{n,n'} \tag{5.4}$$

where $\left\{\hat{A}, \hat{B}\right\} = \hat{A}\hat{B} + \hat{B}\hat{A}$

$\left\{\hat{A}, \hat{B}\right\} = 0$ implies $\hat{A}\hat{B} = -\hat{B}\hat{A}$. Thus exchanging the order of the annihilation or creation operators provides a minus sign for fermions.

If both operators refer to the same state ($n = n'$) we find:

- $\hat{a}_n\hat{a}_n = \hat{a}_n^\dagger\hat{a}_n^\dagger = 0$. Thus it is not possible to annihilate or create two particles in the same state, in accordance with the Pauli principle.

- $\hat{a}_n\hat{a}_n^\dagger = 1-\hat{a}_n^\dagger\hat{a}_n$ as well as $\hat{a}_n^\dagger\hat{a}_n = 1-\hat{a}_n\hat{a}_n^\dagger$. Thus exchanging the order of an annihilation and a creation operator for the same state gives an additional 1.

- $\hat{a}_n^\dagger\hat{a}_n|o_1, o_2, \ldots o_n, \ldots\rangle = \delta_{o_n,1}|o_1, o_2, \ldots o_n, \ldots\rangle$. Thus $\hat{a}_n^\dagger\hat{a}_n$ is the *number operator* counting the number of particles in state n.

Proof: (exemplary for $\hat{a}_{n_1}\hat{a}_{n_2}^\dagger = \delta_{n_1,n_2} - \hat{a}_{n_2}^\dagger\hat{a}_{n_1}$ with $n_1 \leq n_2$)
For $n_1 < n_2$ we find

$$\begin{aligned}
\hat{a}_{n_1}\hat{a}_{n_2}^\dagger|o_1, \ldots o_{n_1}, \ldots o_{n_2}, \ldots\rangle =& \hat{a}_{n_1}\delta_{o_{n_2},0}(-1)^{S_{n_2}}|o_1, \ldots o_{n_1}, \ldots \underset{n=n_2}{1}, \ldots\rangle \\
=& \delta_{o_{n_1},1}\delta_{o_{n_2},0}(-1)^{S_{n_1}}(-1)^{S_{n_2}}|o_1, \ldots \underset{n=n_1}{0}, \ldots \underset{n=n_2}{1}, \ldots\rangle \\
=& \delta_{o_{n_1},1}(-1)^{S_{n_1}}(-1)\hat{a}_{n_2}^\dagger|o_1, \ldots \underset{n=n_1}{0}, \ldots o_{n_2}, \ldots\rangle \\
=& (-1)\hat{a}_{n_2}^\dagger\hat{a}_{n_1}|o_1, \ldots o_{n_1}, \ldots o_{n_2}, \ldots\rangle
\end{aligned}$$

and for $n_1 = n_2$

$$\begin{aligned}
\hat{a}_{n_1}\hat{a}_{n_1}^\dagger|o_1, \ldots o_{n_1}, \ldots\rangle =& \hat{a}_{n_1}\delta_{o_{n_1},0}(-1)^{S_{n_1}}|o_1, \ldots \underset{n=n_1}{1}, \ldots\rangle = \delta_{o_{n_1},0}|o_1, \ldots o_{n_1}, \ldots\rangle \\
=& |o_1, \ldots o_{n_1}, \ldots\rangle - \delta_{o_{n_1},1}|o_1, \ldots o_{n_1}, \ldots\rangle \\
=& |o_1, \ldots o_{n_1}, \ldots\rangle - \delta_{o_{n_1},1}\hat{a}_{n_1}^\dagger(-1)^{S_{n_1}}|o_1, \ldots \underset{n=n_1}{0}, \ldots\rangle \\
=& |o_1, \ldots o_{n_1}, \ldots\rangle - \hat{a}_{n_1}^\dagger\hat{a}_{n_1}|o_1, \ldots o_{n_1}, \ldots\rangle = (1-\hat{a}_{n_1}^\dagger\hat{a}_{n_1})|o_1, \ldots o_{n_1}, \ldots\rangle
\end{aligned}$$

5.1.3 Field operators

We define the field operators[1]

$$\hat{\Psi}(\mathbf{r}) = \sum_n \varphi_n(\mathbf{r})\hat{a}_n \qquad \hat{\Psi}^\dagger(\mathbf{r}) = \sum_n \varphi_n^*(\mathbf{r})\hat{a}_n^\dagger \tag{5.5}$$

which satisfy $\{\hat{\Psi}(\mathbf{r}), \hat{\Psi}(\mathbf{r}')\} = 0$, $\{\hat{\Psi}^\dagger(\mathbf{r}), \hat{\Psi}^\dagger(\mathbf{r}')\} = 0$, and $\{\hat{\Psi}(\mathbf{r}), \hat{\Psi}^\dagger(\mathbf{r}')\} = \delta(\mathbf{r}-\mathbf{r}')$. We find

$$\langle o_1, o_2, \ldots|\hat{\Psi}^\dagger(\mathbf{r})\hat{\Psi}(\mathbf{r})|o_1, o_2, \ldots\rangle = \sum_{nn'} \varphi_{n'}^*(\mathbf{r})\varphi_n(\mathbf{r}) \underbrace{\langle o_1, o_2, \ldots|\hat{a}_{n'}^\dagger\hat{a}_n|o_1, o_2, \ldots\rangle}_{o_n\delta_{n,n'}} = \sum_n o_n|\varphi_n(\mathbf{r})|^2$$

Thus $\hat{\Psi}^\dagger(\mathbf{r})\hat{\Psi}(\mathbf{r})$ gives us the total particle density at $\mathbf{r}$. We may interpret the field operators as follows

- $\hat{\Psi}^\dagger(\mathbf{r})$ creates a particle at position $\mathbf{r}$

- $\hat{\Psi}(\mathbf{r})$ annihilates a particle at position $\mathbf{r}$

Historically, the transition from the Schrödinger wave function $\Psi(\mathbf{r})$ to the field operator $\hat{\Psi}(\mathbf{r})$ was considered as a quantization. Therefore the name *second quantization* is frequently used synonymously for occupation number formalism.

[1]For spin-dependent systems this is generalized by $\hat{\Psi}(\mathbf{r}, s) = \sum_n \varphi_n(\mathbf{r}, s)\hat{a}_n$.

5.1.4 Operators

Now we consider a systems of N identical particles. We have single-particle operators

$$\hat{O}_{\text{single particle}} = \sum_{i=1}^{N} \hat{O}(i)$$

which act on each particle i individually. Typical examples are the kinetic energy $\hat{T}(i) = \hat{\mathbf{p}}^2/2m$, external potentials $\hat{U}(i) = U(\mathbf{r}_i)$, or the spin-orbit interaction $\hat{O}(i) = f(r_i)\hat{\mathbf{L}}_i \cdot \hat{\mathbf{S}}_i$. In the same spirit there are two-particle operators

$$\hat{O}_{\text{two particle}} = \frac{1}{2}\sum_{i=1}^{N}\sum_{j=1}^{N} \hat{O}(i,j)$$

where the Coulomb interaction $\hat{V}^{ee}(i,j) = \frac{e^2}{4\pi\epsilon_0|\mathbf{r}_i - \mathbf{r}_j|}$ is a typical example. Starting with the spatial representations $\hat{O}^{\text{SR}}(\mathbf{r})$, $\hat{O}^{\text{SR}}(\mathbf{r},\mathbf{r}')$ of the individual operators, it is suggestive to write in occupation number formalism

$$\hat{O}_{\text{single particle}} = \int \mathrm{d}^3 r\, \hat{\Psi}^\dagger(\mathbf{r}) \hat{O}^{\text{SR}}(\mathbf{r}) \hat{\Psi}(\mathbf{r})$$
$$\hat{O}_{\text{two particle}} = \frac{1}{2}\int \mathrm{d}^3 r \int \mathrm{d}^3 r'\, \hat{\Psi}^\dagger(\mathbf{r})\hat{\Psi}^\dagger(\mathbf{r}') \hat{O}^{\text{SR}}(\mathbf{r},\mathbf{r}') \hat{\Psi}(\mathbf{r}')\hat{\Psi}(\mathbf{r})$$

Using the definition of the field operators we find the[2]

Operators in occupation number formalism

$$\hat{O}_{\text{single particle}} = \sum_{n,m} O_{nm} \hat{a}_n^\dagger \hat{a}_m \quad \text{with} \quad O_{nm} = \int \mathrm{d}^3 r\, \varphi_n^*(\mathbf{r}) \hat{O}^{\text{SR}}(\mathbf{r}) \varphi_m(\mathbf{r}) \tag{5.6}$$

$$\hat{O}_{\text{two particle}} = \frac{1}{2}\sum_{nn',mm'} O_{nn';m'm} \hat{a}_n^\dagger \hat{a}_{n'}^\dagger \hat{a}_{m'} \hat{a}_m$$
$$\text{with} \quad O_{nn';m'm} = \int \mathrm{d}^3 r \mathrm{d}^3 r'\, \varphi_n^*(\mathbf{r})\varphi_{n'}^*(\mathbf{r}') \hat{O}^{\text{SR}}(\mathbf{r},\mathbf{r}') \varphi_{m'}(\mathbf{r}')\varphi_m(\mathbf{r}) \tag{5.7}$$

These important relations can be proven by checking that the matrix elements for arbitrary many-particle states are identical. For the single-particle case, $\sum_{i=1}^{N} \hat{O}^{\text{SR}}(\mathbf{r}_i)$ has the same matrix elements with Slater determinants like $\hat{O}_{\text{single particle}}$ with the corresponding occupation number states. The two-particle case is analogous but lengthy.

Example:

The single-particle Hamilton-operator of the crystal reads in occupation number formalism

$$\hat{H}_0 = \sum_{n\mathbf{k}} E_n(\mathbf{k}) \hat{a}_{n\mathbf{k}}^\dagger \hat{a}_{n\mathbf{k}} \tag{5.8}$$

A perturbation of lattice periodicity, such as the presence of ionized impurities, provides a Hamilton operator with terms $\hat{a}_{n\mathbf{k}'}^\dagger \hat{a}_{n\mathbf{k}}$, see exercises.

[2]Note, that different notations for the two-particle matrix elements can be found in the literature. E.g., Kittel (1987); Schrieffer (1983) use $O_{nn';m'm} = \langle n, n'|\hat{O}_2(\mathbf{r},\mathbf{r}')|m,m'\rangle$ which provides a different ordering of indices in the matrix element.

5.2 Temporal evolution of expectation values

If the system is in a quantum state $|\phi\rangle$ we can evaluate expectation values of arbitrary operators $\hat{A}$ in the form

$$\langle\hat{A}\rangle = \langle\phi|\hat{A}|\phi\rangle$$

Typically we do not know exactly the quantum state, but can give a probability P_r to find the system in each many-particle quantum state $|\phi_r\rangle$ (which form a complete orthonormal set). Then the expectation value of the operator reads

$$\langle\hat{A}\rangle = \sum_r P_r\langle\phi_r|\hat{A}|\phi_r\rangle \tag{5.9}$$

Using $\mathrm{i}\hbar|\dot{\phi}_r\rangle = \hat{H}|\phi_r\rangle$, the time-dependence of the expectation values is given by

$$\frac{\mathrm{d}}{\mathrm{d}t}\langle\hat{A}\rangle = \sum_r P_r\left(\langle\dot{\phi}_r|\hat{A}|\phi_r\rangle + \langle\phi_r|\hat{A}|\dot{\phi}_r\rangle\right) = \frac{1}{\mathrm{i}\hbar}\sum_r P_n\left(-\langle\phi_r|\hat{H}\hat{A}|\phi_r\rangle + \langle\phi_r|\hat{A}\hat{H}|\phi_r\rangle\right) \tag{5.10}$$

Thus we find

$$\boxed{\frac{\mathrm{d}}{\mathrm{d}t}\langle\hat{A}\rangle = \frac{\mathrm{i}}{\hbar}\langle[\hat{H},\hat{A}]\rangle} \tag{5.11}$$

Thus the time dependence of the expectation value is given by the expectation value of the commutator with the Hamilton operator[3].

5.3 Density operator

Now we want to provide a more general quantum description of a system, where we do not know the specific state, but only can give probabilities P_r to find it in certain states $|\Psi_r\rangle$ (which are orthonormal). First note that such a system can **not** be described by the state $|\Psi\rangle = \sum_r P_r|\Psi_r\rangle$, as such a ket state would be a complete description of a system (this would also not be normalized as $\sum_r P_r^2 < 1$). In contrast, a helpful tool to fully characterize the system is the

$$\boxed{\text{Density operator} \quad \hat{\rho} = \sum_s |\phi_s\rangle P_s\langle\phi_s|} \tag{5.12}$$

E.g., one obtains the expectation value of the observable related to $\hat{A}$ by taking the trace over the product of $\hat{\rho}$ and any operator $\hat{A}$:

$$\text{Trace}\left\{\hat{\rho}\hat{A}\right\} = \sum_r\langle\phi_r|\sum_s|\phi_s\rangle P_s\langle\phi_s|\hat{A}|\phi_r\rangle = \sum_r P_r\langle\phi_r|\hat{A}|\phi_r\rangle = \langle\hat{A}\rangle$$

Note the essential difference between (i) a quantum states $|\Psi\rangle = \frac{1}{\sqrt{2}}(|\uparrow\rangle + |\downarrow\rangle)$ and (ii) a statistical mixture where the states $|\uparrow\rangle$ and $|\downarrow\rangle$ have both the probability 50%. The density operators (and corresponding matrices with respect to the basis $\{|\uparrow\rangle, |\downarrow\rangle\}$) read

$$\hat{\rho}_{(i)} = \frac{1}{2}(|\uparrow\rangle + |\downarrow\rangle)(\langle\uparrow| + \langle\downarrow|) \to \begin{pmatrix}\frac{1}{2} & \frac{1}{2}\\ \frac{1}{2} & \frac{1}{2}\end{pmatrix} \quad \hat{\rho}_{(ii)} = \frac{1}{2}|\uparrow\rangle\langle\uparrow| + \frac{1}{2}|\downarrow\rangle\langle\downarrow| \to \begin{pmatrix}\frac{1}{2} & 0\\ 0 & \frac{1}{2}\end{pmatrix}$$

[3]We derived this equation in the conventional Schrödinger picture, i.e. the states $|\phi_n\rangle$ are time dependent. Alternatively we can consider the states (or the density operator) to be fixed, while the operators are time dependent with $\frac{\mathrm{d}}{\mathrm{d}t}\hat{A}_H(t) = \frac{\mathrm{i}}{\hbar}[\hat{H},\hat{A}_H]$. This is called Heisenberg picture.

The time-dependence of the density operator is given by the *von Neumann equation*:

$$\begin{aligned}\frac{\mathrm{d}}{\mathrm{d}t}\hat{\rho} =& \sum_s \left[\frac{\hat{H}}{\mathrm{i}\hbar}|\phi_s\rangle\right] P_s\langle\phi_s| + \sum_s |\phi_s\rangle P_s \left[\langle\phi_s|\frac{\hat{H}}{-\mathrm{i}\hbar}\right] = \frac{1}{\mathrm{i}\hbar}\sum_s \left\{\hat{H}|\phi_s\rangle P_s\langle\phi_s| - |\phi_s\rangle P_s\langle\phi_s|\hat{H}\right\} \\ =& \frac{1}{\mathrm{i}\hbar}[\hat{H},\hat{\rho}]\end{aligned}$$

Note the difference in sign with respect to Eq. (5.11).[4]

In thermal equilibrium, the density operator reads for fixed particle number N

$$\hat{\rho} = \sum_r |\phi_r\rangle \frac{\exp\left(\frac{-E_r}{k_BT}\right)}{Z}\langle\phi_r| = \frac{\exp\left(\frac{-\hat{H}}{k_BT}\right)}{Z} \quad \text{with} \quad Z = \mathrm{Trace}\left\{\exp\left(\frac{-\hat{H}}{k_BT}\right)\right\}$$

If there is particle exchange with a bath of chemical potential μ, thermodynamics gives us (here N_r is the number of particles in state $|\phi_r\rangle$).

$$\hat{\rho} = \sum_r |\phi_r\rangle \frac{\exp\left(\frac{\mu N_r - E_r}{k_BT}\right)}{Z}\langle\phi_r| = \frac{\exp\left(\frac{\mu\hat{N}-\hat{H}}{k_BT}\right)}{Y} \quad \text{with} \quad Y = \mathrm{Trace}\left\{\exp\left(\frac{\mu\hat{N}-\hat{H}}{k_BT}\right)\right\}$$

where $\hat{N} = \sum_n \hat{a}_n^\dagger \hat{a}_n$ counts the number of particles. If the Hamilton operator separates, $\hat{H} = \sum_n E_n \hat{a}_n^\dagger \hat{a}_n$, this provides us with the Fermi distribution

$$\langle \hat{a}_n^\dagger \hat{a}_n\rangle = \frac{1}{\exp\left(\frac{E_n-\mu}{k_BT}\right)+1} \tag{5.13}$$

5.4 Semiconductor Bloch equation

Now we want to study the interaction of electrons in a semiconductor with a classical light field $F(z,t)$.

$$F(z,t) = \mathbf{e}_x \frac{1}{2}\left(\tilde{F}(z)\mathrm{e}^{\mathrm{i}[(K+\delta k)z-\omega t]} + \tilde{F}^*(z)\mathrm{e}^{-\mathrm{i}[(K+\delta k)z-\omega t]}\right) \tag{5.14}$$

where $K = \sqrt{\epsilon_{\mathrm{host}}}\omega/c$ is the wave vector in the semiconductor without carrier injection. Using $\frac{\mathrm{d}|\tilde{F}(z)|^2}{\mathrm{d}z} = -\alpha|\tilde{F}(z)|^2$, Eq. (4.13) relates $F(z)$ and δk to the change in susceptibility by the nonequilibrium electron distribution in an operating laser.

Taking into account the coupling of the electric field to the dipole moment (compare Sec. 4.4) we find the Hamilton operator in two-band approximation

$$\hat{H} = \sum_{\mathbf{k}} E_c(\mathbf{k})\hat{a}_{c\mathbf{k}}^\dagger \hat{a}_{c\mathbf{k}} + \sum_{\mathbf{k}} E_v(\mathbf{k})\hat{a}_{v\mathbf{k}}^\dagger \hat{a}_{v\mathbf{k}} - \sum_{\mathbf{k}}\left(\mu_{\mathbf{k}}\hat{a}_{c\mathbf{k}}^\dagger \hat{a}_{v\mathbf{k}} + \mu_{\mathbf{k}}^*\hat{a}_{v\mathbf{k}}^\dagger \hat{a}_{c\mathbf{k}}\right)F(z,t) + \hat{H}_{\mathrm{interaction}}$$

where $\mu_{\mathbf{k}} = \mathbf{e}_x \cdot \boldsymbol{\mu}_{cv}(\mathbf{k})$ is the dipole moment of the transition between conduction and valence band from Eq. (4.18).

Using the notation of holes (2.4) we have to replace the electron creation operator $\hat{a}_{v\mathbf{k}}^\dagger$ by the hole annihilation operator $\hat{d}_{-\mathbf{k}}$, resulting in

$$\hat{H} = \sum_{\mathbf{k}'}\left[\left(E_g + \frac{\hbar^2 k'^2}{2m_c}\right)\hat{a}_{\mathbf{k}'}^\dagger \hat{a}_{\mathbf{k}'} + \frac{\hbar^2 k'^2}{2m_h}\hat{d}_{-\mathbf{k}'}^\dagger \hat{d}_{-\mathbf{k}'} - \left(\mu_{\mathbf{k}'}\hat{a}_{\mathbf{k}'}^\dagger \hat{d}_{-\mathbf{k}'}^\dagger + \mu_{\mathbf{k}'}^*\hat{d}_{-\mathbf{k}'}\hat{a}_{\mathbf{k}'}\right)F(z,t)\right] + \hat{H}_{\mathrm{interaction}} \tag{5.15}$$

[4] All equations are in Schrödinger picture here.

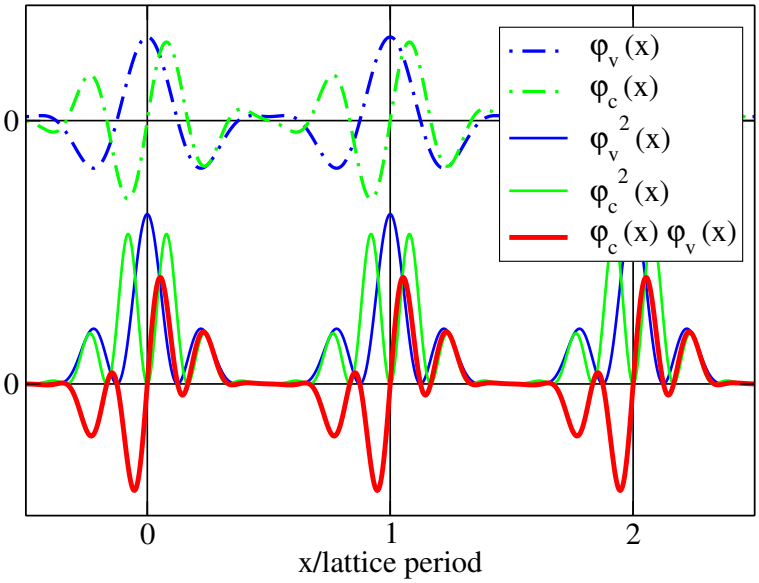

Figure 5.1: Sketch of Bloch functions for conduction and valence band (without the $e^{\mathrm{i}\mathbf{k}\cdot\mathbf{r}}$ factor which is identical for both) together with their absolute values and overlap.

where we set $E = 0$ at the edge of the valence band and use effective mass approximation. Furthermore the index c is skipped and the energy $\sum_{\mathbf{k}} E_v(\mathbf{k})$ of the full valence band has been omitted.

The goal is to evaluate the polarization $\mathbf{P} = P(t)\mathbf{e}_x$. As motivated in Fig. 5.1, the electron densities from conduction or valence band states $|\varphi_{c\mathbf{k}}(\mathbf{r})|^2$ and $|\varphi_{v\mathbf{k}}(\mathbf{r})|^2$ do not provide any displacement of charge from the core positions (symmetry points). In contrast, the product between these states provides a displacement of charge from the core positions given by the dipole moment $\mu_{\mathbf{k}} = e\int \mathrm{d}^3 r x \varphi^*_{c\mathbf{k}}(\mathbf{r})\varphi_{v\mathbf{k}}(\mathbf{r})$ (which is only well-defined for tightly bound states as shown in figure. The definition (4.18) is more general.). Thus the macroscopic polarization becomes

$$P(t) = \frac{1}{V}\sum_{\mathbf{k}} \left(\mu_{\mathbf{k}}\langle \hat{a}^\dagger_{\mathbf{k}}\hat{d}^\dagger_{-\mathbf{k}}\rangle + \mu^*_{\mathbf{k}}\langle \hat{d}_{-\mathbf{k}}\hat{a}_{\mathbf{k}}\rangle\right) \tag{5.16}$$

in occupation number formalism in the two-band limit addressed here. In these equations the spin is included in the $\mathbf{k}$-summations, in order to simplify the notation.

In order to determine the polarization we evaluate the equation of motion for $\langle \hat{d}_{-\mathbf{k}}\hat{a}_{\mathbf{k}}\rangle$, which is given by Eq. (5.11)

$$\frac{\mathrm{d}}{\mathrm{d}t}\langle \hat{d}_{-\mathbf{k}}\hat{a}_{\mathbf{k}}\rangle = \frac{\mathrm{i}}{\hbar}\left\langle \left[\hat{H}, \hat{d}_{-\mathbf{k}}\hat{a}_{\mathbf{k}}\right]\right\rangle$$

For $\mathbf{k}' \neq \mathbf{k}$, we need four exchanges of fermionic annihilation/creation operators to change the order of $\hat{d}_{-\mathbf{k}}\hat{a}_{\mathbf{k}}$ and the part of $\hat{H}$. This provides a factor of $(-1)^4 = 1$, and thus the commutator vanishes for $\mathbf{k}' \neq \mathbf{k}$. For $\mathbf{k}' = \mathbf{k}$ we have

$$\hat{a}^\dagger_{\mathbf{k}}\hat{a}_{\mathbf{k}}\hat{d}_{-\mathbf{k}}\hat{a}_{\mathbf{k}} = (-1)^2\hat{d}_{-\mathbf{k}}\hat{a}^\dagger_{\mathbf{k}}\hat{a}_{\mathbf{k}}\hat{a}_{\mathbf{k}} = 0 \quad \text{and} \quad \hat{d}_{-\mathbf{k}}\hat{a}_{\mathbf{k}}\hat{a}^\dagger_{\mathbf{k}}\hat{a}_{\mathbf{k}} = \hat{d}_{-\mathbf{k}}(1-\hat{a}^\dagger_{\mathbf{k}}\hat{a}_{\mathbf{k}})\hat{a}_{\mathbf{k}} = \hat{d}_{-\mathbf{k}}\hat{a}_{\mathbf{k}}$$

Thus

$$\left[\hat{a}^\dagger_{\mathbf{k}}\hat{a}_{\mathbf{k}}, \hat{d}_{-\mathbf{k}}\hat{a}_{\mathbf{k}}\right] = -\hat{d}_{-\mathbf{k}}\hat{a}_{\mathbf{k}}$$

Similarly

$$\left[\hat{d}^\dagger_{-\mathbf{k}}\hat{d}_{-\mathbf{k}}, \hat{d}_{-\mathbf{k}}\hat{a}_{\mathbf{k}}\right] = -\hat{d}_{-\mathbf{k}}\hat{a}_{\mathbf{k}} \tag{5.17}$$

$$\left[\hat{a}^\dagger_{\mathbf{k}}\hat{d}^\dagger_{-\mathbf{k}}, \hat{d}_{-\mathbf{k}}\hat{a}_{\mathbf{k}}\right] = \hat{a}^\dagger_{\mathbf{k}}\hat{a}_{\mathbf{k}} + \hat{d}^\dagger_{-\mathbf{k}}\hat{d}_{-\mathbf{k}} - 1 \qquad \left[\hat{d}_{-\mathbf{k}}\hat{a}_{\mathbf{k}}, \hat{d}_{-\mathbf{k}}\hat{a}_{\mathbf{k}}\right] = 0 \tag{5.18}$$

$$\left[\hat{a}^\dagger_{\mathbf{k}}\hat{d}^\dagger_{-\mathbf{k}}, \hat{a}^\dagger_{\mathbf{k}}\hat{a}_{\mathbf{k}}\right] = -\hat{a}^\dagger_{\mathbf{k}}\hat{d}^\dagger_{-\mathbf{k}} \qquad \left[\hat{a}^\dagger_{\mathbf{k}}\hat{d}^\dagger_{-\mathbf{k}}, \hat{d}^\dagger_{-\mathbf{k}}\hat{d}_{-\mathbf{k}}\right] = -\hat{a}^\dagger_{\mathbf{k}}\hat{d}^\dagger_{-\mathbf{k}} \tag{5.19}$$

With these commutation relations we find the

Semiconductor Bloch equations

$$\frac{\hbar}{\mathrm{i}}\frac{\mathrm{d}}{\mathrm{d}t}p_{\mathbf{k}}(t) = -\hbar\omega_k p_{\mathbf{k}} - \mu_{\mathbf{k}}F(z,t)\left(n_{e\mathbf{k}}+n_{h-\mathbf{k}}-1\right) + \left\langle\left[\hat{H}_{\text{interaction}},\hat{d}_{-\mathbf{k}}\hat{a}_{\mathbf{k}}\right]\right\rangle \quad (5.20)$$

$$\frac{\hbar}{\mathrm{i}}\frac{\mathrm{d}}{\mathrm{d}t}n_{e\mathbf{k}}(t) = F(z,t)\left(\mu_{\mathbf{k}}p^*_{\mathbf{k}}-\mu^*_{\mathbf{k}}p_{\mathbf{k}}\right) + \left\langle\left[\hat{H}_{\text{interaction}},\hat{a}^\dagger_{\mathbf{k}}\hat{a}_{\mathbf{k}}\right]\right\rangle \quad (5.21)$$

$$\frac{\hbar}{\mathrm{i}}\frac{\mathrm{d}}{\mathrm{d}t}n_{h-\mathbf{k}}(t) = F(z,t)\left(\mu_{\mathbf{k}}p^*_{\mathbf{k}}-\mu^*_{\mathbf{k}}p_{\mathbf{k}}\right) + \left\langle\left[\hat{H}_{\text{interaction}},\hat{d}^\dagger_{-\mathbf{k}}\hat{d}_{-\mathbf{k}}\right]\right\rangle \quad (5.22)$$

where

$$p_{\mathbf{k}} = \langle\hat{d}_{-\mathbf{k}}\hat{a}_{\mathbf{k}}\rangle, \quad n_{e\mathbf{k}} = \langle\hat{a}^\dagger_{\mathbf{k}}\hat{a}_{\mathbf{k}}\rangle, \quad n_{h-\mathbf{k}} = \langle\hat{d}^\dagger_{-\mathbf{k}}\hat{d}_{-\mathbf{k}}\rangle$$

and

$$\hbar\omega_k = E_g + \frac{\hbar^2k^2}{2m_c} + \frac{\hbar^2k^2}{2m_h}$$

5.5 Free carrier gain spectrum

Now we want to discuss the case of free carriers, i.e., the details of $\hat{H}_{\text{interaction}}$ are neglected. The key function of this interaction part is the decay of the polarization which may be treated as

$$\left\langle\left[\hat{H}_{\text{interaction}},\hat{d}_{-\mathbf{k}}\hat{a}_{\mathbf{k}}\right]\right\rangle \approx -\frac{\hbar}{\mathrm{i}}\gamma p_{\mathbf{k}}$$

where $T_2 = 1/\gamma$ is the dipole lifetime. γ can be evaluated microscopically and it is approximately given by the mean total scattering rate of the electron and hole state involved. Typical values are $T_2 \approx 0.1$ ps. Then we find from Eq. (5.20):

$$p_{\mathbf{k}}(t) = -\frac{\mathrm{i}}{\hbar}\int_{-\infty}^{t}\mathrm{d}t'\,\mathrm{e}^{-(\mathrm{i}\omega_k+\gamma)(t-t')}\mu_{\mathbf{k}}F(z,t')\left(n_{e\mathbf{k}}(t')+n_{h-\mathbf{k}}(t')-1\right) \quad (5.23)$$

The t'-dependence of the different terms is sketched in Fig. 5.2. The term $\mathrm{e}^{-\gamma(t-t')}$ ensures that the integrant vanishes for $t-t' \gg T_2$. As the occupations $n_{\mathbf{k}}(t')$ typically vary on a timescale which is longer than ps, we may approximate $n_{\mathbf{k}}(t') \approx n_{\mathbf{k}}(t)$. The electric field, see Eq. (5.14), has components with $\sim \mathrm{e}^{\mathrm{i}\omega t'}$ and $\sim \mathrm{e}^{-\mathrm{i}\omega t'}$. Now $\mathrm{e}^{\mathrm{i}(\omega+\omega_k)t'}$ is always oscillating very fast on the time scale T_2 and therefore only the component $\sim \mathrm{e}^{-\mathrm{i}\omega t'}$ of $F(z,t')$ contributes to the final value of the integral. (The neglect of $\mathrm{e}^{\mathrm{i}\omega t'}$ is called rotating wave approximation.) Together we find:

$$p_{\mathbf{k}}(t) \approx -\frac{\mathrm{i}}{\hbar}\mu_{\mathbf{k}}\frac{\tilde{F}(z)}{2}\mathrm{e}^{\mathrm{i}(K+\delta k)z-\mathrm{i}\omega t}\left(n_{e\mathbf{k}}(t)+n_{h-\mathbf{k}}(t)-1\right)\frac{1}{\gamma+\mathrm{i}(\omega_k-\omega)} \quad (5.24)$$

Now the complex susceptibility is defined as $\chi^{\text{rel}}(\omega) = P(\omega)/[\epsilon_0\epsilon_{\text{host}}F(\omega)]$. From Eqs. (5.16,5.24) we have

$$P(\omega) = \pi\sum_k \frac{1}{V\hbar}|\mu_{\mathbf{k}}|^2\tilde{F}(z)\mathrm{e}^{\mathrm{i}(K+\delta k)z}\left(n_{e\mathbf{k}}(t)+n_{h-\mathbf{k}}(t)-1\right)\frac{1}{\omega-\omega_k+\mathrm{i}\gamma}\,.$$

Identifying $F(\omega) = \pi\tilde{F}(z)\mathrm{e}^{\mathrm{i}(K+\delta k)z}$ from Eq. (5.14) we obtain the susceptibility

$$\chi^{\text{rel}} = \sum_k \frac{|\mu_{\mathbf{k}}|^2}{V\hbar\epsilon_0\epsilon_{\text{host}}}\left(n_{e\mathbf{k}}(t)+n_{h-\mathbf{k}}(t)-1\right)\left(\frac{\omega-\omega_k}{(\omega-\omega_k)^2+\gamma^2}-\mathrm{i}\frac{\gamma}{(\omega-\omega_k)^2+\gamma^2}\right) \quad (5.25)$$

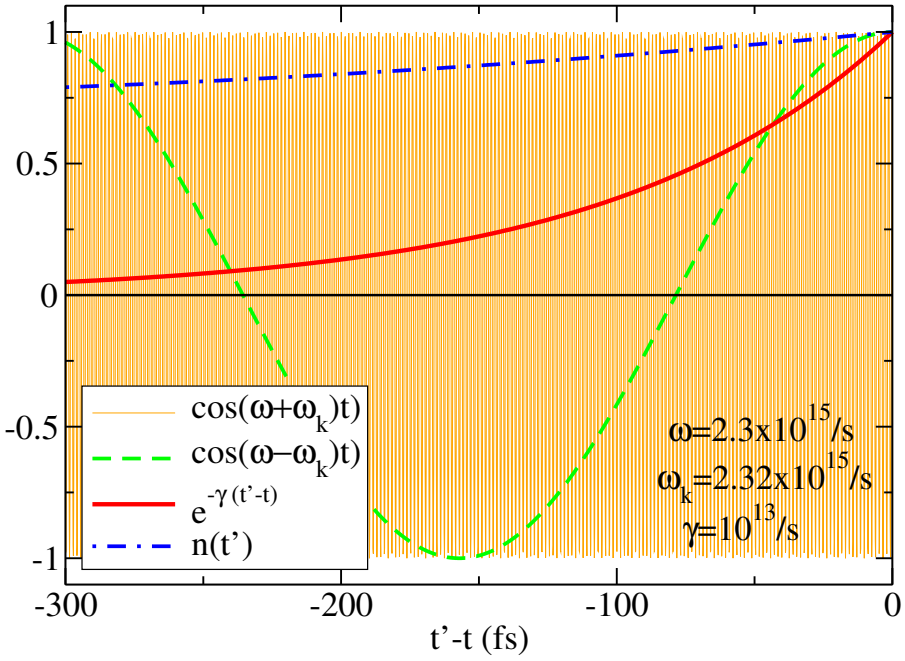

Figure 5.2: Sketch of the different parts of the integrant in Eq. (5.23) with $\hbar\omega_k = E_{\rm gap} + 10$ meV for $E_{\rm gap} = 1.43$eV (GaAs). It is assumed that $n_{\mathbf{k}}(t')$ varies on a ps timescale (probably even slower).

Note that this satisfies the Kramers-Kronig relation. Using $\alpha = \omega\sqrt{\epsilon_{\rm host}}\,{\rm Im}\{\chi^{\rm rel}(\omega)\}/c$, the imaginary part provides us with the earlier result (4.20) for gain in the limit $\gamma \to 0$.

5.5.1 Quasi-equilibrium gain spectrum

For low intensities F^2 of the laser field, Eqs. (5.21,5.22) show that the occupations of the electron and hole states are essentially determined by the interactions. As the electrons and holes dominantly interact with themselves this provides a local thermal equilibrium in each band

$$n_{e\mathbf{k}} \approx \frac{1}{\exp\left(\frac{E_e(\mathbf{k})-\mu_e}{k_BT}\right)+1} = f_e(\mathbf{k}), \quad n_{h\mathbf{k}} \approx \frac{1}{\exp\left(\frac{E_h(\mathbf{k})-\mu_h}{k_BT}\right)+1} = f_h(\mathbf{k})$$

Assuming charge neutrality (if the active region is undoped) the chemical potentials μ_e, μ_h are determined by

$$N = \sum_{\mathbf{k}} f_e(\mathbf{k}) = \sum_{\mathbf{k}} f_h(\mathbf{k})$$

where N is determined by Eq. (4.22).

We find from Eq. (5.25) the material gain $G = -\omega\sqrt{\epsilon_{\rm host}}\,{\rm Im}\{\chi^{\rm rel}(\omega)\}/c$. The change in refractive index is given by $\delta n = \sqrt{\epsilon_{\rm host}}{\rm Re}\{\chi^{\rm rel}(\omega)\}/2$, where we have to subtract the result for the bare semiconductor (i.e. $f_e(\mathbf{k}) = f_h(\mathbf{k}) \equiv 0$) in the evaluation of ${\rm Re}\{\chi^{\rm rel}\}$. Results are shown in Figure 5.3. We find:

- We have gain in the region $E_g \lesssim \hbar\omega \lesssim \mu_h + \mu_e$.
- The gain becomes weaker with increasing γ.
- Numerically, we find approximately $G = A_g(N - N_g)$ as in Eq. (4.23) at the gain peak. Here N_g increases and A_g drops with temperature.
- Gain is associated with a change in the refractive index of the semiconductor.

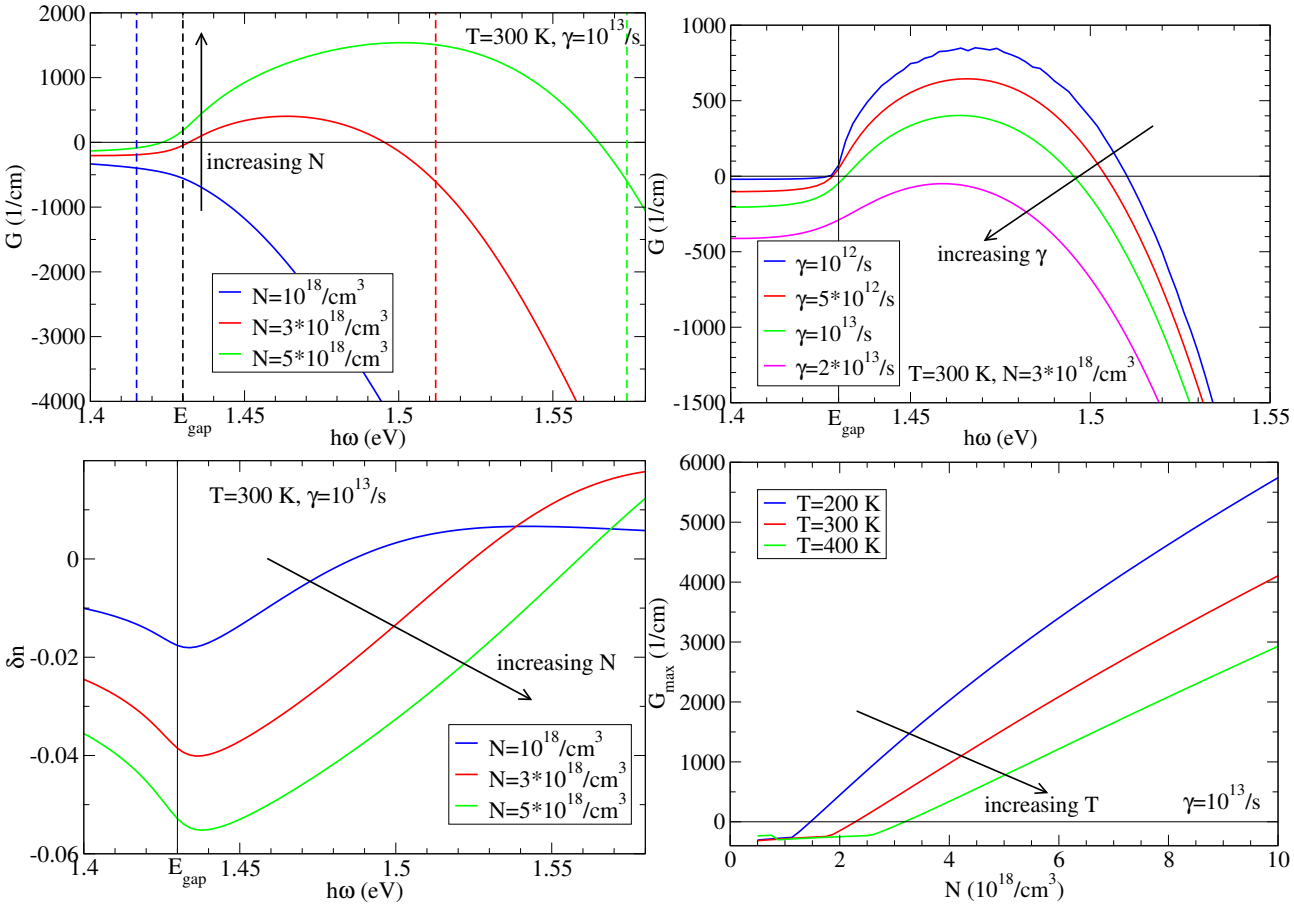

Figure 5.3: Gain for a GaAs-laser material calculated from Eq. (5.25) using effective mass approximation with $m_e = 0.067$, $m_h = 0.52$ (the real valence band structure of GaAs is dominated by 3 bands, which are represented by a single parabolic band for simplicity here), $\mu_k = e \times 0.473\text{nm}$, $E_{gap} = 1.43\text{eV}$, $\epsilon_{\text{host}} = 13$.

5.5.2 Spectral hole burning

At high intensities I of the optical field, gain saturation occurs, as discussed in subsection 4.5.1. The treatment tacitly assumes that even at high intensities $n_{e\mathbf{k}}$ and $n_{h\mathbf{k}}$ are given by Fermi distribution. In contrast, Eqs. (5.21,5.22,5.24) show, that $n_{e\mathbf{k}}$ and $n_{h-\mathbf{k}}$ are diminished for those $\mathbf{k}$-values satisfying $|\omega - \omega_k| \lesssim \gamma$, which is called *spectral hole burning*. This effect reduces the inversion in particular for those states, which are responsible for the laser transition, and thus gain is stronger reduced than estimated by the treatment in 4.5.1. On the other hand scattering processes effectively restore a quasi-equilibrium in the bands, and thus this effect is only prominent at very high intensities, in particular for short laser pulses.

Chapter 6

Electron-Electron interaction

The electron-electron interaction is a two-particle operator. In the basis of Bloch states with Bloch vector $\mathbf{k}, \mathbf{l}$ and band indices m, n, Eq. (5.7) provides the two-particle operator in occupation number representation.

$$\hat{V}_{ee} = \frac{1}{2} \sum_{m\mathbf{l},m'\mathbf{l}',n'\mathbf{k}',n\mathbf{k}} V_{m\mathbf{l},m'\mathbf{l}',n'\mathbf{k}',n\mathbf{k}} \hat{a}^\dagger_{m\mathbf{l}} \hat{a}^\dagger_{m'\mathbf{l}'} \hat{a}_{n'\mathbf{k}'} \hat{a}_{n\mathbf{k}} \tag{6.1}$$

with the matrix elements

$$V_{m\mathbf{l},m'\mathbf{l}',n'\mathbf{k}',n\mathbf{k}} = \int \mathrm{d}^3 r \int \mathrm{d}^3 r' \varphi^*_{m\mathbf{l}}(\mathbf{r}) \varphi^*_{m'\mathbf{l}'}(\mathbf{r}') \frac{e^2}{4\pi\epsilon_{\mathrm{host}}\epsilon_0 |\mathbf{r}-\mathbf{r}'|} \varphi_{n'\mathbf{k}'}(\mathbf{r}') \varphi_{n\mathbf{k}}(\mathbf{r})$$

The calculation of the matrix elements is essentially simplified by applying the Fourier decomposition of the (screened) Coulomb potential, which reads:

$$\frac{e^2 \mathrm{e}^{-\lambda|\mathbf{r}|}}{4\pi\epsilon_0\epsilon_{\mathrm{host}}|\mathbf{r}|} = \frac{1}{V} \sum_{\mathbf{q}} V_q^\lambda \mathrm{e}^{\mathrm{i}\mathbf{q}\cdot\mathbf{r}} = \int \mathrm{d}^3 q V_q^\lambda \frac{\mathrm{e}^{\mathrm{i}\mathbf{q}\cdot\mathbf{r}}}{(2\pi)^3} \quad \text{with} \quad V_q^\lambda = \frac{e^2}{\epsilon_{\mathrm{host}}\epsilon_0(|\mathbf{q}|^2+\lambda^2)} \tag{6.2}$$

and is used at many places throughout this chapter. In particular we use the symbol V_q in the limit $\lambda \to 0$ (no screening). Here we are considering a finite crystal of volume V, so that we have a discrete set of Bloch vectors, which facilitates the numbering.

Inserting the discrete Fourier transformation, the two spatial integrals disentangle. Using Eqs. (1.12,2.10) and neglecting Umklapp processes the $\mathbf{r}$ integral provides

$$\int \mathrm{d}^3 r \, \varphi^*_{m\mathbf{l}}(\mathbf{r}) \mathrm{e}^{\mathrm{i}\mathbf{q}\cdot\mathbf{r}} \varphi_{n\mathbf{k}}(\mathbf{r}) \approx \delta_{nm} \delta_{\mathbf{l},\mathbf{k}+\mathbf{q}} \tag{6.3}$$

assuming $u_{m(\mathbf{k}+\mathbf{q})}(\mathbf{r}) \approx u_{m\mathbf{k}}(\mathbf{r})$, which holds for small $\mathbf{q}$. In the same way we find

$$\int \mathrm{d}^3 r' \, \varphi^*_{m'\mathbf{l}'}(\mathbf{r}') \mathrm{e}^{-\mathrm{i}\mathbf{q}\cdot\mathbf{r}'} \varphi_{n\mathbf{k}'}(\mathbf{r}') \approx \delta_{n'm'} \delta_{\mathbf{l}',\mathbf{k}'-\mathbf{q}}$$

Putting things together provides

$$V_{m\mathbf{l},m'\mathbf{l}',n'\mathbf{k}',n\mathbf{k}} = \frac{1}{V} \sum_{\mathbf{q}} V_q \delta_{nm} \delta_{\mathbf{l},\mathbf{k}+\mathbf{q}} \delta_{n'm'} \delta_{\mathbf{l}',\mathbf{k}'-\mathbf{q}}$$

which reduces the number of running indices in Eq. (6.1) dramatically and we obtain the

Operator for electron-electron interaction in occupation number formalism

$$\hat{V}_{\mathrm{ee}} \approx \frac{1}{2V} \sum_{n\mathbf{k},n'\mathbf{k}'} \sum_{\mathbf{q}} V_q \hat{a}^\dagger_{n(\mathbf{k}+\mathbf{q})} \hat{a}^\dagger_{n'(\mathbf{k}'-\mathbf{q})} \hat{a}_{n'\mathbf{k}'} \hat{a}_{n\mathbf{k}} \quad \text{with} \quad V_q = \frac{e^2}{\epsilon_{\mathrm{host}}\epsilon_0 |\mathbf{q}|^2} \tag{6.4}$$

This can be interpreted as follows: Two electron with $\mathbf{k}$ and $\mathbf{k}'$ interact by transferring the crystal momentum $\mathbf{q}$ as indicated in the Feynman diagram on the right. Note that the sum of quasimomenta $\hbar\mathbf{k} + \hbar\mathbf{k}'$ is conserved by the interaction. Here the respective band index is kept by the interaction. This is actually an approximation, see Eq. (6.3), and transitions between bands (as happening in the Auger effect, e.g.) are possible for $\mathbf{q} \neq 0$ albeit their likelihood is much smaller than the processes considered is Eq. (6.4).

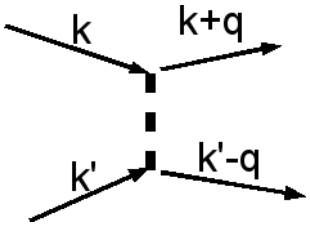

6.1 Coulomb effects for interband transitions

6.1.1 The Hamiltonian

Restricting Eq. (6.4) to the valence and conduction band we find

$$\hat{V}_{\rm ee} = \frac{1}{2V}\sum_{\mathbf{k},\mathbf{k}'}\sum_{\mathbf{q}} V_q \left(\hat{a}^\dagger_{(\mathbf{k}+\mathbf{q})}\hat{a}^\dagger_{(\mathbf{k}'-\mathbf{q})}\hat{a}_{\mathbf{k}'}\hat{a}_{\mathbf{k}} + \hat{d}^\dagger_{(\mathbf{k}+\mathbf{q})}\hat{d}^\dagger_{(\mathbf{k}'-\mathbf{q})}\hat{d}_{\mathbf{k}'}\hat{d}_{\mathbf{k}} - 2\hat{a}^\dagger_{(\mathbf{k}+\mathbf{q})}\hat{d}^\dagger_{(\mathbf{k}'-\mathbf{q})}\hat{d}_{\mathbf{k}'}\hat{a}_{\mathbf{k}}\right) \tag{6.5}$$

where we replaced $\mathbf{k} \to -\mathbf{q} - \mathbf{k}$ and $\mathbf{k}' \to \mathbf{q} - \mathbf{k}'$ for the hole operators[1]. ($\mathbf{k}, \mathbf{k}'$ contain also the spin here.) The electron-electron interaction is a part of $\hat{H}_{\rm interaction}$ in Eqs. (5.20-5.22) and we find e.g.

$$\begin{aligned}\left[\hat{V}_{\rm ee}, \hat{d}_{-\mathbf{k}_0}\hat{a}_{\mathbf{k}_0}\right] = \frac{1}{V}\sum_{\mathbf{k}'}\sum_{\mathbf{q}} V_q\Big(&\hat{a}^\dagger_{(\mathbf{k}'+\mathbf{q})}\hat{d}_{-\mathbf{k}_0}\hat{a}_{\mathbf{k}'}\hat{a}_{\mathbf{k}_0+\mathbf{q}} + \hat{d}^\dagger_{(\mathbf{k}'-\mathbf{q})}\hat{d}_{\mathbf{k}'}\hat{a}_{\mathbf{k}_0}\hat{d}_{-\mathbf{k}_0-\mathbf{q}} \\ &- \hat{a}^\dagger_{(\mathbf{k}'+\mathbf{q})}\hat{d}_{(\mathbf{q}-\mathbf{k}_0)}\hat{a}_{\mathbf{k}'}\hat{a}_{\mathbf{k}_0} - \hat{d}^\dagger_{(\mathbf{k}'-\mathbf{q})}\hat{d}_{-\mathbf{k}_0}\hat{d}_{\mathbf{k}'}\hat{a}_{\mathbf{k}_0-\mathbf{q}} + \hat{d}_{(\mathbf{q}-\mathbf{k}_0)}\hat{a}_{(\mathbf{k}_0-\mathbf{q})}\delta_{\mathbf{k}',\mathbf{q}-\mathbf{k}_0}\Big)\end{aligned}$$

Thus the right-hand side of the equation of motion for the polarization (5.20) contains higher expectation values such as $\langle\hat{a}^\dagger_{(\mathbf{k}'+\mathbf{q})}\hat{d}_{-\mathbf{k}_0}\hat{a}_{\mathbf{k}'}\hat{a}_{\mathbf{k}_0+\mathbf{q}}\rangle$. The same holds for the equations for n_e and n_h. Thus the Eqs. (5.20-5.22) constitute no longer a closed system as exploited in Sec. 5.5. In contrast we should take into account the equation of motion for the two-particle expectation values $\langle\hat{a}^\dagger_{(\mathbf{k}'+\mathbf{q})}\hat{d}_{-\mathbf{k}_0}\hat{a}_{\mathbf{k}'}\hat{a}_{\mathbf{k}_0+\mathbf{q}}\rangle$, which will itself generate three-particle expectation values on the right hand side. This process will generate an infinite hierarchy of many-particle expectation values. Thus, approximations have to be done on a certain stage.

6.1.2 Semiconductor Bloch equations in HF approximation

The simplest approximation is to assume that the expectation values for four operators factorize into products of expectation values of two operators. For simple states (such as slater states) the expectation values vanish unless an electron creation operator is paired with an annihilation operator and we find

$$\langle\hat{a}^\dagger_{(\mathbf{k}'+\mathbf{q})}\hat{d}_{-\mathbf{k}_0}\hat{a}_{\mathbf{k}'}\hat{a}_{\mathbf{k}_0+\mathbf{q}}\rangle \approx \langle\hat{a}^\dagger_{(\mathbf{k}'+\mathbf{q})}\hat{a}_{\mathbf{k}_0+\mathbf{q}}\rangle\langle\hat{d}_{-\mathbf{k}_0}\hat{a}_{\mathbf{k}'}\rangle - \langle\hat{a}^\dagger_{(\mathbf{k}'+\mathbf{q})}\hat{a}_{\mathbf{k}'}\rangle\langle\hat{d}_{-\mathbf{k}_0}\hat{a}_{\mathbf{k}_0+\mathbf{q}}\rangle$$

[1] Additional terms $\sum_{\mathbf{k}}(\hat{a}^\dagger_{\mathbf{k}}\hat{a}_{\mathbf{k}} + \hat{d}^\dagger_{\mathbf{k}}\hat{d}_{\mathbf{k}})V_0\frac{1}{V}\sum_{\mathbf{k}'} + \frac{1}{2V}\sum_{\mathbf{k},\mathbf{k}'}V_0 - \frac{1}{2V}\sum_{\mathbf{k},\mathbf{q}}V_q$ describe the electron-electron interaction of the full valence band and are subsumed in redefined single particle energies.

where the minus sign is a result of the ordering of the operators.[2] For spatially independent quantities, the respective expectation values vanish unless they have the same $\mathbf{k}$ ($-\mathbf{k}$ for hole operators), see Eq. (6.21). Thus we find

$$\langle \hat{a}^\dagger_{(\mathbf{k}'+\mathbf{q})} \hat{d}_{-\mathbf{k}_0} \hat{a}_{\mathbf{k}'} \hat{a}_{\mathbf{k}_0+\mathbf{q}} \rangle \approx \langle \hat{a}^\dagger_{(\mathbf{k}'+\mathbf{q})} \hat{d}_{-\mathbf{k}_0} \hat{a}_{\mathbf{k}'} \hat{a}_{\mathbf{k}_0+\mathbf{q}} \rangle_{\mathrm{HF}} = \delta_{\mathbf{k}',\mathbf{k}_0} n_{e\mathbf{k}_0+\mathbf{q}} p_{\mathbf{k}_0} - \delta_{\mathbf{q},0} n_{e\mathbf{k}'} p_{\mathbf{k}_0} \tag{6.6}$$

which is called Hartree-Fock approximation (HF). Using the same procedure for all two-particle expectation values we obtain the Semiconductor Bloch equations in Hartree-Fock approximation

$$\frac{\mathrm{d}}{\mathrm{d}t} p_{\mathbf{k}}(t) = -\mathrm{i}\omega_k^{\mathrm{ren}} p_{\mathbf{k}} - \mathrm{i}\Omega_k(t)\left(n_{e\mathbf{k}} + n_{h-\mathbf{k}} - 1\right) + \left(\frac{\partial p_{\mathbf{k}}}{\partial t}\right)_{\mathrm{col}} \tag{6.7}$$

$$\frac{\mathrm{d}}{\mathrm{d}t} n_{e\mathbf{k}}(t) = \mathrm{i}\Omega_k(t) p^*_{\mathbf{k}} - \mathrm{i}\Omega^*_k(t) p_{\mathbf{k}} + \left(\frac{\partial n_{e\mathbf{k}}}{\partial t}\right)_{\mathrm{col}} \tag{6.8}$$

$$\frac{\mathrm{d}}{\mathrm{d}t} n_{h-\mathbf{k}}(t) = \mathrm{i}\Omega_k(t) p^*_{\mathbf{k}} - \mathrm{i}\Omega^*_k(t) p_{\mathbf{k}} + \left(\frac{\partial n_{h-\mathbf{k}}}{\partial t}\right)_{\mathrm{col}} \tag{6.9}$$

where the terms ω_k and $\mu_{\mathbf{k}} F(z,t)$ in Eqs. (5.20-5.22) are replaced by

$$\hbar\omega_k^{\mathrm{ren}} = E_g + \frac{\hbar^2 k^2}{2m_c} + \frac{\hbar^2 k^2}{2m_h} - \frac{1}{V}\sum_{\mathbf{q}} V_q \left(n_{e\mathbf{k}+\mathbf{q}} + n_{h-\mathbf{k}-\mathbf{q}}\right)$$

$$\hbar\Omega_k = \mu_{\mathbf{k}} F(z,t) + \frac{1}{V}\sum_{\mathbf{q}} V_q p_{\mathbf{k}-\mathbf{q}}$$

containing the *exchange shift* and the *Coulomb field renormalization*, respectively.

We find that the electron-electron interaction reduces the transition energies with increasing excitation (increasing N). Furthermore the polarizations of different $\mathbf{k}$-values couple to each other.

6.1.3 Excitons*

Let us now solve Eq. (6.7) in the limit of low densities $n_e \approx 0$, $n_h \approx 0$. Furthermore we assume that $\mu_{\mathbf{k}} = \mu_{cv}$ does not depend on k. The Fourier transformation of Eq. (6.7) in time reads:

$$-\mathrm{i}\omega p_{\mathbf{k}}(\omega) = -\frac{\mathrm{i}}{\hbar}\left(E_g + \frac{\hbar^2 k^2}{2m_r}\right) p_{\mathbf{k}}(\omega) + \frac{\mathrm{i}}{\hbar}\mu_{cv} F(\omega) + \frac{\mathrm{i}}{\hbar}\frac{1}{V}\sum_{\mathbf{q}} V_q p_{\mathbf{k}-\mathbf{q}}(\omega) - \gamma p_{\mathbf{k}}(\omega)$$

Performing a second Fourier transformation in space

$$p_{\mathbf{k}}(\omega) = \int \mathrm{d}^3 r\, p(\mathbf{r},\omega) \mathrm{e}^{-\mathrm{i}\mathbf{k}\cdot\mathbf{r}} \tag{6.10}$$

we obtain with Eq. (6.2) and the convolution theorem $\frac{1}{V}\sum_{\mathbf{q}} V_q p_{\mathbf{k}-\mathbf{q}}(\omega) \to \int \mathrm{d}^3 r V(\mathbf{r}) p(\mathbf{r},\omega)$

$$\left[E_g - \frac{\hbar^2}{2m_r}\Delta - \frac{e^2}{4\pi\epsilon_{\mathrm{host}}\epsilon_0 |\mathbf{r}|} - \hbar(\omega + \mathrm{i}\gamma)\right] p(\mathbf{r},\omega) = \mu_{cv} F(\omega)\delta(\mathbf{r}) \tag{6.11}$$

[2] One might argue, that this is a double-counting. However, this can be formalized by the assumption, that the joint cumulant $\langle abcd\rangle_c$ of the four-operator expectation value $\langle abcd\rangle$ vanishes. Using

$$\begin{aligned}\langle abcd\rangle =& \langle abcd\rangle_c + \langle abc\rangle\langle d\rangle + \langle abd\rangle\langle c\rangle + \langle acd\rangle\langle b\rangle + \langle bcd\rangle\langle a\rangle - 2\langle ab\rangle\langle c\rangle\langle d\rangle - 2\langle ac\rangle\langle b\rangle\langle d\rangle - 2\langle ad\rangle\langle b\rangle\langle c\rangle \\ & - 2\langle cd\rangle\langle a\rangle\langle b\rangle - 2\langle bd\rangle\langle a\rangle\langle c\rangle - 2\langle bc\rangle\langle a\rangle\langle d\rangle + \langle ab\rangle\langle cd\rangle \underbrace{+\langle ac\rangle\langle bd\rangle + \langle ad\rangle\langle bc\rangle} + 6\langle a\rangle\langle b\rangle\langle c\rangle\langle d\rangle\end{aligned}$$

the underbraced terms provide the HF approximation (taking into account the sign changes by permutation of fermionic operators), while all other expectation values vanish due to the conservation of particle number.

In order to solve Eq. (6.11) we first solve the eigenvalue equation

$$\left[-\frac{\hbar^2}{2m_r}\Delta - \frac{e^2}{4\pi\epsilon_{\rm host}\epsilon_0|\mathbf{r}|}\right]\Psi_\alpha(\mathbf{r}) = E_\alpha\Psi_\alpha(\mathbf{r})$$

which is called *Wannier equation*. It is identical with the equation for the hydrogen atom where $m_r = m_e m_p/(m_e+m_p)$ is the reduced mass taking into account the proton motion as well. Thus, for $E_\alpha < 0$ we have a discrete set of levels with energies

$$E_\alpha = -\frac{m_r e^4}{32\pi^2\epsilon_{\rm host}^2\epsilon_0^2\hbar^2}\frac{1}{n_\alpha^2} = -{\rm Ryd}^*\frac{1}{n_\alpha^2}$$

where n_α is the principal quantum number of the state $\alpha = (n,l,m)$. Ryd* is the effective Rydberg constant taking into account the effective mass and the dielectric constant. These states are bound states between a conduction band electron and a hole in the valence band, which is called *Wannier exciton*. The wave function $\Psi_\alpha(\mathbf{r})$ describes the relative motion between the electron and the hole.

In addition, we obtain a continuous set of states with energies $E_\alpha \geq 0$, so that the functions $\Psi_\alpha(\mathbf{r})$ form a complete orthonormal system.

Decomposing

$$p(\mathbf{r},\omega) = \sum_\alpha p_\alpha(\omega)\Psi_\alpha(\mathbf{r})$$

we find from Eq. (6.11) after multiplying with $\Psi^*_{\alpha'}(\mathbf{r})$ and integrating over space:

$$p_{\alpha'}(\omega) = \frac{\mu_{cv}F(\omega)\Psi^*_{\alpha'}(0)}{E_g + E_{\alpha'} - \hbar(\omega+{\rm i}\gamma)}$$

which provides us with

$$p(\mathbf{r},\omega) = \sum_\alpha \frac{\mu_{cv}F(\omega)\Psi^*_\alpha(0)\Psi_\alpha(\mathbf{r})}{E_g + E_\alpha - \hbar(\omega+{\rm i}\gamma)}$$

Inserting into Eq. (6.10) we find

$$p_{\mathbf{k}}(\omega) = \sum_\alpha \frac{\mu_{cv}F(\omega)\Psi^*_\alpha(0)}{E_g + E_\alpha - \hbar(\omega+{\rm i}\gamma)}\int {\rm d}^3r\, \Psi_\alpha(\mathbf{r}){\rm e}^{-{\rm i}\mathbf{k}\cdot\mathbf{r}}$$

Finally, the polarization[3] is given by $P(\omega) = \frac{2({\rm for\ spin})}{(2\pi)^3}\int {\rm d}^3\, k\mu^*_{cv}p_{\mathbf{k}}(\omega)$ and we find the susceptibility:

$$\chi^{\rm rel} = \frac{2|\mu_{cv}|^2}{\epsilon_0\epsilon_{\rm host}}\sum_\alpha \frac{|\Psi_\alpha(0)|^2}{E_g + E_\alpha - \hbar(\omega+{\rm i}\gamma)}$$

For $\gamma \to 0$ this provides absorption at sharp exciton peaks located at $\hbar\omega = E_{\rm gap} - {\rm Ryd}^*/n^2$, as well as a continuum absorption spectrum above the band gap, see Fig. 6.1[4].

6.2 The Hartree-Fock approximation

In Eq. (6.6) we defined the Hartree-Fock approximation on the level of expectation values. Here we want to perform the equivalent approximation on the operator level. We start with the general two-particle operator

$$\hat{O}_{\rm TP} = \hat{a}^\dagger_n\hat{a}^\dagger_{n'}\hat{a}_{m'}\hat{a}_m \tag{6.12}$$

[3]We neglect the additional term $\mu_{cv}p^*_{\mathbf{k}}(-\omega)$ from Eq. (5.16), which is negligible for $\hbar\gamma \ll E_g$. This corresponds to the rotation wave approximation.

[4]For a further discussion, see Sec. 3.2 of Chow and Koch (1999).

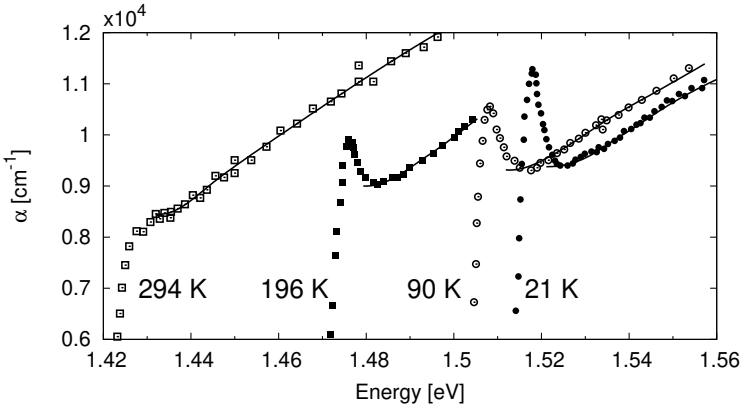

Figure 6.1: Absorption in GaAs for different temperatures. Note that the band gap decreases with temperature. At low temperature an exciton peak becomes visible. After M.D. Surge, Physical Review **127**, 768 (1962).

and look for an equivalent operator $\hat{O}^{\mathrm{HF}}$ containing only *single-particle* operators (and numbers) which satisfies

$$\langle o_1', o_2', \ldots | \hat{O}^{\mathrm{HF}} | o_1, o_2, \ldots \rangle = \langle o_1', o_2', \ldots | \hat{O}_{\mathrm{TP}} | o_1, o_2, \ldots \rangle \tag{6.13}$$

If this would hold for arbitrary states, the operators would be identical. $\hat{O}_{\mathrm{TP}}$ contains two annihilation and two creation operator. Thus its matrix elements vanish unless the states $|o_1', o_2', \ldots\rangle$ and $|o_1, o_2, \ldots\rangle$ (i) are identical, (ii) have an exchange in occupation [i.e. $(o_i, o_j) = (1, 0)$ and $(o_i', o_j') = (0, 1)$] for one pair of states (i, j), or (iii) have an exchange in occupation for two different pairs of states. In contrast, a single-particle operator provides always zero for case (iii). Thus, the best approximation is obtained by the requirement, that the matrix elements agree for Slater states $|o_1, o_2, \ldots\rangle$, $|o_1', o_2', \ldots\rangle$, which are identical or differ by exchanging the occupation in an arbitrary pair of states. As shown below this requirement is satified by the

Hartree-Fock approximation

$$\begin{aligned} \hat{O}_{\mathrm{TP}} = \hat{a}_n^\dagger \hat{a}_{n'}^\dagger \hat{a}_{m'} \hat{a}_m \quad \rightarrow \quad \hat{O}^{\mathrm{HF}} =& \hat{a}_{n'}^\dagger \hat{a}_{m'} \langle \hat{a}_n^\dagger \hat{a}_m \rangle + \hat{a}_n^\dagger \hat{a}_m \langle \hat{a}_{n'}^\dagger \hat{a}_{m'} \rangle - \langle \hat{a}_{n'}^\dagger \hat{a}_{m'} \rangle \langle \hat{a}_n^\dagger \hat{a}_m \rangle \\ & - \hat{a}_{n'}^\dagger \hat{a}_m \langle \hat{a}_n^\dagger \hat{a}_{m'} \rangle - \hat{a}_n^\dagger \hat{a}_{m'} \langle \hat{a}_{n'}^\dagger \hat{a}_m \rangle + \langle \hat{a}_{n'}^\dagger \hat{a}_m \rangle \langle \hat{a}_n^\dagger \hat{a}_{m'} \rangle \end{aligned} \tag{6.14}$$

Here the expectation values have to be taken self-consistently with the true state of the system. The first line is commonly referred to as Hartree-term and the second as Fock-term. Note that the expectation value $\langle \hat{O}^{\mathrm{HF}} \rangle$ is identical to the Hartree-Fock approximation for the expectation value $\langle \hat{O}_{\mathrm{TP}} \rangle$ used in (6.6), showing the equivalence between both definitions. Indeed there are many different ways to define a Hartree-Fock approximation, which essentially boil down to the same thing.

6.2.1 Proof*

We first consider the case (ii) of different states, which can be written as $|o_1', o_2', \ldots\rangle = \hat{a}_i \hat{a}_j^\dagger |o_1, o_2, \ldots\rangle$ with $i \neq j$. (Here we neglect a factor (-1) for an odd number of occupied states between i and j for simplicity.)

$$\begin{aligned} &\langle o_1, o_2, \ldots | \hat{a}_j \hat{a}_i^\dagger \hat{a}_n^\dagger \hat{a}_{n'}^\dagger \hat{a}_{m'} \hat{a}_m | o_1, o_2, \ldots \rangle \\ &= \delta_{o_m,1} \delta_{o_{m'},1} \left(\delta_{m,n} \delta_{n',j} \delta_{m',i} - \delta_{m',n} \delta_{n',j} \delta_{m,i} + \delta_{m',n'} \delta_{n,j} \delta_{m,i} - \delta_{m,n'} \delta_{n,j} \delta_{m',i} \right) \end{aligned}$$

For $|\Psi\rangle = |o_1, o_2, \ldots\rangle$ we may replace $\delta_{o_m,1}\delta_{m,n} = \langle\Psi|\hat{a}_n^\dagger \hat{a}_m|\Psi\rangle$ [5] and find that the single-particle operator

$$\hat{O}_{\rm SP}^{\rm HF} = \hat{a}_{n'}^\dagger \hat{a}_{m'} \langle\Psi|\hat{a}_n^\dagger \hat{a}_m|\Psi\rangle - \hat{a}_{n'}^\dagger \hat{a}_m \langle\Psi|\hat{a}_n^\dagger \hat{a}_{m'}|\Psi\rangle + \hat{a}_n^\dagger \hat{a}_m \langle\Psi|\hat{a}_{n'}^\dagger \hat{a}_{m'}|\Psi\rangle - \hat{a}_n^\dagger \hat{a}_{m'} \langle\Psi|\hat{a}_{n'}^\dagger \hat{a}_m|\Psi\rangle$$

satisfies Eq. (6.13) for arbitrary states which differ by exchanging the occupation of two states. Now consider the case (i) of identical states $|o_1', o_2', \ldots\rangle = |o_1, o_2, \ldots\rangle$, which provides

$$\langle o_1, o_2, \ldots|\hat{a}_n^\dagger \hat{a}_{n'}^\dagger \hat{a}_{m'} \hat{a}_m|o_1, o_2, \ldots\rangle = \delta_{o_m,1}\delta_{o_{m'},1}(\delta_{n,m}\delta_{n',m'} - \delta_{n,m'}\delta_{m,n'})$$

We find

$$\begin{aligned}\langle o_1, o_2, \ldots|\hat{O}_{\rm TP}|o_1, o_2, \ldots\rangle =& \langle o_1, o_2, \ldots|\hat{O}_{\rm SP}^{\rm HF}|o_1, o_2, \ldots\rangle \\ & \underbrace{-\langle\Psi|\hat{a}_{n'}^\dagger \hat{a}_{m'}|\Psi\rangle\langle\Psi|\hat{a}_n^\dagger \hat{a}_m|\Psi\rangle + \langle\Psi|\hat{a}_n^\dagger \hat{a}_{m'}|\Psi\rangle\langle\Psi|\hat{a}_{n'}^\dagger \hat{a}_m|\Psi\rangle}_{=O_{\text{double counting}}^{\rm HF}}\end{aligned}$$

As the state $|o_1, o_2, \ldots\rangle$ is normalized this double counting correction $O_{\text{double counting}}^{\rm HF}$ can be established by adding this number to $\hat{O}_{\rm SP}^{\rm HF}$. This does not affect the case (ii) where $|o_1', o_2', \ldots\rangle$ and $|o_1, o_2, \ldots\rangle$ are orthogonal. Thus $\hat{O}^{\rm HF} = \hat{O}_{\rm SP}^{\rm HF} + O_{\text{double counting}}^{\rm HF}$ is the effective operator to approximate $\hat{O}_{\rm TP}$, which provides Eq. (6.14).

6.2.2 Application to the Coulomb interaction

The Coulomb interaction reads in occupation number representation

$$\hat{V}_{\rm ee} = \frac{1}{2}\sum_{ss'}\int {\rm d}^3r \int {\rm d}^3r'\, \hat{\Psi}^\dagger(\mathbf{r}, s)\hat{\Psi}^\dagger(\mathbf{r}', s')\frac{e^2}{4\pi\epsilon_0|\mathbf{r}-\mathbf{r}'|}\hat{\Psi}(\mathbf{r}', s')\hat{\Psi}(\mathbf{r}, s)$$

Now we want to replace this two-particle interaction by an effective mean field model, which operates on single particles, i.e. containing only one annihilation and one creation operator. The other two operators are replaced by their expectation value. Here we have four possibilities:

- $\hat{\Psi}^\dagger(\mathbf{r}, s)\hat{\Psi}(\mathbf{r}, s)$ and $\hat{\Psi}^\dagger(\mathbf{r}', s')\hat{\Psi}(\mathbf{r}', s')$ provide the same result exchanging the particle coordinates and yield the *Hartree term*

$$\begin{aligned}\hat{V}_{\rm Hartree} =& \sum_s \int {\rm d}^3r \hat{\Psi}^\dagger(\mathbf{r}, s)\hat{\Psi}(\mathbf{r}, s)\int {\rm d}^3r' \frac{e^2}{4\pi\epsilon_0|\mathbf{r}-\mathbf{r}'|}\sum_{s'}\langle\hat{\Psi}^\dagger(\mathbf{r}', s')\hat{\Psi}(\mathbf{r}', s')\rangle \\ & - \frac{1}{2}\sum_{ss'}\int {\rm d}^3r \int {\rm d}^3r' \frac{e^2}{4\pi\epsilon_0|\mathbf{r}-\mathbf{r}'|}\langle\hat{\Psi}^\dagger(\mathbf{r}, s)\hat{\Psi}(\mathbf{r}, s)\rangle\langle\hat{\Psi}^\dagger(\mathbf{r}', s')\hat{\Psi}(\mathbf{r}', s')\rangle\end{aligned}$$

  which describes the interaction of the electron (with charge $-e$) at $\mathbf{r}$ with the classical electric potential $\phi(\mathbf{r}) = \sum_{s'}\int {\rm d}^3r' \frac{-e}{4\pi\epsilon_0|\mathbf{r}-\mathbf{r}'|}n(\mathbf{r}')$ of the electron distribution.

- $\hat{\Psi}^\dagger(\mathbf{r}, s)\hat{\Psi}(\mathbf{r}', s')$ and $\hat{\Psi}^\dagger(\mathbf{r}', s')\hat{\Psi}(\mathbf{r}, s)$ provide the *Fock term*

$$\begin{aligned}\hat{V}_{\rm Fock} =& -\int {\rm d}^3r \int {\rm d}^3r' \sum_{s,s'}\hat{\Psi}^\dagger(\mathbf{r}, s)\hat{\Psi}(\mathbf{r}', s')\frac{e^2}{4\pi\epsilon_0|\mathbf{r}-\mathbf{r}'|}\langle\hat{\Psi}^\dagger(\mathbf{r}', s')\hat{\Psi}(\mathbf{r}, s)\rangle \\ & + \frac{1}{2}\sum_{s,s'}\int {\rm d}^3r \int {\rm d}^3r' \frac{e^2}{4\pi\epsilon_0|\mathbf{r}-\mathbf{r}'|}\langle\hat{\Psi}^\dagger(\mathbf{r}, s)\hat{\Psi}(\mathbf{r}', s')\rangle\langle\hat{\Psi}^\dagger(\mathbf{r}', s')\hat{\Psi}(\mathbf{r}, s)\rangle\end{aligned}$$

[5] The following equations hold for the state $|\Psi\rangle = |o_1', o_2', \ldots\rangle$ as well. I believe that $|\Psi\rangle = \alpha|o_1, o_2, \ldots\rangle + \beta|o_1', o_2', \ldots\rangle$ with $|\alpha|^2 + |\beta|^2 = 1$ is also possible, but could not proof it yet.

which describes the *exchange interaction* due to the antisymmetry of the electronic wave function. It constitutes a single-particle interaction with a nonlocal potential.

In both cases we have subtracted the product of the expectation values as in the mean field model for the Heisenberg model, see Sec. 3.3.4. The remaining terms of the full interaction $\hat{V}_{\text{correlations}} = \hat{V}_{\text{ee}} - \hat{V}_{\text{Hartree}} - \hat{V}_{\text{Fock}}$ are called *correlation energy*, and cannot be expressed as a single-particle potential.

Now we insert $\hat{\Psi}(\mathbf{r}, s) = \sum_{\mathbf{k}\sigma} \varphi_{c\mathbf{k}}(\mathbf{r})\chi_\sigma(s)\hat{a}_{\mathbf{k}\sigma}$ for a single conduction band with two spins, $\chi_\sigma(s) = \delta_{\sigma,s}$. (In this paragraph we write the spin state σ explicitly, while it is tacitly included within $\mathbf{k}$ otherwise.) If we restrict to a homogeneous electron gas [i.e. setting $\langle \hat{a}^\dagger_{\mathbf{k}'\sigma'}\hat{a}_{\mathbf{k}\sigma}\rangle = \delta_{\mathbf{k}',\mathbf{k}}\delta_{\sigma\sigma'}\langle \hat{a}^\dagger_{\mathbf{k}\sigma}\hat{a}_{\mathbf{k}\sigma}\rangle$, see Eq. (6.21)] we obtain the Hartree-Fock part

$$\begin{aligned}\hat{V}_{\text{HF}} =& \frac{1}{V}\sum_{\mathbf{k}\sigma\mathbf{k}'\sigma'} V_0 \left[\langle \hat{a}^\dagger_{\mathbf{k}'\sigma'}\hat{a}_{\mathbf{k}'\sigma'}\rangle \hat{a}^\dagger_{\mathbf{k}\sigma}\hat{a}_{\mathbf{k}\sigma} - \frac{1}{2}\langle \hat{a}^\dagger_{\mathbf{k}'\sigma'}\hat{a}_{\mathbf{k}'\sigma'}\rangle\langle \hat{a}^\dagger_{\mathbf{k}\sigma}\hat{a}_{\mathbf{k}\sigma}\rangle\right] \\ & - \frac{1}{V}\sum_{\mathbf{k}\sigma\mathbf{q}} V_q \left[\langle \hat{a}^\dagger_{(\mathbf{k}+\mathbf{q})\sigma}\hat{a}_{(\mathbf{k}+\mathbf{q})\sigma}\rangle \hat{a}^\dagger_{\mathbf{k}\sigma}\hat{a}_{\mathbf{k}\sigma} - \frac{1}{2}\langle \hat{a}^\dagger_{(\mathbf{k}+\mathbf{q})\sigma}\hat{a}_{(\mathbf{k}+\mathbf{q})\sigma}\rangle\langle \hat{a}^\dagger_{\mathbf{k}\sigma}\hat{a}_{\mathbf{k}\sigma}\rangle\right]\end{aligned} \tag{6.15}$$

6.3 The free electron gas*

Let us consider a free electron gas of density $n = N/V$ and evaluate the expectation value of the total energy

$$E_G = \langle \Psi_G | \hat{T} + \hat{V}_{\text{Background}} + \hat{V}_{\text{ee}} | \Psi_G \rangle$$

where $|\Psi_G\rangle$ is the N-particle ground state, $\hat{T} = \sum_{\mathbf{k}} \frac{\hbar^2 k^2}{2m}\hat{a}^\dagger_{\mathbf{k}}\hat{a}_{\mathbf{k}}$ is the kinetic energy and $\hat{V}_{\text{Background}}$ describes the interaction with a homogeneous positive background charge of the same density n (this is called jellium model). It can be shown that the Slater state $|\Psi_F\rangle$ (F stands for Fermi sphere), where all k-states up to

$$k_F = (3\pi^2 n)^{1/3} \quad \text{corresponding to} \quad E_F = \frac{\hbar^2}{2m}(3\pi^2 n)^{2/3} \tag{6.16}$$

are occupied, is the ground state of the Hamiltonian, if we restrict the Coulomb interaction to its Hartree-Fock part $\hat{V}_{\text{HF}}$ from Eq. (6.15). Then we find (see, e.g. Sec. 5.4 of Czycholl (2004))

- The kinetic energy per particle reads

$$\langle \Psi_F | \hat{T} | \Psi_F \rangle = \sum_{\mathbf{k}}^{k_F} \frac{\hbar^2 k^2}{2m} = 2(\text{for spin})\frac{V}{(2\pi)^3}\int_0^{k_F} \mathrm{d}k\, 4\pi k^2 \frac{\hbar^2 k^2}{2m} = N\frac{3}{5}E_F$$

- The Hartree part

$$\frac{1}{2V}\sum_{\mathbf{k}\mathbf{k}'} V_0 \left[2\hat{a}^\dagger_{\mathbf{k}}\hat{a}_{\mathbf{k}}\langle \hat{a}^\dagger_{\mathbf{k}'}\hat{a}_{\mathbf{k}'}\rangle - \langle \hat{a}^\dagger_{\mathbf{k}}\hat{a}_{\mathbf{k}}\rangle\langle \hat{a}^\dagger_{\mathbf{k}'}\hat{a}_{\mathbf{k}'}\rangle\right]$$

  exactly cancels with $\hat{V}_{\text{Background}}$.

- The Fock part yields (after some tedious calculation)

$$\langle \Psi_F | - \frac{1}{2V}\sum_{\mathbf{k}\mathbf{q}} V_q \left(2\hat{a}^\dagger_{\mathbf{k}}\hat{a}_{\mathbf{k}} - \langle \hat{a}^\dagger_{\mathbf{k}}\hat{a}_{\mathbf{k}}\rangle\right)\langle \hat{a}^\dagger_{(\mathbf{k}+\mathbf{q})}\hat{a}_{(\mathbf{k}+\mathbf{q})}\rangle | \Psi_F\rangle = -N\frac{3e^2}{16\pi^2\epsilon_0}k_F$$

The total energy per particle is now a function of the density n, which can be conveniently expressed using

$$\mathrm{Ryd} = \frac{m_e e^4}{32\pi^2\epsilon_0^2\hbar^2} = 13.6\mathrm{eV} \quad a_B = \frac{4\pi\epsilon_0\hbar^2}{m_e e^2} = 0.53\text{Å} \quad \frac{1}{n} = \frac{4}{3}\pi a_B^3 r_s^3$$

where r_s is the mean distance between the electrons in units of the Bohr radius. Then we find the total energy per particle

$$\frac{E_G^{\mathrm{HF}}}{N} = \frac{2.2099\mathrm{Ryd}}{r_s^2} - \frac{0.9163\mathrm{Ryd}}{r_s} \tag{6.17}$$

in Hartree-Fock approximation. This energy has its minimum at $r_s = 4.823$ corresponding to an electron density $1.43 \times 10^{22}/\mathrm{cm}^3$ with the value $E_G^{\mathrm{HF}}/N = -0.095\mathrm{Ryd} = -1.3\mathrm{eV}$. These values are comparable with the densities and separation energies of alkali metals ($4.7\times10^{22}/\mathrm{cm}^3$ and 1.63 eV for Li; $0.9\times10^{22}/\mathrm{cm}^3$ and 0.804 eV for Cs, see tables 1.4 and 3.1 of Kittel (1996)). Thus we have an approximate description of the binding in metals. For higher densities (lower r_s) too much kinetic energy is needed to satisfy the Pauli principle. On the other hand, for lower densities (higher r_s) the attractive interaction between the positive background and the electrons (which is not fully compensated by electronic repulsion due to the Fock part) becomes too weak.

Treating the correlation part $\hat{V}_{\mathrm{ee}} - \hat{V}_{\mathrm{HF}}$ within perturbation theory (a complex task) one finds further terms [6]

$$\frac{E_G}{N} = \frac{2.2099\mathrm{Ryd}}{r_s^2} - \frac{0.9163\mathrm{Ryd}}{r_s} + 0.0622\mathrm{Ryd}\log r_s - 0.094\mathrm{Ryd} + \mathcal{O}(r_s)$$

Metals have densities of the order of $5\times10^{22}/\mathrm{cm}^3$ (see table 1 of Kittel (1996)), resulting in $r_s \approx 3$. Thus, the kinetic energy and the Fock part dominate the energy and correlation corrections are somewhat smaller, but become very important for densities less than $5 \times 10^{21}/\mathrm{cm}^3$.

6.3.1 A brief glimpse of density functional theory

As seen above, the complicated many-particle interactions can be divided into the Hartree term, the exchange term, and further correlation effects. For a given particle, these result in effective potentials depending on all other particles. In density functional theory this interaction is described via the density $n(\mathbf{r})$ of the electron gas. For the Hartree term this provides the potential

$$V_H(\mathbf{r}) = \int \mathrm{d}^3r' \frac{e^2 n(\mathbf{r}')}{4\pi\epsilon_0|\mathbf{r}-\mathbf{r}'|}\,,$$

while corresponding functionals for the exchange and correlation terms, subsumed in $V_{XC}(\mathbf{r})$, can be shown to exist for the ground state, but are not explicitly known. A common approximation is the local density approximation (LDA): Considering a fictitious homogeneous electron gas with the sum of exchange and correlation energy $E_{XC}(n)$ (as partially evaluated above) and sets $V_{XC}(\mathbf{r}) = \frac{\mathrm{d}E_{XC}(n(\mathbf{r}))}{\mathrm{d}n}$. Thus one obtains the single-particle Hamiltonian

$$\hat{H}_{\mathrm{Kohn-Sham}}\{n(\mathbf{r})\} = -\frac{\hbar^2}{2m}\Delta + V_{\mathrm{lattice}}(\mathbf{r}) + V_H(\mathbf{r}) + V_{XC}(\mathbf{r})$$

which is a functional of $n(\mathbf{r})$ via the effective potentials V_H and V_{XC}. Numerical solution of the Kohn-Sham equations $\hat{H}_{\mathrm{Kohn-Sham}}\varphi_n(\mathbf{r}) = E_n\varphi_n(\mathbf{r})$ provides the eigenvalues E_n and

[6] according to Sec 5.1 of Mahan: *Many Particle Physics* (Plenum 1993)

eigenfunctions $\varphi_n(\mathbf{r})$. Occupying the N lowest energy-eigenstates until charge neutrality is reached, the density reads $n(\mathbf{r}) = \sum_{n=1}^{N} |\varphi_n(\mathbf{r})|^2$. Now one has to find a self-consistent solution, so that the evaluated density equals the input in $\hat{H}_{\mathrm{Kohn-Sham}}\{n(\mathbf{r})\}$, which is done iteratively. In this way one obtains the ground state energy and its spatial density distribution of the many-particle system. This allows, e.g., for the determination of the equilibrium configuration of a set of atoms, (i.e. the positions with lowest total energy), which is of high relevance both in chemistry and solid state physics. Frequently, the energies E_n are also considered as electronic excitation energies, which is however problematic, as the heuristic justification given above can only be validated for ground states of the system. For more information see, e.g., the notes by K. Capelle `http://arxiv.org/abs/cond-mat/0211443`.

6.4 The Lindhard-Formula for the dielectric function

6.4.1 Derivation

If we consider spatially inhomogeneous electric fields, the polarization reads

$$\mathbf{P}(\mathbf{r},t) = \epsilon_0 \int \mathrm{d}^3 r' \mathrm{d}t' \, \chi(\mathbf{r}-\mathbf{r}', t-t') \mathbf{F}(\mathbf{r}', t')$$

which results in

$$\mathbf{P}(\mathbf{q},\omega) = \epsilon_0 \chi(\mathbf{q},\omega)\mathbf{F}(\mathbf{q},\omega) \quad \text{or} \quad \mathbf{P}(\mathbf{q},\omega) = \chi^{\mathrm{rel}}(\mathbf{q},\omega)\epsilon_0\epsilon_{\mathrm{host}}\mathbf{F}(\mathbf{q},\omega)$$

after Fourier transformation in space and time. Now we have $\nabla \cdot \mathbf{P}(\mathbf{r},t) = -\rho_{\mathrm{ind}}(\mathbf{r},t)$ and $\mathbf{F}(\mathbf{r},t) = -\nabla\phi(\mathbf{r},t)$ in the quasistatic case, where $\frac{\partial}{\partial t}\mathbf{A}(\mathbf{r},t)$is negligible. Thus

$$\begin{aligned} \rho_{\mathrm{ind}}(\mathbf{q},\omega) =& -\mathrm{i}\mathbf{q}\cdot\mathbf{P}(\mathbf{q},\omega) = -\mathrm{i}\mathbf{q}\cdot\epsilon_0\epsilon_{\mathrm{host}}\chi^{\mathrm{rel}}(\mathbf{q},\omega)\mathbf{F}(\mathbf{q},\omega) \\ =& \mathrm{i}\mathbf{q}\cdot\epsilon_0\epsilon_{\mathrm{host}}\chi^{\mathrm{rel}}(\mathbf{q},\omega)\mathrm{i}\mathbf{q}\phi(\mathbf{q},\omega) = -q^2\epsilon_0\epsilon_{\mathrm{host}}\chi^{\mathrm{rel}}(\mathbf{q},\omega)\phi(\mathbf{q},\omega) \end{aligned} \tag{6.18}$$

and the ratio $\rho_{\mathrm{ind}}(\mathbf{q},\omega)/\phi(\mathbf{q},\omega)$ provides us with the susceptibility.[7]

Now we want to evaluate this charge density induced by the potential for a free electron gas. Using Eq. (6.3) the electrical potential $\phi(\mathbf{r},t) = \frac{1}{V}\sum_{\mathbf{q}} \mathrm{e}^{\mathrm{i}\mathbf{q}\cdot\mathbf{r}}\phi(\mathbf{q},t)$ results in the Hamilton-operator[8]

$$\hat{H} = \underbrace{\sum_{n\mathbf{k}} E_n(\mathbf{k})\hat{a}^\dagger_{n\mathbf{k}}\hat{a}_{n\mathbf{k}}}_{=\hat{H}_0} + \underbrace{\frac{(-e)}{V}\sum_{n\mathbf{k}}\sum_{\mathbf{q}}\phi(\mathbf{q},t)\hat{a}^\dagger_{n(\mathbf{k}+\mathbf{q})}\hat{a}_{n\mathbf{k}}}_{=\delta\hat{H}} \tag{6.19}$$

for the electrons in the crystal, where the Bloch states are the natural basis. The charge density, averaged over a unit cell, is given by

$$\rho(\mathbf{r}) = -e\langle\Psi^\dagger(\mathbf{r})\Psi(\mathbf{r})\rangle = -e\sum_{n\mathbf{k},n'\mathbf{k}'}\varphi^*_{n',\mathbf{k}'}(\mathbf{r})\varphi_{n\mathbf{k}}(\mathbf{r})\langle\hat{a}^\dagger_{n'\mathbf{k}'}\hat{a}_{n\mathbf{k}}\rangle \tag{6.20}$$

with the Fourier transformation using Eq. (6.3)

$$\rho(\mathbf{q}) \approx -e\sum_{n\mathbf{k}}\langle\hat{a}^\dagger_{n(\mathbf{k}-\mathbf{q})}\hat{a}_{n\mathbf{k}}\rangle \quad \Leftrightarrow \quad \rho(\mathbf{r}) \approx \frac{-e}{V}\sum_{\mathbf{q}}\sum_{n\mathbf{k}}\langle\hat{a}^\dagger_{n(\mathbf{k}-\mathbf{q})}\hat{a}_{n\mathbf{k}}\rangle\mathrm{e}^{\mathrm{i}\mathbf{q}\cdot\mathbf{r}} \tag{6.21}$$

[7] This is actually the longitudinal part of the susceptibility tensor. A full calculation for the tensor structure can be found in S.L. Adler, Phys. Rev. **126**, 413 (1962). As discussed there, the tensor becomes diagonal for cubic crsytals and $q \to 0$, so that our result (6.22) is general in this case.

[8] Note that $\phi(\mathbf{q},t)$ will both contain external potentials and the potential of the electron gas itself. Thus this Hamilton operator treats the electron-electron interaction in Hartree approximation.

which holds for small $\mathbf{q}$ disregarding any charge fluctuations on the atomic scale.

Now we consider the equation of motion for the expectation value $\langle \hat{a}^\dagger_{n(\mathbf{k}-\mathbf{q})} \hat{a}_{n\mathbf{k}} \rangle$

$$\frac{\mathrm{d}}{\mathrm{d}t}\langle \hat{a}^\dagger_{n(\mathbf{k}-\mathbf{q})} \hat{a}_{n\mathbf{k}} \rangle = \frac{\mathrm{i}}{\hbar}\left\langle \left[\hat{H}, \hat{a}^\dagger_{n(\mathbf{k}-\mathbf{q})} \hat{a}_{n\mathbf{k}}\right] \right\rangle - \gamma \left(\langle \hat{a}^\dagger_{n(\mathbf{k}-\mathbf{q})} \hat{a}_{n\mathbf{k}} \rangle - \delta_{\mathbf{q},0} f_n(\mathbf{k}) \right)$$

where the latter term phenomenologically restores the homogeneity if $\delta\hat{H}$ vanishes. We find

$$\begin{aligned}\frac{\mathrm{d}}{\mathrm{d}t}\langle \hat{a}^\dagger_{n(\mathbf{k}-\mathbf{q})} \hat{a}_{n\mathbf{k}} \rangle =& \frac{\mathrm{i}}{\hbar}[E_n(\mathbf{k}-\mathbf{q}) - E_n(\mathbf{k})]\langle \hat{a}^\dagger_{n(\mathbf{k}-\mathbf{q})} \hat{a}_{n\mathbf{k}} \rangle - \gamma \left(\langle \hat{a}^\dagger_{n(\mathbf{k}-\mathbf{q})} \hat{a}_{n\mathbf{k}} \rangle - \delta_{\mathbf{q},0} f_n(\mathbf{k}) \right) \\ &+ \frac{\mathrm{i}}{\hbar}\frac{(-e)}{V}\sum_{\mathbf{q}'} \phi(\mathbf{q}', t) \left(\langle \hat{a}^\dagger_{n(\mathbf{k}+\mathbf{q}'-\mathbf{q})} \hat{a}_{n\mathbf{k}} \rangle - \langle \hat{a}^\dagger_{n(\mathbf{k}-\mathbf{q})} \hat{a}_{n(\mathbf{k}-\mathbf{q}')} \rangle \right)\end{aligned}$$

For $\mathbf{q} \neq 0$, the expectation value $\langle \hat{a}^\dagger_{n(\mathbf{k}-\mathbf{q})} \hat{a}_{n\mathbf{k}} \rangle$ is of order ϕ in the potential. Thus we have

$$\langle \hat{a}^\dagger_{n(\mathbf{k}+\mathbf{q}'-\mathbf{q})} \hat{a}_{n\mathbf{k}} \rangle = f_n(\mathbf{k})\delta_{\mathbf{q}',\mathbf{q}} + \mathcal{O}\{\phi\}$$

and we find after Fourier-transformation in time

$$\begin{aligned}-\mathrm{i}\omega\langle \hat{a}^\dagger_{n(\mathbf{k}-\mathbf{q})} \hat{a}_{n\mathbf{k}} \rangle_\omega =& \left(\frac{\mathrm{i}}{\hbar}[E_n(\mathbf{k}-\mathbf{q}) - E_n(\mathbf{k})] - \gamma \right) \langle \hat{a}^\dagger_{n(\mathbf{k}-\mathbf{q})} \hat{a}_{n\mathbf{k}} \rangle_\omega + 2\pi\gamma\delta(\omega)\delta_{\mathbf{q},0} f_n(\mathbf{k}) \\ &+ \frac{\mathrm{i}}{\hbar}\frac{(-e)}{V}\phi(\mathbf{q},\omega)\left(f_n(\mathbf{k}) - f_n(\mathbf{k}-\mathbf{q})\right) + \mathcal{O}\{\phi^2\}\end{aligned}$$

with the solution

$$\langle \hat{a}^\dagger_{n(\mathbf{k}-\mathbf{q})} \hat{a}_{n\mathbf{k}} \rangle_\omega = 2\pi\delta(\omega)\delta_{\mathbf{q},0} f_n(\mathbf{k}) + \frac{e}{V}\frac{f_n(\mathbf{k}) - f_n(\mathbf{k}-\mathbf{q})}{E_n(\mathbf{k}-\mathbf{q}) - E_n(\mathbf{k}) + \hbar\omega + \mathrm{i}\hbar\gamma}\phi(\mathbf{q},\omega) + \mathcal{O}\{\phi^2\}\,.$$

Eq. (6.21) gives us the induced charge

$$\rho_{\mathrm{ind}}(\mathbf{q},\omega) = \frac{e^2}{V}\phi(\mathbf{q},\omega)\sum_{n\mathbf{k}} \frac{f_n(\mathbf{k}-\mathbf{q}) - f_n(\mathbf{k})}{E_n(\mathbf{k}-\mathbf{q}) - E_n(\mathbf{k}) + \hbar\omega + \mathrm{i}\hbar\gamma} + \mathcal{O}\{\phi^2\}$$

by the potential ϕ and Eq. (6.18) provides us with the

Lindhard formula for the dielectric function

$$\chi^{\mathrm{rel}}(\mathbf{q},\omega) = -\frac{e^2}{q^2\epsilon_{\mathrm{host}}\epsilon_0 V}\sum_{n\mathbf{k}} \frac{f_n(\mathbf{k}-\mathbf{q}) - f_n(\mathbf{k})}{E_n(\mathbf{k}-\mathbf{q}) - E_n(\mathbf{k}) + \hbar\omega + \mathrm{i}\hbar\gamma} \tag{6.22}$$

which is the central result of this section.

We find:

- Entirely filled or entirely empty bands do not contribute to $\chi(\mathbf{q},\omega)$
- In the limit $\gamma \to 0$ we find

  $$\mathrm{Im}\{\chi(\mathbf{q},\omega)\} = \frac{e^2}{q^2\epsilon_{\mathrm{host}}\epsilon_0 V}\sum_{n\mathbf{k}} (f_n(\mathbf{k}) - f_n(\mathbf{k}+\mathbf{q}))\pi\delta\left(E_n(\mathbf{k}) + \hbar\omega - E_n(\mathbf{k}+\mathbf{q})\right)$$

  Thus $\mathrm{Im}\{\chi(\mathbf{q},\omega)\} > 0$ if there is a possibility for electronic transitions between an occupied state at $\mathbf{k}$ and an empty state $\mathbf{k}+\mathbf{q}$ at a higher energy (difference $\hbar\omega$). For a free electron gas $E_n(\mathbf{k}) = \hbar^2k^2/2m$ which is filled up to k_F this provides $\mathrm{Im}\{\chi(\mathbf{q},\omega)\} \neq 0$ for $\hbar^2(q^2 - 2k_Fq)/2m \leq \hbar\omega \leq \hbar^2(2k_Fq + q^2)/2m$, see Fig. 6.2. Thus $\chi(\mathbf{q},\omega)$ is real both in the high-frequency and large q limit.
- $\mathrm{Im}\{\chi(\mathbf{q},\omega)\} \to 0$ for $\omega \to 0$ as $f_n(\mathbf{k}+\mathbf{q}) = f_n(\mathbf{k})$ for $E_n(\mathbf{k}+\mathbf{q}) = E_n(\mathbf{k})$ in equilibrium.

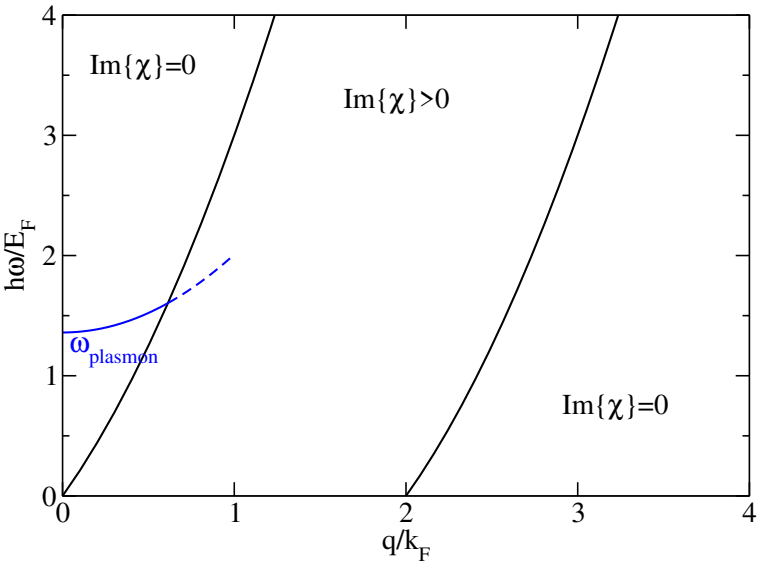

Figure 6.2: General behavior of the Lindhard dielectric function. The ratio $\hbar\omega_{\text{Plasmon}}/E_F = 1.36$ is appropriate for aluminum (n=$1.8 \times 10^{23}/cm^3$ corresponding to $E_F = 11.6eV$, $k_F = 1.75 \times 10^8/cm$).

6.4.2 Plasmons

Now we consider the dielectric function (6.22) in the limit of small q. Replacing $\mathbf{k} \to \mathbf{k} + \mathbf{q}$ in a part of the sum we find for $\gamma \to 0$

$$\text{Re}\{\chi(\mathbf{q},\omega)\} = -\frac{e^2}{q^2\epsilon_{\text{host}}\epsilon_0 V}\sum_{n\mathbf{k}} f_n(\mathbf{k})\left(\frac{1}{E_n(\mathbf{k}) - E_n(\mathbf{k}+\mathbf{q}) + \hbar\omega} - \frac{1}{E_n(\mathbf{k}-\mathbf{q}) - E_n(\mathbf{k}) + \hbar\omega}\right)$$

Using $E_n(\mathbf{k} \pm \mathbf{q}) = E_n(\mathbf{k}) \pm \mathbf{q}\cdot\nabla E_n(\mathbf{k}) + q^2\hbar^2/2m_n(\mathbf{k})$ we find for small q

$$\text{Re}\{\chi(\mathbf{q},\omega)\} \approx -\frac{e^2}{q^2\epsilon_{\text{host}}\epsilon_0 V}\sum_{n\mathbf{k}} f_n(\mathbf{k})\left(\frac{1}{\hbar\omega - \mathbf{q}\cdot\nabla E_n(\mathbf{k})}\right)^2\left(\frac{q^2\hbar^2}{m_n(\mathbf{k})} + \mathcal{O}\{q^4\}\right) \qquad (6.23)$$

In the limit $\mathbf{q} \to 0$ we thus obtain

$$\chi^{\text{rel}}(0,\omega) = -\frac{\omega^2_{\text{plasma}}}{\omega^2} \quad \text{with} \quad \omega^2_{\text{plasma}} = \frac{e^2}{\epsilon_{\text{host}}\epsilon_0 V}\sum_{n\mathbf{k}}\frac{f_n(\mathbf{k})}{m_n(\mathbf{k})} \qquad (6.24)$$

For $\omega = \omega_{\text{plasma}}$ we find $\epsilon_{\text{tot}} = (1 + \chi^{\text{rel}})\epsilon_{\text{host}} =$ and we have a natural oscillation of the system (see section 4.1.2), which is called *plasma oscillation*. For a single band with constant mass we obtain $\omega^2_{\text{plasma}} = e^2 n/(m\epsilon_{\text{host}}\epsilon_0)$, which is the classical frequency of a homogeneous charge-density oscillating with respect to a positive background. We find that $\hbar\omega_{\text{plasma}}$ is of the order of 10 eV for metals with densities $\sim 10^{23}/\text{cm}^3$. Read Sec 11.9 of Ibach and Lüth (2003) for more details! Correspondingly, the equation $\chi^{\text{rel}}(\mathbf{q},\omega) = -1$ provides us with the plasma frequencies[9] $\omega_{\text{plasma}}(\mathbf{q})$ for wavelike oscillations with finite $\mathbf{q}$, as indicated in Fig. 6.2.

For $\omega < \omega_{\text{plasma}}$ we have $\epsilon_{\text{tot}} < 0$ and the refractive index $\tilde{n}(\omega)$ is purely imaginary. As discussed in section 4.1.2 this implies total reflection of electromagnetic waves. Therefore metals with $\omega_{\text{plasma}} > \omega_{\text{light}}$ reflect visible light.

[9] For parabolic bands one finds $\omega_{\text{plasma}}(\mathbf{q}) = \omega_{\text{plasma}}\left[1 + \frac{3v_F^2}{10\omega^2_{\text{plasma}}}q^2 + \ldots\right]$, after Kittel (1996).

6.4.3 Static screening

In thermal equilibrium we have $f_n(\mathbf{k}) = f_F(E_n(\mathbf{k}))$ and for small $\mathbf{q}$ we can expand

$$f_n(\mathbf{k}-\mathbf{q}) \approx f_n(\mathbf{k}) + \frac{\mathrm{d}f_F(E_n(\mathbf{k}))}{\mathrm{d}E}[E_n(\mathbf{k}-\mathbf{q}) - E_n(\mathbf{k})]$$

Then Eq. (6.22) provides us for $\omega = 0$ and $\gamma \to 0$ with

$$\chi^{\mathrm{rel}}(\mathbf{q},0) \approx \frac{\lambda^2}{q^2} \quad \text{for small } q \qquad \text{with} \quad \lambda^2 = \frac{e^2}{\epsilon_{\mathrm{host}}\epsilon_0 V}\sum_{n\mathbf{k}}\left(-\frac{\mathrm{d}f_F(E_n(\mathbf{k}))}{\mathrm{d}E}\right) \tag{6.25}$$

Thus we find $\epsilon_{\mathrm{tot}} = \epsilon_{\mathrm{host}}(1+\lambda^2/q^2)$. Now

$$\rho_{\mathrm{free}}(\mathbf{r},t) = \nabla\cdot\mathbf{D}(\mathbf{r},t) = \nabla\cdot\int \mathrm{d}^3r'\int \mathrm{d}t'\epsilon_{\mathrm{tot}}(\mathbf{r}-\mathbf{r}',t-t')\mathbf{F}(\mathbf{r}',t')$$

and $\mathbf{F}(\mathbf{r},t) = -\nabla\phi(\mathbf{r},t)$ provides after Fourier transformation

$$\rho_{\mathrm{free}}(\mathbf{q},\omega) = q^2\epsilon_0\epsilon_{\mathrm{tot}}(\mathbf{q},\omega)\phi(\mathbf{q},\omega) \quad \Rightarrow \quad \phi(\mathbf{q},0) = \frac{\rho_{\mathrm{free}}(\mathbf{q},0)}{\epsilon_0\epsilon_{\mathrm{host}}(q^2+\lambda^2)}$$

which corresponds to

$$\phi(\mathbf{r}) = \int \mathrm{d}^3r' \frac{\rho_{\mathrm{free}}(\mathbf{r}')\mathrm{e}^{-\lambda|\mathbf{r}-\mathbf{r}'|}}{4\pi\epsilon_0\epsilon_{\mathrm{host}}|\mathbf{r}-\mathbf{r}'|}$$

where Eq. (6.2) has been used. Thus we obtain a screened potential of an external test charge. For a nondegenerate semiconductor we have $\frac{\mathrm{d}f_F(E)}{\mathrm{d}E} \approx -f_F(E)/(k_BT)$ and Eq. (6.25) provides us with the inverse Debye screening length

$$\lambda^2_{\mathrm{Debye}} = \frac{ne^2}{\epsilon_0\epsilon_{\mathrm{host}}k_BT} \tag{6.26}$$

For a degenerate metal we have $\frac{\mathrm{d}f_F(E)}{\mathrm{d}E} \approx -\delta(E_n(\mathbf{k})-E_F)$ providing us with the inverse Thomas-Fermi screening length

$$\lambda^2_{\mathrm{TF}} = \frac{e^2}{\epsilon_{\mathrm{host}}\epsilon_0}D(E_F) \tag{6.27}$$

Assuming a parabolic band structure, we find with Eqs. (1.9,1.11) the screening length $\lambda^{-1}_{\mathrm{TF}} = 0.6$ Å for a typical metallic electron density of $5\times10^{22}/\mathrm{cm}^3$ and $m_{\mathrm{eff}} = m_e$. Thus, the electron-electron interaction is only effective on a very short range in metals. Read also Sec 6.5 of Ibach and Lüth (2003), or Chapter 10 of Kittel (1996).

Chapter 7

Superconductivity

7.1 Phenomenology

Plenty of materials exhibit an intriguing effect at low temperatures, as first observed by H. Kammerlingh Onnes (Leiden 1911)[1] for Hg below 4.2 K.

- For many metals the resistance drops abruptly to "zero", i.e. below any measurement resolution, at the critical temperature T_c (typically a few K). See Fig. 7.1. Data for different materials is given in Fig. 7.2.
- The magnetic field satisfies $\mathbf{B} = 0$ inside the material[2]. Thus, the magnetization $\mathbf{M}$ exactly compensates the magnetizing field $\mathbf{H}$ (Meißner-Ochsenfeld effect).
- Superconductivity vanishes above a critical field $\mathbf{H}_c$.
- The heat capacity exhibits a discontinuity at the transition temperature T_c. This indicates a phase transition (of second order) between a normal and a superconducting phase.
- Superconductivity is an effect due to the electron gas of the solid. There is no change of lattice structure at the transition.
- There is an energy gap 2Δ of the order of 1 meV in the excitation spectrum, which can be manifested by the absorption of microwaves. Electron tunneling (see Fig. 7.3) and the exponential behavior $\mathrm{e}^{-\Delta/k_B T}$ in the specific heat[3] for $T \ll T_c$ show the gap as well.

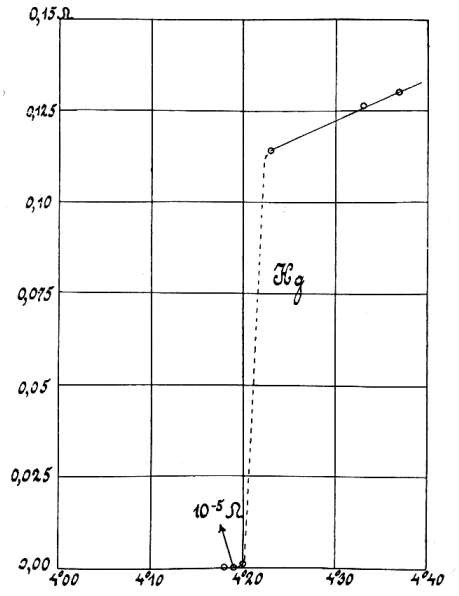

Figure 7.1: Original measurement of the resistance of Hg as a function of temperature. At 4.2 K, the resistance drops abruptly below the resolution of the measurement.(from Wikipedia Commons)

Consult your textbook for details (e.g. Sects. 10.1+2 of Ibach and Lüth (2003))!

[1] For history, see `http://nobelprize.org/nobel_prizes/physics/laureates/1913/onnes-lecture.pdf` and D. van Delft and P. Kes, Physics Today **63**(9), 38 (2010)

[2] Note that for type-2 superconductors there is a finite magnetic induction $\mathbf{B}$ within the superconductor for fields $\mathbf{H}_{c1} < \mathbf{H} < \mathbf{H}_{c2}$, while the material is still superconductive.

[3] page 344 of Kittel (1996).

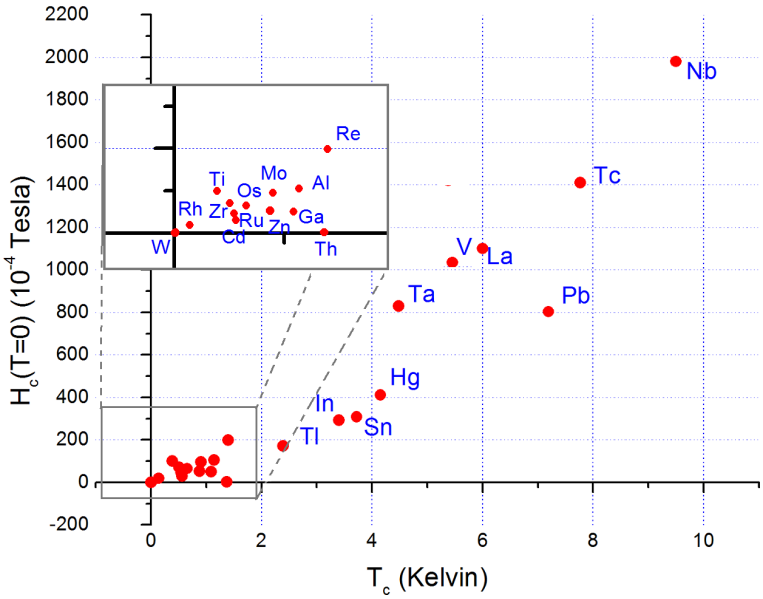

Figure 7.2: Critical temperature and critical magnetic fields of several materials (from Wikipedia Commons)

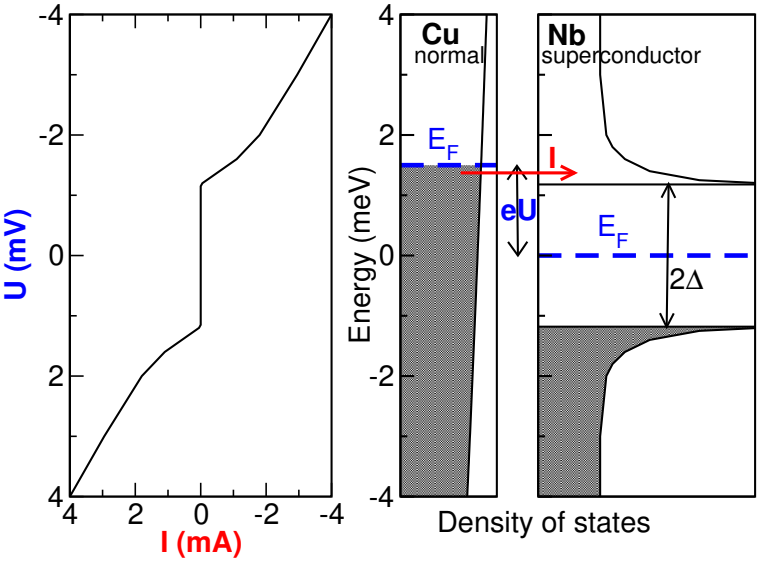

Figure 7.3: Tunneling current from copper to niobium at 0.38 K, see M.G. Castellano *et al.* IEEE Trans. Appli. Supercond. **7**, 3251 (1997). The vanishing current for $|V| \lesssim 1$ mV indicates the presence of a gap in the single particle spectrum, as indicated on the right hand side.

The experimental results can be interpreted by the existence of superconducting electron density n_s establishing a superconducting current density $\mathbf{j}_s$. The vanishing resistance indicates that there is no friction term in the acceleration of electrons, thus $m\dot{\mathbf{v}}_s = -e\mathbf{F}$ or the

1. London equation: $$\frac{\mathrm{d}}{\mathrm{d}t}\mathbf{j}_s = \frac{n_s e^2}{m}\mathbf{F} \tag{7.1}$$

In addition there is a normal part of the electron density $n_n = n - n_s$, which contributes to a normal current density $\mathbf{j}_n = \sigma_n \mathbf{F}$. This is called the two-fluid model.

The key point is the gap $2\Delta(T)$ for creating normal fluid excitation from the superconducting component. This gap vanishes for $T \to T_c$ and the distinction between normal and superconducting component vanishes similar to the difference between a gas and a liquid at the critical point.

With Maxwell's equation $\nabla \times \mathbf{F} = -\dot{\mathbf{B}}$ and Eq. (7.1) we find $\frac{\mathrm{d}}{\mathrm{d}t}(\nabla \times \mathbf{j}_s + \frac{n_s e^2}{m}\mathbf{B}) = 0$ and thus $\nabla \times \mathbf{j}_s + \frac{n_s e^2}{m}\mathbf{B} = \text{const}$. The observation of zero magnetic induction within a superconductor suggests, that the constant is zero and thus we obtain the

2. London equation: $\nabla \times \mathbf{j}_s = -\dfrac{n_s e^2}{m}\mathbf{B}$ (7.2)

Together with the Maxwell equation $\nabla \times \mathbf{B} = \mu_0 \mathbf{j}$ (stationary case) we find $\Delta \mathbf{B} = \frac{\mu_0 n_s e^2}{m}\mathbf{B}$. This provides a spatial decay

$$\begin{aligned} \mathbf{B}(x) &= B(0)\mathbf{e}_z \mathrm{e}^{-x/\lambda_L} \\ \mathbf{j}(x) &= \tfrac{B(0)}{\lambda_L \mu_0}\mathbf{e}_y \mathrm{e}^{-x/\lambda_L} \end{aligned} \quad \text{with the } \textit{penetration length} \quad \lambda_L = \sqrt{\frac{m}{\mu_0 n_s e^2}} \tag{7.3}$$

at the surface ($x = 0$) of superconducting material. We find that a surface current of a depth $\lambda_L \sim 30nm$ shields the outer magnetic field.

7.2 BCS Theory

The BCS theory was developed by Bardeen, Cooper, and Schrieffer in 1957 to describe superconductivity. The theory is rather general for a system of interacting fermions with an *attractive* interaction

$$\hat{V}_a = \frac{1}{2V}\sum_{\mathbf{k}\mathbf{k}'}\sum_{\sigma\sigma'}\sum_{\mathbf{q}} V_{\mathbf{k},\mathbf{k}'}(\mathbf{q})\hat{a}^\dagger_{\sigma(\mathbf{k}+\mathbf{q})}\hat{a}^\dagger_{\sigma'(\mathbf{k}'-\mathbf{q})}\hat{a}_{\sigma'\mathbf{k}'}\hat{a}_{\sigma\mathbf{k}} \tag{7.4}$$

(In this chapter $\mathbf{k}$ does not include spin.) Next to the electron gas, it is also of importance for the structure of nuclei and atomic Fermi gases. Here we assume for simplicity

$$V_{\mathbf{k},\mathbf{k}'}(\mathbf{q}) = \begin{cases} -V_0 & \text{for} \quad |E_{\mathbf{k}} - E_{\mathbf{k}+\mathbf{q}}| < \hbar\omega_D \quad \text{and} \quad |E_{\mathbf{k}'} - E_{\mathbf{k}'-\mathbf{q}}| < \hbar\omega_D \\ 0 & \text{otherwise} \end{cases} \tag{7.5}$$

This can be motivated by an effective interaction with the lattice, where the exchange of virtual acoustic phonons with $\omega < \omega_D$ (the Debye cut-off frequency) provides an attractive interaction as shown in Sec. 7.2.5[4]. The idea is that the first electron creates a distortion of the lattice, which attracts the second electron, similar to two heavy balls on a spring mattress.

The following treatment given here follows the lines given in Sec. 10.3+4 of Ibach and Lüth (2003) and Chapter 2 of Schrieffer (1983). While the former is easier to read, the latter provides a much deeper discussion of the matter.

7.2.1 The Cooper pair

We consider a sea of electrons $|\Psi_F\rangle$ occupying the states $k < k_F$ and add two electrons. Their wave function can be written as

$$\Psi_{\mathrm{Pair}}(\mathbf{r}_1, s_1, \mathbf{r}_2, s_2) = \varphi(\mathbf{r})\mathrm{e}^{\mathrm{i}\mathbf{K}\cdot\mathbf{R}}\chi(s_1, s_2) \quad \text{with} \quad \mathbf{R} = \frac{\mathbf{r}_1 + \mathbf{r}_2}{2} \quad \text{and} \quad \mathbf{r} = \mathbf{r}_1 - \mathbf{r}_2 \tag{7.6}$$

in relative and center-of-mass coordinates. Decomposing into plane waves we have

$$\varphi(\mathbf{r}) = \frac{1}{V}\sum_{\mathbf{k}} g(\mathbf{k})\mathrm{e}^{\mathrm{i}\mathbf{k}\cdot\mathbf{r}} = \frac{1}{V}\sum_{\mathbf{k}} g(\mathbf{k})\mathrm{e}^{\mathrm{i}\mathbf{k}\cdot\mathbf{r}_1}\mathrm{e}^{-\mathrm{i}\mathbf{k}\cdot\mathbf{r}_2}$$

[4]See, e.g., Sec. 10.3 of Ibach and Lüth (2003) for a qualitative discussion and Chap. 8 of Kittel (1987) or Sec. 11.2 of Czycholl (2004) for details.

where we are only allowed to use states with $k > k_F$ due to the Pauli principle. In the following we neglect the center of mass motion (which will increase the energy) and set $\mathbf{K} = 0$ for simplicity. Then we may write the state as

$$|\Psi\rangle = \sum_{\sigma_1\sigma_2} S_{\sigma_1\sigma_2} \sum_{\mathbf{k}} g(\mathbf{k}) \hat{a}^\dagger_{\sigma_1\mathbf{k}} \hat{a}^\dagger_{\sigma_2-\mathbf{k}} |\Psi_F\rangle \tag{7.7}$$

Then the stationary Schrödinger equation $(\hat{H}_0+\hat{V}_a)|\Psi\rangle = E|\Psi\rangle$ with the interaction of Eq. (7.4) provides us with

$$(E_k + E_{-k})g(\mathbf{k}) + \frac{1}{V}\sum_{\mathbf{k}'} V_{\mathbf{k}',-\mathbf{k}'}(\mathbf{k}-\mathbf{k}')g(\mathbf{k}') = Eg(\mathbf{k})$$

where we neglected all contributions from the homogeneous Fermi sea $|\Psi_F\rangle$, which would affect the energy of all possible two-particle excitations in a similar way. Then the approximation (7.5) provides the relation

$$g(\mathbf{k}) = \frac{V_0}{2E_k - E} \int_{\mathrm{Min}\{E_F,(E_k-\hbar\omega_D)\}}^{E_k+\hbar\omega_D} \mathrm{d}E_{k'} \frac{D(E)}{2} g(k')$$

where $D(E)$ is the density of states for both spin directions. Setting $D(E) \approx D(E_F)$ and assuming that $g(k) \approx 0$ for $E_k > E_F + \hbar\omega_D$ we obtain the relation

$$g(\mathbf{k}) = \frac{D(E_F)}{2} \frac{V_0}{2E_k - E} \int_{E_F}^{E_F+\hbar\omega_D} \mathrm{d}E_{k'} g(k')$$

which requires the self-consistency condition

$$1 = \frac{V_0 D(E_F)}{2} \int_{E_F}^{E_F+\hbar\omega_D} \mathrm{d}E_k \frac{1}{2E_k - E} = \frac{V_0 D(E_F)}{4} \log\left(\frac{2E_F + 2\hbar\omega_D - E}{2E_F - E}\right)$$

providing us with the ground state energy

$$E = 2E_F - \frac{2\hbar\omega_D}{\exp\left(\frac{4}{V_0 D(E_F)}\right) - 1} \approx 2E_F - 2\hbar\omega_D \exp\left(-\frac{4}{V_0 D(E_F)}\right) \tag{7.8}$$

in the limit of weak interaction $V_0 D(E_F) \ll 1$. In this case $2\hbar\omega_D \gg |2E_F - E|$, which justifies the approximation $g(\mathbf{k}) \approx g(k_F)\frac{2E_F-E}{2E_k-E} \to 0$ for $E_k > E_F + \hbar\omega_D$ as applied above.

We find

- The attractive interaction provides a bound state between electron pairs, which is called *Cooper pair*.
- The ground state energy of the Cooper pair is well separated from excited energies in the relative motion, which are above $2E_F$. In contrast, the center-of-mass motion with finite $\mathbf{K}$ in Eq. (7.6) provides a continuous spectrum[5].
- As $g(\mathbf{k}) = g(-\mathbf{k})$ the wave function $\varphi(\mathbf{r}_1 - \mathbf{r}_2)$ is symmetric in the particle indices. To guarantee antisymmetry, $\chi(s_1, s_2)$ in Eq. (7.6) must be antisymmetric, i.e. a singlet state. This means that $S_{\sigma_1\sigma_2} = 0$ for equal spins in Eq. (7.7).

[5]See Sec. 2.2 of Schrieffer (1983) for a general treatment of these issues.

- Using $g(\mathbf{k}) = g(-\mathbf{k})$ the Cooper pair (7.7) can be written as

$$|\Psi\rangle_{\text{Cooper Pair}} = \sum_{\mathbf{k}} g(\mathbf{k}) \hat{a}^\dagger_{\uparrow\mathbf{k}} \hat{a}^\dagger_{\downarrow-\mathbf{k}} |\Psi_F\rangle$$

  which differs essentially from a simple Slater state $\hat{a}^\dagger_n \hat{a}^\dagger_m |\Psi_F\rangle$. In particular it is isotropic in space, while exhibiting strong correlations between $\uparrow \mathbf{k}$ and $\downarrow -\mathbf{k}$.

- The binding energy of the Cooper pair (7.8) is a non-analytic function in the variable V_0 at $V_0 = 0$. This means that it cannot be represented by a Taylor series in the vicinity around $V_0 = 0$. (This can be verified by the vanishing of all derivatives with respect to V_0.) Thus, its energy (7.8) cannot be obtained by standard perturbation theory in the interaction which would provide a Taylor series in V_0.

7.2.2 The BCS ground state

As the formation of the Cooper pair lowers the energy, the Fermi sea $|\Psi_F\rangle$ is unstable in the presence of the attractive interaction. Thus we consider a new trial state

$$|\Psi_{BCS}\rangle = \prod_{\mathbf{k}} \left(\sin\Theta_k + \mathrm{e}^{\mathrm{i}\varphi_\mathbf{k}} \cos\Theta_k \hat{a}^\dagger_{\uparrow\mathbf{k}} \hat{a}^\dagger_{\downarrow-\mathbf{k}} \right) |0\rangle \tag{7.9}$$

describing internal correlations[6]. Note that this constitutes only an approximation for the exact ground state, which is in practice impossible to determine. If we set $\Theta_k = 0$ for $k < k_F$ and $\Theta_k = \pi/2$ for $k > k_F$ we recover the Fermi sea $|\Psi_F\rangle$ as a special case. We also restrict $0 \leq \theta_k \leq \pi/2$, so that both $\cos\Theta_k$ and $\sin\Theta_k$ are not negative (all other possibilities can be taken into account for by a different total sign, which is meaningless for quantum states, or a redefinition $\varphi_k \to \varphi_k \pm \pi$).

For calculations we define

$$|\Psi^{\mathbf{k}_0}_{BCS}\rangle = \prod_{\mathbf{k}\neq\mathbf{k}_0} \left(\sin\Theta_k + \mathrm{e}^{\mathrm{i}\varphi_\mathbf{k}} \cos\Theta_k \hat{a}^\dagger_{\uparrow\mathbf{k}} \hat{a}^\dagger_{\downarrow-\mathbf{k}} \right) |0\rangle$$

which has zero occupation of the states $\uparrow \mathbf{k}_0$ and $\downarrow -\mathbf{k}_0$. Thus $\hat{a}_{\uparrow\mathbf{k}_0} |\Psi^{\mathbf{k}_0}_{BCS}\rangle = \hat{a}_{\downarrow-\mathbf{k}_0} |\Psi^{\mathbf{k}_0}_{BCS}\rangle = 0$. As $\left[\left(\sin\Theta_k + \mathrm{e}^{\mathrm{i}\varphi_\mathbf{k}} \cos\Theta_k \hat{a}^\dagger_{\uparrow\mathbf{k}} \hat{a}^\dagger_{\downarrow-\mathbf{k}} \right), \left(\sin\Theta_{k'} + \mathrm{e}^{\mathrm{i}\varphi_{\mathbf{k}'}} \cos\Theta_{k'} \hat{a}^\dagger_{\uparrow\mathbf{k}'} \hat{a}^\dagger_{\downarrow-\mathbf{k}'} \right) \right] = 0$ due to the even number of permutations for the fermionic operators $a^\dagger$, the order in the product can be chosen arbitrarily and we find

$$\begin{aligned}
\langle\Psi_{BCS}|\Psi_{BCS}\rangle =& \langle\Psi^{\mathbf{k}}_{BCS}| \left(\sin\Theta_k + \mathrm{e}^{-\mathrm{i}\varphi_\mathbf{k}} \cos\Theta_k \hat{a}_{\downarrow-\mathbf{k}} \hat{a}_{\uparrow\mathbf{k}} \right) \left(\sin\Theta_k + \mathrm{e}^{\mathrm{i}\varphi_\mathbf{k}} \cos\Theta_k \hat{a}^\dagger_{\uparrow\mathbf{k}} \hat{a}^\dagger_{\downarrow-\mathbf{k}} \right) |\Psi^{\mathbf{k}}_{BCS}\rangle \\
=& \langle\Psi^{\mathbf{k}}_{BCS}| \sin^2\Theta_k + \cos^2\Theta_k |\Psi^{\mathbf{k}}_{BCS}\rangle \,.
\end{aligned}$$

Repeating this operation, we proof the normalization $\langle\Psi_{BCS}|\Psi_{BCS}\rangle = 1$. Furthermore we find the single-particle expectation value

$$\begin{aligned}
&\langle\Psi_{BCS}|\hat{a}^\dagger_{\uparrow\mathbf{k}} \hat{a}_{\uparrow\mathbf{k}}|\Psi_{BCS}\rangle \\
&= \langle\Psi^{\mathbf{k}}_{BCS}| \left(\sin\Theta_k + \mathrm{e}^{-\mathrm{i}\varphi_\mathbf{k}} \cos\Theta_k \hat{a}_{\downarrow-\mathbf{k}} \hat{a}_{\uparrow\mathbf{k}} \right) \hat{a}^\dagger_{\uparrow\mathbf{k}} \hat{a}_{\uparrow\mathbf{k}} \left(\sin\Theta_k + \mathrm{e}^{\mathrm{i}\varphi_\mathbf{k}} \cos\Theta_k \hat{a}^\dagger_{\uparrow\mathbf{k}} \hat{a}^\dagger_{\downarrow-\mathbf{k}} \right) |\Psi^{\mathbf{k}}_{BCS}\rangle \\
&= \cos^2\Theta_\mathbf{k} \langle\Psi^{\mathbf{k}}_{BCS}| \hat{a}_{\downarrow-\mathbf{k}} \hat{a}_{\uparrow\mathbf{k}} \hat{a}^\dagger_{\uparrow\mathbf{k}} \hat{a}_{\uparrow\mathbf{k}} \hat{a}^\dagger_{\uparrow\mathbf{k}} \hat{a}^\dagger_{\downarrow-\mathbf{k}} |\Psi^{\mathbf{k}}_{BCS}\rangle = \cos^2\Theta_\mathbf{k}
\end{aligned} \tag{7.10}$$

[6] According to Sec. 2.4 of Schrieffer (1983) this can be written as an anti-symmetrized product of N/2 identical two-particle wave functions $\varphi(\mathbf{r}_1 - \mathbf{r}_2)$ for φ_k =const. However such a state would have a constant particle number in contrast to $|\Psi_{BCS}\rangle$.

and similarly $\langle\Psi_{BCS}|\hat{a}^\dagger_{\downarrow-\mathbf{k}}\hat{a}_{\downarrow-\mathbf{k}}|\Psi_{BCS}\rangle = \cos^2\Theta_\mathbf{k}$. Thus the expectation value of the total particle number is $N = 2\sum_k \cos^2\Theta_\mathbf{k}$.

The total energy is given by the expectation value $E = \langle\Psi_{BCS}|\hat{H}_0 + \hat{V}_a|\Psi_{BCS}\rangle$. We note, that all elements are zero, unless the operators in the $\hat{V}_a$ are pairs of the form $\hat{a}^\dagger_{\uparrow\mathbf{k}}\hat{a}^\dagger_{\downarrow-\mathbf{k}}$, $\hat{a}_{\uparrow\mathbf{k}}\hat{a}_{\downarrow-\mathbf{k}}$, $\hat{a}^\dagger_{\uparrow\mathbf{k}}\hat{a}_{\uparrow\mathbf{k}}$, or $\hat{a}^\dagger_{\downarrow-\mathbf{k}}\hat{a}_{\downarrow-\mathbf{k}}$. Together we find

$$\begin{aligned} E =& \sum_\mathbf{k} 2E_\mathbf{k}\cos^2\Theta_\mathbf{k} + \frac{1}{V}\sum_{\mathbf{kq}\neq 0} V_{\mathbf{k},-\mathbf{k}}(\mathbf{q})\mathrm{e}^{\mathrm{i}(\varphi_\mathbf{k}-\varphi_{\mathbf{k}+\mathbf{q}})}\cos\Theta_{\mathbf{k}+\mathbf{q}}\sin\Theta_{\mathbf{k}+\mathbf{q}}\sin\Theta_\mathbf{k}\cos\Theta_\mathbf{k} \\ &\underbrace{+\frac{2}{V}\sum_{\mathbf{kk'}} V_{\mathbf{k},\mathbf{k'}}(0)\cos^2\Theta_\mathbf{k}\cos^2\Theta_{\mathbf{k'}} - \frac{1}{V}\sum_{\mathbf{kq}} V_{\mathbf{k},\mathbf{k}+\mathbf{q}}(\mathbf{q})\cos^2\Theta_\mathbf{k}\cos^2\Theta_{\mathbf{k}+\mathbf{q}}}_{\text{Hartree-Fock terms}} \end{aligned} \tag{7.11}$$

The occurrence of expressions $\hat{a}^\dagger_{\uparrow\mathbf{k}}\hat{a}_{\uparrow\mathbf{k}}$ and $\hat{a}^\dagger_{\downarrow-\mathbf{k}}\hat{a}_{\downarrow-\mathbf{k}}$ provide the Hartree-Fock terms, which describe the interaction of single-particle states (with occupation $\cos^2\Theta_\mathbf{k}$) with each other. For a fixed particle number N these provide a contribution to the energy, which does not crucially depend on the actual values of $\Theta_\mathbf{k}$. Thus we neglect these terms in the following in accordance with the literature. This corresponds to the effective interaction

$$\hat{V}_a^{\text{eff}} = \frac{1}{V}\sum_\mathbf{k}\sum_{\mathbf{q}\neq 0} V_{\mathbf{k},-\mathbf{k}}(\mathbf{q})\hat{a}^\dagger_{\uparrow\mathbf{k}+\mathbf{q}}\hat{a}^\dagger_{\downarrow-\mathbf{k}-\mathbf{q}}\hat{a}_{\downarrow-\mathbf{k}}\hat{a}_{\uparrow\mathbf{k}} = \frac{1}{V}\sum_{\mathbf{kk'}} V^{\text{eff}}_{\mathbf{k},\mathbf{k'}}\hat{a}^\dagger_{\uparrow\mathbf{k'}}\hat{a}^\dagger_{\downarrow-\mathbf{k'}}\hat{a}_{\downarrow-\mathbf{k}}\hat{a}_{\uparrow\mathbf{k}}\,, \tag{7.12}$$

with $V^{\text{eff}}_{\mathbf{k},\mathbf{k'}} = -V_0\Theta(\hbar\omega_D - |E_k - E_{k'}|)$ see, e.g. Schrieffer (1983).

The combination of terms $\hat{a}^\dagger_{\uparrow\mathbf{k}}\hat{a}^\dagger_{\downarrow-\mathbf{k}}$ and $\hat{a}_{\uparrow\mathbf{k'}}\hat{a}_{\downarrow-\mathbf{k'}}$ describe the interaction process annihilating one pair of particles (called *Cooper pair*) and creating another. This provides a term proportional to $\cos\Theta_{\mathbf{k'}}\sin\Theta_{\mathbf{k'}}\sin\Theta_\mathbf{k}\cos\Theta_\mathbf{k}$ in the energy (7.11). Eq. (7.10) shows that this term is finite if the states $\mathbf{k}$ and $\mathbf{k'}$ are neither fully occupied ($\Theta = 0$) or empty ($\Theta = \pi/2$). For the case of attractive interaction (negative matrix element) it provides a reduction of energy for partially occupied paired states (i.e. $0 \leq \Theta_\mathbf{k} \leq \pi/2$) and identical phase $\varphi_\mathbf{k} = \varphi$ =const so that the attractive interaction adds up with positive prefactors. This shows that a fixed phase relation between all pairs is crucial for a low energy of the BCS state. φ is the *phase of the BCS state* and is important for the Josephson effect, e.g.

We are looking for the minimum of E for a fixed particle number $N = 2\sum_k \cos^2\Theta_\mathbf{k}$. This can be achieved by considering the variation of $E - N\mu$ with respect to any Θ_k, where μ is the chemical potential (the Lagrange multiplier), which can be determined at a later stage to fix the particle number N. Thus we obtain the conditions:

$$\begin{aligned} \frac{\partial(E-N\mu)}{\partial\Theta_k} =& -2(E_\mathbf{k}-\mu)\underbrace{2\cos\Theta_\mathbf{k}\sin\Theta_\mathbf{k}}_{=\sin 2\Theta_\mathbf{k}} + \frac{2}{V}\sum_\mathbf{q} V_{\mathbf{k},-\mathbf{k}}(\mathbf{q})\underbrace{\cos\Theta_{\mathbf{k}+\mathbf{q}}\sin\Theta_{\mathbf{k}+\mathbf{q}}}_{=\frac{1}{2}\sin 2\Theta_{\mathbf{k}+\mathbf{q}}}\underbrace{(\cos^2\Theta_\mathbf{k} - \sin^2\Theta_\mathbf{k})}_{=\cos 2\Theta_\mathbf{k}} \\ =& 0 \end{aligned}$$

using $V_{\mathbf{k},-\mathbf{k},\mathbf{q}} = V_{\mathbf{k},-\mathbf{k},-\mathbf{q}}$. Now we set $\mathbf{k'} = \mathbf{k} + \mathbf{q}$ and use the approximation (7.5) implying the restriction $|E_{k'} - E_k| < \hbar\omega_D$. This provides us with

$$(E_\mathbf{k} - \mu)\tan 2\Theta_\mathbf{k} = -\Delta_\mathbf{k} \quad \text{with} \quad \Delta_\mathbf{k} = \frac{V_0}{2}\int_{E_\mathbf{k}-\hbar\omega_D}^{E_\mathbf{k}+\hbar\omega_D} \mathrm{d}E_{k'}\frac{1}{2}D(E_{k'})\sin 2\Theta_{k'} \tag{7.13}$$

Using $\tan 2\Theta = \sin 2\Theta/\sqrt{1-\sin^2 2\Theta}$ we find

$$\sin 2\Theta_\mathbf{k} = \frac{\Delta_\mathbf{k}}{\sqrt{\Delta_\mathbf{k}^2 + (E_\mathbf{k}-\mu)^2}} \tag{7.14}$$

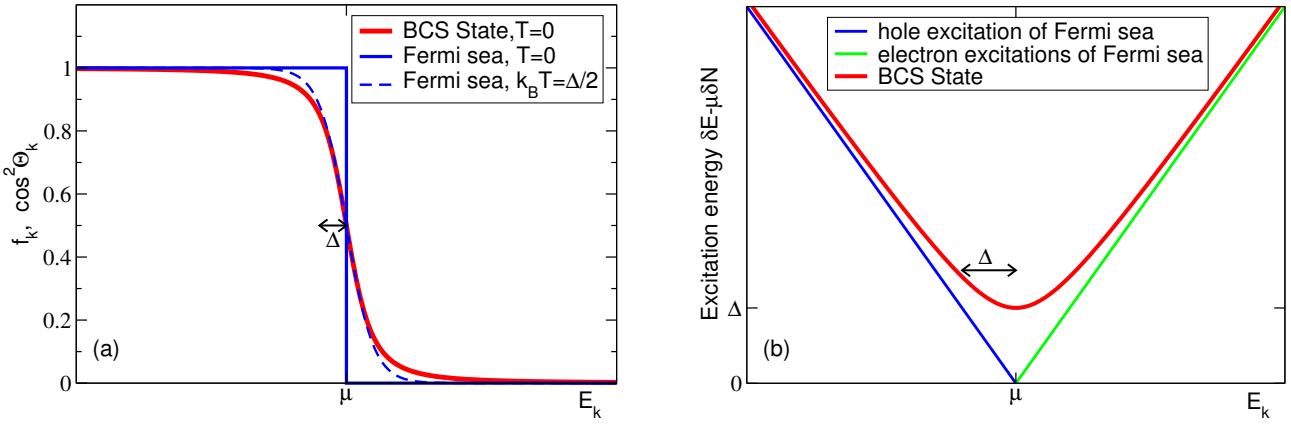

Figure 7.4: (a) occupation of single-particle states/Cooper pairs as a function of the single particle energy E_k. (b) Excitation energies of the BCS state in comparison with excitations of the Fermi sea at zero temperature.

and with $\sin 2\theta = 2\sqrt{1-\cos^2\Theta}\cos\Theta$ we obtain a minimum for E at

$$\cos^2\Theta_{\mathbf{k}} = \frac{1}{2}\left(1 - \frac{E_{\mathbf{k}}-\mu}{\sqrt{(E_{\mathbf{k}}-\mu)^2+\Delta_{\mathbf{k}}^2}}\right) \tag{7.15}$$

Now $\cos^2\Theta_{\mathbf{k}}$ is the probability to find a pair $\mathbf{k}$. Fig. 7.4(a) shows:

- For $E_k < \mu - \Delta_k$, the states are essentially occupied
- For $E_k > \mu + \Delta_k$, the states are essentially empty
- There is a smooth transition between 1 and 0 around $E_k = \mu$ with a width of $2\Delta_k$

Fig. 7.4(a), shows that $\cos^2\Theta_{\mathbf{k}}$ resembles a Fermi distribution with $k_BT = \Delta/2$. However, this similarity is misleading: At first, we are considering the ground state of a quantum system, which is most relevant for zero temperature here. Secondly, the values $\cos\Theta_{\mathbf{k}}$ are the expansion coefficients of a many-particle quantum state (7.9), where a defined phase relation between all parts exists. In contrast, the Fermi occupation function describes the average occupation of a level in a statistical ensemble, where all phase relations between different states are washed out.

Provided $\Delta_k \ll \hbar\omega_D$, Eq. (7.13) shows that $\Delta_k = \Delta$ becomes independent of E_k for $|E_k - \mu| \ll \hbar\omega_D$. Inserting Eq. (7.14) gives

$$\Delta \approx \Delta\frac{V_0 D(\mu)}{4}\int_{\mu-\hbar\omega_D}^{\mu+\hbar\omega_D} \mathrm{d}E_k \frac{1}{\sqrt{\Delta^2+(E_k-\mu)^2}} = \Delta\frac{V_0 D(\mu)}{2}\sinh\left(\frac{\hbar\omega_D}{\Delta}\right)$$

with the solution[7]

$$\Delta = \frac{\hbar\omega_D}{\operatorname{arcsinh}[2/V_0 D(\mu)]} \approx 2\hbar\omega_D \exp\left(\frac{-2}{V_0 D(\mu)}\right) \tag{7.16}$$

in the limit $V_0 D(\mu) \ll 1$.

[7]The additional solution $\Delta = 0$ provides the normal state $|\Psi_F\rangle$ which exhibits a larger energy.

7.2.3 Excitations from the BCS state

Now we consider a single-particle excitation of the BCS state:

$$|\mathbf{k}_0\rangle = \frac{1}{\sin\Theta_{\mathbf{k}_0}}\hat{a}^\dagger_{\uparrow\mathbf{k}_0}|\Psi_{\rm BCS}\rangle = \hat{a}^\dagger_{\uparrow\mathbf{k}_0}\prod_{\mathbf{k}\neq\mathbf{k}_0}\left(\sin\Theta_k + \cos\Theta_k\hat{a}^\dagger_{\uparrow\mathbf{k}}\hat{a}^\dagger_{\downarrow-\mathbf{k}}\right)|0\rangle \tag{7.17}$$

Applying the effective interaction (7.12) we find the energy

$$\langle\mathbf{k}_0|\hat{H}_0+\hat{V}_a^{\rm eff}|\mathbf{k}_0\rangle = E_{\rm BCS} + E_{\mathbf{k}_0}(1-2\cos^2\Theta_{\mathbf{k}_0}) - \underbrace{\frac{1}{V}\sum_{\mathbf{k}'\neq\mathbf{k}_0}V^{\rm eff}_{\mathbf{k}_0\mathbf{k}'}\cos\Theta_{\mathbf{k}'}\sin\Theta_{\mathbf{k}'}}_{=-\Delta_{\mathbf{k}_0}}\underbrace{2\sin\Theta_{\mathbf{k}_0}\cos\Theta_{\mathbf{k}_0}}_{\sin(2\Theta_{\mathbf{k}_0})}$$

and the number of electrons

$$\langle\mathbf{k}_0|\hat{N}|\mathbf{k}_0\rangle = N_{\rm BCS} + (1-2\cos^2\Theta_{\mathbf{k}_0})\,.$$

Thus, the state $|\mathbf{k}_0\rangle$ corresponds to a single-particle excitation for $E_{\mathbf{k}_0}\gg\mu$ and a hole excitation for $E_{\mathbf{k}_0}\ll\mu$, while its nature is a mixture of both for $E_{\mathbf{k}_0}\approx\mu$. Now, for the effective energy of the excitation, one has to take into account the change in the particle reservoir as well. Thus we obtain with Eqs. (7.14,7.15)

$$\delta E(\mathbf{k}_0)-\mu\delta N = \langle\mathbf{k}_0|\hat{H}_0+\hat{V}_a^{\rm eff}|\mathbf{k}_0\rangle - E_{\rm BCS} - \mu(\langle\mathbf{k}_0|\hat{N}|\mathbf{k}_0\rangle - N_{\rm BCS}) = \sqrt{(E_{\mathbf{k}_0}-\mu)^2+\Delta_{k_0}^2} \tag{7.18}$$

Thus creating an excitation containing a single-particle state $\mathbf{k}_0$ costs at least the energy Δ as shown in Fig. 7.4(b). This explains the gap observed in the tunneling experiment from Fig. 7.3. In comparison for the non-interacting Fermi sea $|\Psi_F\rangle$ we have electron excitations for $\hat{a}^\dagger_{\sigma\mathbf{k}_0}|\Psi_F\rangle$ for $E_{\mathbf{k}_0}>\mu=E_F$ and hole excitations for $\hat{a}_{\sigma\mathbf{k}_0}|\Psi_F\rangle$ for $E_{\mathbf{k}_0}<\mu=E_F$ with $\delta E(\mathbf{k}_0)-\mu\delta N = |E_{\mathbf{k}_0}-\mu|$. Here excitations are possible at arbitrary small energies, which allows for absorption at low frequencies, as obtained by the Lindhard theory in Fig. 6.2.

The BCS state from Eq. (7.9) is the ground state, which is taken by the system at zero temperature. With increasing temperature, single-particle excitations become more frequently. Thereby the superfluid density decreases and so does the energy gap, which finally vanishes at

$$k_BT_c \approx 0.57\Delta(T=0) \tag{7.19}$$

as shown in Sec. 10.6 of Ibach and Lüth (2003) or Sec. 11.2.4 of Snoke (2008).

7.2.4 Electron transport in the BCS state

The presence of an electric field causes a shift in the Bloch vector according to $\hbar\dot{\mathbf{k}} = -e\mathbf{F}$. This will cause a center of mass motion $\hbar\dot{\mathbf{K}} = -2e\mathbf{F}$ for the Cooper pair from Eq. (7.6) and correspondingly the BCS state will be shifted by $\mathbf{K}/2$

$$|\Psi^{\mathbf{K}}_{BCS}\rangle = \prod_{\mathbf{k}}\left(\sin\Theta_k + \cos\Theta_k\hat{a}^\dagger_{\uparrow(\mathbf{K}/2+\mathbf{k})}\hat{a}^\dagger_{\downarrow(\mathbf{K}/2-\mathbf{k})}\right)|0\rangle$$

carrying the current density $\mathbf{j}_s = -en_s\hbar\mathbf{K}/2m$ for a parabolic band $E_k=\hbar^2k^2/2m$ as depicted in Fig. 7.5(b). This justifies the London equation (7.1). The state $|\Psi^{\mathbf{K}}_{BCS}\rangle$ exhibits a fixed phase relation between pairs with total crystal momentum $2\mathbf{K}=\mathbf{k}_1+\mathbf{k}_2$ and has thus similar properties as the $\mathbf{K}=0$ BCS ground state (7.9). In particular there is the same gap Δ (provided

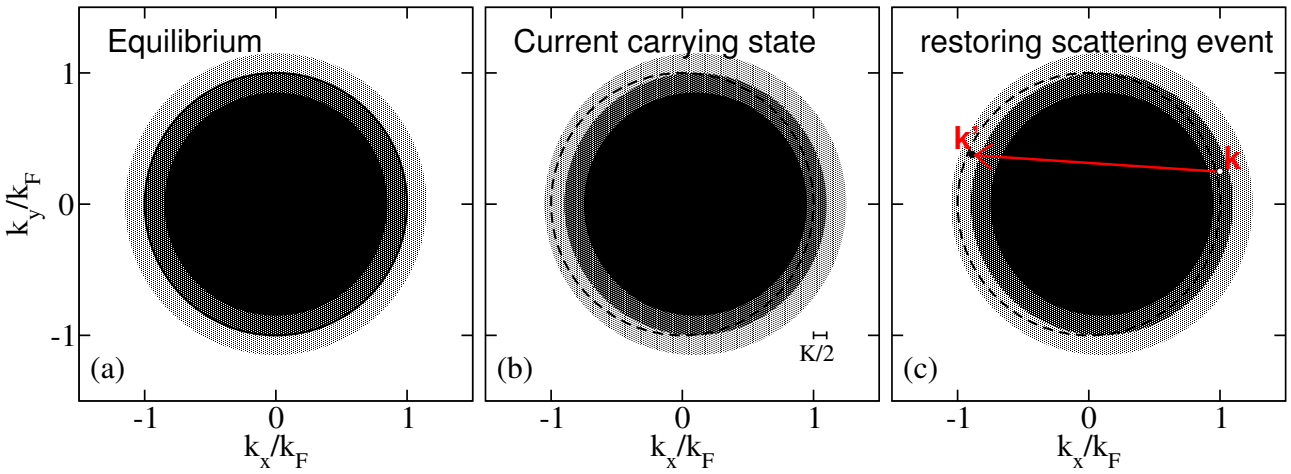

Figure 7.5: The superconducting state (a) in equilibrium, (b) after acceleration by a pulse with finite electric field in x direction, (c) a possible scattering process tho restore equilibrium.

$\hbar^2 \mathbf{K} k_F/m \ll \hbar\omega_D$). For a single particle scattering process as indicated in Fig. 7.5(c) we have the energy balance

$$\delta E = E_{\mathbf{k}'} + 2\Delta - E_{\mathbf{k}} \geq E_{k_F - K/2} - E_{k_F + K/2} + 2\Delta \tag{7.20}$$

as the breaking of the pair $\uparrow(\mathbf{k}), \downarrow(\mathbf{K}-\mathbf{k})$ and adding the electron at another place $\mathbf{k}'$ corresponds to two single particle excitations. Thus, for small $\mathbf{K}$, any single particle scattering event to restore the equilibrium *costs* energy in contrast to the simple Fermi sea, where Δ is zero. Therefore the probability to change the entire state $|\Psi^{\mathbf{K}}_{BCS}\rangle$ is negligible small. The latter would either imply N subsequent single-particle excitations with the cost of a total energy of $\sim N\Delta$ or the collective scattering of *all* particles within a single process. Both scenarios become extremely unlikely for a macroscopic system. This explains, that scattering does not restore the zero-current state as in a normal metal.

However the energy balance (7.20) becomes negative for $K > 2\Delta m/\hbar^2 k_F$, when the gain in kinetic energy by single-particle excitations can compensate the gap energy Δ, so that a macroscopic number of electrons will leave the BCS condensate, causing a breakdown of superconductivity. Thus there is a

critical current density

$$j_c \approx \frac{e n_s \Delta}{\hbar k_F} \tag{7.21}$$

which provides us with a critical magnetic field $H_c \approx \lambda_L j_c$ from Eq. (7.3). See also exercises as well as Sec. 10.6 of Ibach and Lüth (2003). With Eq. (7.19) we thus understand the approximately linear increase of H_c with T_c displayed in Fig. 7.2.

7.2.5 Justification of attractive interaction*

In order to justify Eq. (7.5) we consider a model of free electrons with phonon interaction described by the Fröhlich Hamiltonian

$$\hat{H} = \underbrace{\sum_{\mathbf{k}} E_k \hat{a}^\dagger_{\mathbf{k}} \hat{a}_{\mathbf{k}} + \sum_{\mathbf{q}} \hbar\omega_q \hat{b}^\dagger_{\mathbf{q}} \hat{b}_{\mathbf{q}}}_{=\hat{H}_0} + \underbrace{\sum_{\mathbf{k},\mathbf{q}} g_q \hat{a}^\dagger_{\mathbf{k}+\mathbf{q}} \hat{a}_{\mathbf{k}} (\hat{b}_{\mathbf{q}} + \hat{b}^\dagger_{-\mathbf{q}})}_{=\hat{H}_i} \tag{7.22}$$

A *canonical transformation* changes all states via $|X\rangle \to |\mathcal{X}\rangle = \hat{U}|a\rangle$ and operators as $\hat{O} \to \hat{\mathcal{O}} = \hat{U}\hat{O}\hat{U}^\dagger$ with an unitarian operator $\hat{U}$ (i.e. $\hat{U}^\dagger = \hat{U}^{-1}$). Such a transformation maintains all physical properties such as equations of motion and expectation values. A convenient choice is $\hat{U} = \exp(-\mathrm{i}\hat{S})$, where $\hat{S}$ is hermitian (i.e. $\hat{S}^\dagger = \hat{S}$). Then we find

$$\begin{aligned}\hat{\mathcal{H}} =& \exp(-\mathrm{i}\hat{S})\hat{H}\exp(\mathrm{i}\hat{S}) = \left(1 - \mathrm{i}\hat{S} - \frac{1}{2}\hat{S}^2\right)\hat{H}\left(1 + \mathrm{i}\hat{S} - \frac{1}{2}\hat{S}^2\right) + \mathcal{O}(S^3)\\ =& \hat{H} + \mathrm{i}[\hat{H},\hat{S}] + \frac{1}{2}[\hat{S},[\hat{H},\hat{S}]] + \mathcal{O}(S^3)\end{aligned}$$

The idea is to find an operator $\hat{S}$, which cancels the electron-phonon interaction $\hat{H}_i$ in order g. This is the case if $\mathrm{i}[\hat{H}_0,\hat{S}] = -\hat{H}_i$ holds, which is achieved by setting

$$\hat{S} = \mathrm{i}\sum_{\mathbf{k}',\mathbf{q}'} g_{q'}\left(\frac{\hat{a}^\dagger_{\mathbf{k}'+\mathbf{q}'}\hat{a}_{\mathbf{k}'}\hat{b}_{\mathbf{q}'}}{E_{\mathbf{k}'+\mathbf{q}'} - E_{\mathbf{k}'} - \hbar\omega_{q'}} + \frac{\hat{a}^\dagger_{\mathbf{k}'+\mathbf{q}'}\hat{a}_{\mathbf{k}'}\hat{b}^\dagger_{-\mathbf{q}'}}{E_{\mathbf{k}'+\mathbf{q}'} - E_{\mathbf{k}'} + \hbar\omega_{q'}}\right)$$

Using $g_{-q} = g_q^*$ and $\omega_q = \omega_{-q}$ this provides us with

$$\hat{\mathcal{H}} = \hat{H}_0 + \frac{\mathrm{i}}{2}[\hat{H}_i,\hat{S}] + \mathcal{O}(g^3) = \hat{H}_0 + \hat{V}_a + \hat{V}_{\text{Polaron}} + \hat{V}_{\text{sp}} + \mathcal{O}(g^3)$$

Here

$$\hat{V}_a = \sum_{\mathbf{k},\mathbf{k}',\mathbf{q}} \frac{\hbar\omega_q|g_q|^2}{(E_{\mathbf{k}'-\mathbf{q}} - E_{\mathbf{k}'})^2 - (\hbar\omega_q)^2}\hat{a}^\dagger_{\mathbf{k}+\mathbf{q}}\hat{a}^\dagger_{\mathbf{k}'-\mathbf{q}}\hat{a}_{\mathbf{k}'}\hat{a}_{\mathbf{k}}$$

is the interaction used in Eq. (7.4). It is attractive if $|E_{\mathbf{k}'-\mathbf{q}} - E_{\mathbf{k}'}| < \hbar\omega_q$, which suggests the approximation (7.5), as ω_D is an estimate for the maximum frequency of the acoustic branch.

$$\hat{V}_{\text{Polaron}} = -\sum_k\left(\sum_q \frac{|g_q|^2}{E_{\mathbf{k}+\mathbf{q}} - E_{\mathbf{k}} + \hbar\omega_q}\right)\hat{a}^\dagger_{\mathbf{k}}\hat{a}_{\mathbf{k}}$$

is the polaron shift, which renormalizes the single particle energies and can be tacitly incorporated into $\hat{H}_0$. The remaining term

$$\hat{V}_{\text{sp}} = -\frac{1}{2}\sum_{\mathbf{k}'\mathbf{q}\mathbf{q}'} g_{q'}g_q\left(\frac{(\hat{b}_{\mathbf{q}} + \hat{b}^\dagger_{-\mathbf{q}})\hat{b}_{\mathbf{q}'}}{E_{\mathbf{k}'+\mathbf{q}'} - E_{\mathbf{k}'} - \hbar\omega_{q'}} + \frac{\hat{b}^\dagger_{-\mathbf{q}'}(\hat{b}_{\mathbf{q}} + \hat{b}^\dagger_{-\mathbf{q}})}{E_{\mathbf{k}'+\mathbf{q}'} - E_{\mathbf{k}'} + \hbar\omega_{q'}}\right)\left(\hat{a}^\dagger_{\mathbf{k}'+\mathbf{q}'+\mathbf{q}}\hat{a}_{\mathbf{k}'} - \hat{a}^\dagger_{\mathbf{k}'+\mathbf{q}'}\hat{a}_{\mathbf{k}'-\mathbf{q}}\right)$$

also modifies the single particle levels, if there are specific excitations of the phonon spectrum. However it does not constitute an interaction between the electrons.